School of Electrical Engineering, Computing and Mathematical Sciences

Performance Optimisation of Standalone and Grid Connected Microgrid Clusters

Munira Batool

This thesis is presented for the Degree of

Doctor of Philosophy

of

Curtin University

April 2018

Declaration

To the best of my knowledge and belief, this thesis contains no material previously published by any other person, except where due acknowledgment has been made.

This thesis contains no material which has been accepted for the award of any other degree or diploma in any university.

Munira Batool

13 April 2018

Abstract

Remote and regional areas are usually supplied by isolated and self-sufficient electricity supply systems. These systems, often referred to as microgrids, rely on renewable energy-based non-dispatchable distributed energy resources to reduce the overall cost of electricity production. Microgrids can operate in the standalone as well as the interconnected mode. Standalone hybrid remote area microgrids, can provide reasonably priced electricity in geographically isolated and edge of grid locations, for operators. To achieve a reliable operation of microgrids alongside minimal fossil fuel consumption and maximum penetration of renewables, the voltage and frequency should be maintained to within acceptable limits.

Emergencies, such as overloading and excessive generation by renewable sources, can lead to significant voltage or frequency deviation in these power systems. As a result, protective relays may trip some of the sources or loads, to prevent system instability. These problems can be resolved by utilising the optimisation-based technique that is proposed and validated within this research. To this end, a suitable optimisation problem is needed.

In this research an objective function is developed, which focuses on minimizing the power loss in the tie-lines amongst microgrids and the dependency of a microgrid to its neighbouring microgrids, as well as maximizing the contribution of renewable sources in electricity generation while minimizing the fuel consumption and greenhouse gas emissions from conventional generators along with frequency and voltage deviations.

Additionally, this research will propose a new market model that maximises returns for the investment of energy providers, microgrid clusters and distributed network operator. The formulated objective function is then solved with a Genetic Algorithm, using different combinations of operators. The performance of the proposal is evaluated by several numerical analyses in Matlab.

Acknowledgements

I would like to express my sincere gratitude and thanks to Prof. Syed Islam for his continuous support and excellent supervision during this research. Their valuable knowledge, guidance, motivation and support helped me throughout all the many hours spent conducting this research and writing this thesis.

I dedicate my thesis to my parents, for their love and providing me with unfailing support and continuous encouragement, throughout my years of study and throughout the process of researching and writing this thesis. This accomplishment would not have been possible without their support.

Moreover, I dedicate this thesis to my husband, Fawad Nawaz and my lovely sons, Arqum Fawad and Huzayl Fawad, for their understanding. Without my husband's love and sincere support, and my sons' inspiration, I would not have been able to tackle the challenges during my studies. I am very fortunate to have my family by my side, who enrich my life with love and happiness.

I am also thankful to all my friends for their emotional support, companionship, entertainment, love and care.

Finally, I thank Allah, for assisting me to work through all of the difficulties that have challenged me during this research. I have experienced His guidance day by day. He is the one who allowed me to complete my degree. I will keep trusting Him for my future. Thank you, Allah.

Publications arising from this Thesis

Journal papers

1. **Munira Batool**, Farhad Shahnia and Syed M. Islam, "A multi-level supervisory emergency control for the operation of remote area microgrid clusters", *Journal of Modern Power Systems and Clean Energy*, 2019, doi:10.1007/s40565-018-0481-6.
2. **Munira Batool**, Farhad Shahnia and Syed M. Islam, "Impact of scaled fitness functions in a floating-point genetic algorithm to optimize the operation of standalone microgrids", *IET Renewable Power Generation*, 2019, doi: 10.1049/iet-rpg.2018.5519.
3. **Munira Batool**, Syed M. Islam and Farhad Shahnia, "A VPP Market Model for Clustered Microgrid Optimization including Distribution Network Operations", under 2nd review in *IET Generation, Transmission and Distribution*, GTD-2018-5275.

Conference papers

4. **Munira Batool**, Syed M. Islam and Farhad Shahnia, "Power transaction management amongst coupled microgrids in remote areas", IEEE PES Innovative Smart Grid Technologies (ISGT), Auckland, 2017.
5. **Munira Batool**, Syed M. Islam and Farhad Shahnia, "Master control unit based power exchange strategy for interconnected microgrids", 27th Australian Universities Power Engineering Conference (AUPEC), Melbourne, 2017.
6. **Munira Batool**, Syed M. Islam and Farhad Shahnia, "Selection of sustainable standalone microgrid for optimal operation of remote area town", One Curtin Postgraduate Conference (OCPC), Malaysia, 2017.
7. **Munira Batool**, Syed M. Islam and Farhad Shahnia, "Stochastic modelling of the output power of photovoltaic generators in various weather conditions", 26th Australian

Universities Power Engineering Conference (AUPEC), Brisbane, 2016.

Book Chapter

8. **Munira Batool**, Syed M. Islam and Farhad Shahnia, "Operations of a clustered microgrid", in *Variability, Scalability, and Stability of Microgrid*, IET Press, 2019.

Statement of Contributions by Others

The purpose of this statement is to summarize and identify the intellectual input by PhD candidate Ms. Munira Batool and co-authors on the study publications contained herein.

Ms. Munira Batool was the principal author of aforementioned publications listed in the previous section. She designed the included methodologies, developed the associated simulation files, performed interpretations and analysis on the results, and wrote the manuscript. The overall percentage of her contribution is about 60%.

Prof. Syed Islam and Dr. Farhad Shahnia, in their role as Supervisors as well as Co-authors, was involved with evaluating the research contribution and editing the manuscript. Also, they helped in data interpretation, wrote parts of the manuscript, and acted as the corresponding author. Overall percentage of their mutual contribution is about 40%.

I affirm that the details stated in the Statement of Contribution are true and correct.

Ms. Munira Batool (PhD Candidate)

Date: 29/03/2019

Signature: 

Prof. Syed Islam (Supervisor)

Date: 29/03/2019

Signature: 

Dr. Farhad Shahnia (PhD Co-supervisor)

Date: 29/03/2019

Signature: *Farhad Shahnia*

Table of Contents

List of Figures

List of Tables

Nomenclature

A. List of Abbreviations

BSS	Battery storage system
DDER	Dispatchable distributed energy resource
DER	Distributed energy resource
DG	Diesel generator
DNO	Distribution network operator
DRS	Droop regulated system
IOE	Internet of energy
IOEP	Internet of energy provider
ISS	Interconnecting static switch
ISP	Internal service provider
MG	Microgrid
MMA	Multi-microgrid area
MPPT	maximum power point tracking
NDER	Non-dispatchable distributed energy resource
OF	Objective function
PDF	Probability Density Function

PV	Photovoltaic
RC	Renewable curtailment
RPL	Renewable penetration level
SoC	State of charge
SEC	Supervisory emergency controller
SRI	Spinning reserve index
SSP	Shared service provider

B. Parameters and variables

$\alpha, \beta, \gamma, \delta$	Constants
$\Delta f, \Delta f^{\max}$	Frequency deviation and its maximum permissible limit
$\Delta V, \Delta V^{\max}$	Voltage deviation and its maximum permissible limit
ΔT	Time period
η	Gearbox efficiency
λ	Tip-speed ratio
ρ	Standard atmosphere air density
∂	Emission factor
Θ	Blade pitch angle
a, b	Beta distribution shape parameters for sunny condition
A	Wind turbine's blade sweep area
B	Beta distribution
BSS, DG, load, microgrid,	Vector representing corresponding BSSs, DGs, loads, microgrids, NDERs, lines and buses respectively

NDD, line, bus

$cost_{BSS}, C^{BSS}$	Operational and lifeloss cost of BSS
$cost_{curt}$	Cost of curtailing NDERs
$cost_{DG}$	Operational cost of DG
$cost_{em}$	Cost of emissions of DGs
C^{cfp}	Carbon foot print cost
$cost_{fuel}$	Cost of fuel consumption by DGs
$cost_{loss}$	Cost of loss
$cost_{shed}, C_{\text{curt}}^{\text{load}}$	Cost of load-shedding
$C_{\text{curt}}^{\text{NDERs}}$	Curtailment cost of non-dispatchable distributed energy resource
C^{trans}	Power import/export cost
c_v	Scale index
C_P	Coefficient of performance
d, e	Beta distribution shape parameters for cloudy condition
FF	Fill Factor
$f(X)$	PDF for sunny condition
$f(C)$	PDF for cloudy condition
$f(R)$	PDF for rainy condition
$f, f^{min}, f^{max},$ $f^{nom}, \Delta f$	Frequency and its lower, upper, nominal values and its deviation from nominal value
$FF_{op}, FF_{int}, FF_{vf}$	Operational, interruption and technical fitness functions
g, h	Beta distribution shape parameters for rainy condition
I_{mpp}	Current at maximum power point [A]

I_{sc}	Short-circuit current [A]
I_{sco}	Short-circuit current in normal conditions [A]
$I_{sc}(S)$	Mismatched short-circuit current due to shading [A]
I_l, $(I_l)^{max}$	Line current and its maximum
j, l, x, y	Indices
$k_1, k_2, k_3, k_4, N, \gamma, \mu, \psi$	Constants
k_i	Temperature coefficient of I_{sc} [A/ºC]
k_v	Temperature coefficient of V_{OC} [V/ºC]
m	By pass diode ideality factor
m^{DDER}, n^{DDER}	Droop coefficients of a DDER
$m^{\mathrm{DRS}}, n^{\mathrm{DRS}}$	Droop coefficients of droop regulated system
$N_{bus}, N_{DDER},$ N_{load}, N_{NDER}	Number of buses, DDERs, loads and NDERs in the microgrid
$N_{\mathrm{bus}}, N_{\mathrm{exp}}$	Number of buses and experts
N_{cell}	Number of cells connected in PV module
nl	Diode ideality factor [between 0 and 1]
OF_{BSS}	Objective function of the cost of battery energy storage systems
OF_{cont}	Desirable contributions cost
OF_{curt}	Objective function of curtailing non-dispatchable distributed energy resource/load
OF_{DG}	Objective function of diesel generator cost
OF_{loss}	Tie line power loss cost
OF_{oper}	Operational cost
OF_{tech}	Technical cost

OF_{trans}	Power import/export cost
P_{cap}^{BSS}	Nominal capacity of BSS
P_C	Expected output power at cloudy condition
P^{DDER}, Q^{DDER}	Active and reactive power of DDER
P_R	Expected output power at rainy condition
P_X	Expected output power at sunny condition
q	Charge on electron [Col]
$P_{cap}^{DG}, P_{LB}^{DG}, Q^{DG}$	Nominal capacity, minimum loading and reactive power of DG
$P_{cap}^{load}, P^{load},$ $Q^{load}, P_{shed}^{load}$	Nominal active power of load, active and reactive power consumed by the load, and the level of load-shedding
P^{loss}, $(P^{loss})^{max}$	Power loss in lines and its maximum
$P^{NDER}, P_{curt}^{NDER}$	Output power of NDERs and its curtailed level
P^{nom}, Q^{nom}	Active and reactive power consumed by the load at nominal frequency
P_{cap}^{wind}, P^{wind}	Nominal and active power of wind-based NDER
P_{KE}	Power harnessed by wind turbines because of the wind's kinetic energy
P_{mech}	Wind turbine's input mechanical power
P_{pv}	Output power of photovoltaic based NDERs
$P_{\text{wind}}, P_{\text{wind}}^{\max}$	Nominal and maximum power from wind based NDERs
P^{trans}	Power transacted between microgrids
$Q_k^{\text{DG}}, Q^{\text{load}}$	Reactive power of diesel generator, load
q_{step}	Blade pitch of the gearbox
$Ratio^{DDER}$	Ratio of power supplied by each DDER

R_s	Cell series resistance [Ω]
R_{sh}	Cell shunt resistance [Ω]
S	Shading factor
$S^{BSS}, S^{DDER}, S^{load},$ S^{line}, S^{NDER}	Apparent power of BSS, DDER, load, line and NDER
$SoC, SoC^{min},$ SoC^{max}	SoC and its minimum and maximum values
T	Cell temperature [ºC]
$Time$	Time period
T_{amb}	Ambient Temperature ($20 < T_{amb} < 48$°C)
T_O	Nominal operating temperature (25ºC)
v	Wind speed
V_d	Diode voltage [V]
$\|V\|, V^{min}, V^{max},$ $V^{nom}, \Delta V$	Voltage magnitude and its lower, upper, nominal values and its deviation from nominal value
V_{mpp}	Voltage at maximum power point [V]
V_{OC}	Open Circuit voltage [V]
V_x	Array voltage [V]
Y^{bus}	Y-bus of the network
w	Weighting

Chapter 1. Introduction

Traditionally, electric power-based companies have been vertically integrated and one company has controlled the generation, transmission and distribution facilities. However, in recent years, power companies have gone through a series of restructures which have given rise to independent generation, distribution and transmission authorities resulting in the emergence of market models. Although these companies are playing their role in maintaining the balance between supply and demand, but majority of countries around the world have experienced a significant increase in renewable power generation and distributed energy resources, which is predicted to rise in the coming future years [1-2]. To cope up with this situation, new power supply models have emerged and the role of renewables needs to be managed. Customers are now becoming prosumers. Microgrid technology has emerged in the last decade, as one of the rapidly growing electricity provision for both remote areas and urban distribution, providing significant benefits to customers and distribution network operators. In this thesis the optimisation of microgrids and microgrid clusters is carried out for both islanded and grid connected modes.

1.1 Microgrid

Microgrid, by definition, is a group of interconnected, distributed energy resources and loads with definite technical boundaries which act as a single controllable entity, as presented in Fig 1.1.

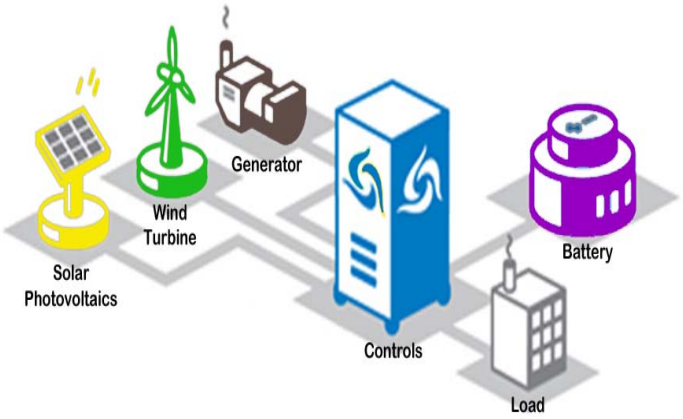

Fig 1.1 An overview of generation and demand in a microgrid.

The concept of microgrids was introduced by Thomson Edison in 1882, when his company installed 50 DC-microgrids during four years, but the massive utility grids with large centralised power plants faded them away [3]. In recent years this microgrid technology is catching attention because of its several benefits. Some advantages are listed in Table 1.1.

Microgrids are well known for their independent handling of demand management problems. Maintaining the supply and demand balance instantaneously, has always been a crucial issue, especially in recent years, resulting from the high rate of peak load growth. In the traditional way of the demand-supply match, generation conforms to load consumption however, this method is not always applicable and cost-effective.

1.2 Remote Areas

Electricity systems in remote area locations, usually work in the state of a standalone system. The concept of self-sufficient power systems, for remote area towns, arose from the fact that the expansion of the utility feeder over long distances, is not economical, considering that the load demand is that of only a few megawatts [4]. The difficulty to extend the utility grids in remote areas result in the use of independent diesel generators for the supply of

Table 1.1. Benefits of microgrid.

Value Proposition	Explanation
Reliability	• Off-grid capability for grid outages • Ensure load prioritisation with essential and non-essential loads • Management of synchronisation and re-synchronisation • Monitoring of energy reserves • Rapid resolution of issues
Efficiency	• Power quality • Optimal dispatching and unit commitment • Managing of intermittent energy sources • Ease of maintenance and operation
Sustainability	• Control of system variables like cost, revenue, emissions etc. • Possibility to incorporate software models for control purpose
Security	• Resilient to natural disasters and provide rapid restoration

electricity. However, the cost of fuel has a negative impact on the economic development of these regions [5]. The natural provision of renewable energy sources in remote locations can solve the power supply problems when used alongside diesel generator. The inclusion of renewables inclusion result in only the maintainace cost but main problem is to look on the cost of fuelling and transporting this fuel for the diesel denerators, creates another problem. [6-8]. Therefore, with increased interest in the concept of microgrid technology, for remote locations, many problems have arisen and a variety of solutions have been

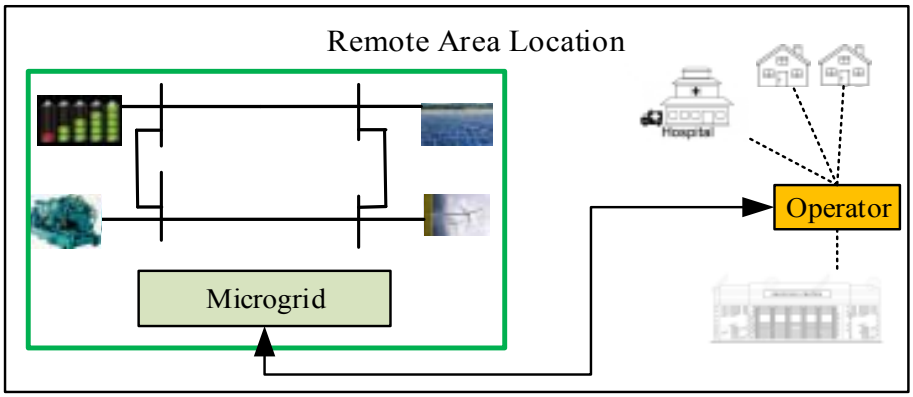

Fig 1.2 Schematic diagram for the remote area location with microgrid.

proposed by microgrid developers and researchers [9-11]. In previous research, it has been indicated that the main architecture of the proposed microgrid has been hybrid in nature, in that the microgrid includes storage systems with renewables, However they are usually intermittent by nature. which can often increase load management problems [12]. A schemetic diagram ,of a remote area location with a microgrid, is presented in Fig. 1.2.

1.3 Research Motivation

Cost management research, has so far focused mainly on microgrids, with less attention given to the unpredictable nature of the distributed resources of generation, which leads to crucial problems in the area of the transmission and distribution, such as the creation of a demand-supply imbalance and a cold load pick up. The main objectives of this research are to firstly examine the operation of microgrids, specifically in cases of emergency situations, in which overloading and excessive generation, occurs and secondly identify appropriate strategies for cost minimisation.

On the other hand, an innovative stochastic based power system is proposed for microgrid applications. Practical photovoltaic and wind generators are designed and simulated in Matlab.

Their numerical analysis is then carried out by the Monte Carlo principle. The load pattern is randomly generated and included within the planning horizon. The minimal optimum values of dispatchable energy sources are identified using a specialised control technique. Thus attempts are made to create a realistic scenario for analysis, under the specified time series sequence.

The above studies are provided in the research literature and correlate with many open research topics, which can be resolved. Achieving the successful operation of microgrids, in remote area locations. The problems that require resolution include:

- inaccessibility to energy services and chronic power shortages in remote areas,
- the need to build a sustainable and robust power transmission and distribution system in remote area towns,
- power systems for remote locations should be reliable, intelligent and environment friendly,
- the cost of fuel for diesel generators and their transportation to long distances,
- optimal operation of microgrids in remote locations by giving consideration to economic factors,
- successful emergency situation handling, for these off-grid areas, and last but not the least,
- minimise costs of operation without the deviation of the technical factors.

1.4 Research Objectives

The primary goal of this research is to develop an optimisation approach for the suitable operation of standalone and microgrid clusters. Thereby, the specific research objectives are:

Objective 1: Developing an optimisation-based controller, for remote area microgrids, to

address the emergencies.

Objective 2: Improving the techniques used to regulate the voltage magnitude and frequency in a standalone microgrid at least cost.

Objective 3: Considering various system features such as the control of resources, the life loss value of available storage systems, power contribution from neighbouring microgrids, and the power loss in tie lines.

Objective 4: Evaluating the interplay, between different operators of the optimisation solver, used in solving the considered problem.

Objective 5: Proposing a new market model to enable optimization of clustered microgrids connected by distribution networks in conditions of energy balance, and emergency situations.

1.5 Scope of the Thesis

This research aims to determine the best strategy for the safe and cost-effective operation, of the designed microgrid system, working both in the autonomous and grid connected mode, with optimum value of its sources. Along with the uncertain nature of solar, wind and load demands, to achieve the best possible solution, for the stable operation of the designed microgrid.

1.6 Significance of Research

Microgrid is considered to be the future of power distribution networks, with the benefit of lower cost, self-healing, minimised power losses and maximum savings of energy, higher reliability and appreciable power generation ratio, from renewable based energy resources. This research focuses on achieving the lowest cost of operation within acceptable limits of technical factors, as well as the usage of a battery storage system so as to reduce the uncertainty

of the generation of renewable energy. The main contribution of this research, is to address the emergency situation which can occur within hybrid power systems used for remote towns. This work also aims for a pollution free environment by reducing the emission factors. The aforementioned factors are explained in existing literature within limited publications. Therefore, an additional aim of this research, is to address the significant gap of available research, by addressing particular research issues and then solving them through the use of optimisation techniques.

1.7 Dissertation Structure

The remainder of this thesis is organised as follows.

- **Chapter 2** describes a brief literature review of the existing, related research, on the optimisation of microgrids. This chapter provides an evaluation and insight of the microgrids operation methods, with different sources of electricity generation. It also explains the different existing methods within the field of microgrid control and optimisation that are applicable to the remote location microgrids.
- **Chapter 3** defines the main challenges and research issues which needs to be solved so as to achieve the goal of the safe and economic operation of microgrids.
- **Chapter 4** proposes the models which are used to develop the main framework of the microgrid, in addition to the analysis methods which are required for the safe operation and optimisation solver.
- In **Chapter 5**, the optimisation solver, which is used to determine the most suitable control variables of an optimisation problem, for a standalone microgrid are discussed, while considering the scaling operator and its various functions inside the solver.

- **Chapter 6** proposes an optimisation based controller, which operates under a sequential-based multilayer action scheme, to address the emergencies of overloading and excessive generation in clusters of microgrids.
- **Chapter 7** proposes a market model to enable optimization of clustered but sparse microgrids, connected by distribution networks in conditions of energy balance, and emergency situations such as overloading or over-generation, within the cluster.
- **Chapter 8** briefly explains the completed dissertation work, by highlighting the goals achieved and explaining the advantages of the proposed phenomenon. It also identifies the key points that can provide pathways for future work in this area.

Chapter 2. Literature Review

2.1 Introduction

A microgrid is usually referred to as a cluster of Distributed Energy Resources (DERs) and loads within close proximity and connected with each other through a network [13]. It is believed to be a very good and advantageous power system, for electricity supply, especially for the edge of grid areas and remote locations. This is because it can operate in the capacity of standalone, as well as grid-connected modes [14]. From the perspective of energy generation economics hybrid microgrids that are composed of some dispatchable units, like diesel generators or gas opertaed synchronous generators, as well as non-dispatchable renewable sources, for instance solar and wind, prove to be very beneficial for the microgrid owners[15]. Such microgrids usually have energy storage systems, such as batteries, to become self-adequate during the intermittencies of renewable sources.

Microgrids are growing in power industry as an essential part. For instance, [16] provides an insight to four types of microgrids which can be used in different situations while applying the same technology. First is known as costomer microgrids or true microgrids.which are operated from a single point of common coupling (PCC) and are self goverened in nature e.g. ship microgrids. Second type is Utility or community microgrids which involves a segment of the regulated utility grid, whereas virtual microgrids (commonly known as vgrids) is the third type in power industry. Vgrids have distributed energy resources (DERs) at multilpe site locations but they all are coordinated such that they can be presented as a single control entity

to the main grid. Lastly microgrids existing in remote areas are those which are not able to operated in a grid-connected mode and are reffered to as isolted power systems.

2.2 Microgrids in Remote Area Locations

Due to technical and geographical limitations, it is not always possible to extend the existing transmission and distribution lines to very remote and regional areas. Thereby, utilities usually build a local power generation and distribution network at such locations. As an example, with the exception of the towns on Australia's East Coast (these are supplied through the National Electricity Market (NEM)) and those few towns located in the South West (these are supplied through the South-West Interconnected System (SWIS)), most other towns in Australia's regional and remote areas, (in which almost 31% of the Australian population live), are supplied by local generators running on diesel or gas [17]. However, in addition to this type of generation being expensive, the fuel transportation is sometimes difficult because of roads' seasonal inaccessibility, and it pollutes the environment [18]. In addition to the lower reliability, the utilities also experience larger power losses due to long lines in those areas. This also results in high expenditure on supply, operation and maintenance, which are usually borne by the utilities. To reduce the overall cost of electricity generation, the utilities prefer to utilize renewable energy-based DERs and maximize their contribution to electricity generation [19-20]. These systems are usually designed to operate in isolation and be self-sufficient, they are often referred to as isolated microgrids. For example, the techno-economic analysis in [21], demonstrates that the local utility, can reduce its electricity supply cost by 70%, when the rural town of Laverton in Western Australia, is supplied by a group of renewable sources, along with smaller sized diesel generators. Likewise, [22] shows that the levelised cost of electricity generation, can be reduced by almost 50%, when a group of renewable energy resources are used to supply the electricity demand of Rottnest Island (18 km west of Australia's west coast)

which thereby increases the contribution of renewable energies by up to 75%.

2.3 Distributed Energy Resources (DERs)

New green energy policies are adopted in order to reduce global warming. This concept leads to the application of renewable energy sources which meet the increasing demand for electricity. This step also helps in lowering the greenhouse gas emissions. Amongst other existing renewable energy sources, Wind and Solar are easily available and naturally renewable sources of energy. The most beneficial feature of using Wind and Solar energies is the minimal costs required for their maintenance. Due to the above reasons Wind and Solar are considered to be the main building components of smart distribution networks, like microgrids. The levels of ambient temperature and solar irradiance, on top of the photovoltaic (PV) cells internal characteristics, are the main factors. These key points also affect the PV module's level of generated power output. Additionally, the clouds passing in the sky, which also pass over the solar cells, intermittently produce a shading effect. This will result in frequent intermittent increases and/or decreases, in the instantaneously generated output of power, which is produced by the PV/solar cells. Alternatively, wind based sources, are mainly effected by the speed of wind, the height of installation and the area location. Therefore ,intermittent renewable generation from Solar and Wind energies, can cause large voltage and frequency deviations, due to their unpredictable fluctuations in power output [23]. If renewable-based Non-Dispatchable DERs (NDERs) are coupled with appropriate power smoothing Battery Storage Systems (BSS), they will act as Dispatchable DERs (DDERs), such as Diesel Generators (DGs), which can effectively operate in a grid forming mode. For instance, they would be responsible for the control of voltage and frequency control in instances of modifications on consumer demand, using various techniques such as droop control [24-25].

2.4 Droop regulated control strategy

It is proposed that some modified droop control techniques (such as intelligent, adaptive, cost-based techniques) or optimisation-based controls, could improve the microgrid performance and stability, as well as improve the power-sharing amongst the DDERs [26-29].If the proper sharing of active and reactive power from DDERs is determined properly, it can minimise the overall microgrid operation costs.(e.g. Using an event-based demand response management technique [30], including smart loads in the microgrid [31], and using an optimal selection of droop parameters [32]). The abovementioned methods are applied for a microgrid which is operating under a decentralised control (i.e., without a microgrid secondary controller), and thereby, the microgrid frequency, is the only way for a DDER to get information about the status of the microgrid. On the other hand, [33-35] highlights the design and performance of the microgrid secondary controller, while [36], and describes the combination of the primary controllers of DDERs, with microgrid secondary controllers, to solve the optimal power-sharing problem amongst DDERs. In [37], a microgrid secondary controller-based technique, has been proposed so as to optimize the DDERs set-points and to minimise the power losses and fuel costs of the microgrid. On the other hand, instead of modifying the output power of DDERs, other alternatives have been suggested separately in [38-41], such as load-shedding, renewable curtailment, and charging/discharging control of the BSS.

2.5 Standalone Microgrids in Remote Areas

Microgrids are commonly known as standalone remote area power systems with a hybrid nature. They are famous for providing electricity at affordable prices in remote area locations. To achieve economical and reliable operation of the hybrid systems, several considerations are

desirable: the burning of minimum fossil fuel, the maximum penetration of renewable sources, minimum power losses, along with effective management and control of the voltage and frequency required to achieve a maximum balance of power. Considering the required criteria, which includes the reduced cost of energy generation, increased penetration level of renewables, and the enhanced active control of the system, it is apparent that central or distributed, optimising-based control mechanisms, are required to guarantee a better performance from standalone microgrids [42]. An optimal standalone microgrid is the one which has the minimum of imbalance between generation and demand (e.g., the frequency and voltage of microgrids are kept under permissible, predefined limits) while operating at the least cost for the owner.

2.6 Provisionally Coupled Microgrids in Remote Areas

Due to the incentives that the governments are currently providing to attract private investors who are willing to build and operate renewable energy sources [43], it is highly probable that a large remote area, can accommodate multiple isolated microgrids, each with it's own individual operator (owner) [43]. In such situations, to improve the reliability, resiliency and self-healing of isolated microgrids existing in remote areas, it is suggested in [44-46], that the microgrids have some sort of physical connection to each other, so as to support each other during emergencies. Therefore, [47] suggests that during emergency situations, these adjacent, individually operating isolated microgrids, are temporarily coupled. These emergency situations can be power shortfalls, excessive generation and short-circuit faults. The management of the microgrid restoration process, after experiencing faults, is explained in [48] while [49-50] identifies those microgrid clusters with self-healing capabilities. The main aim of this research is the enhancement of the microgrids resilience against extensive overloading or events of excessive generation. The idea of coupled

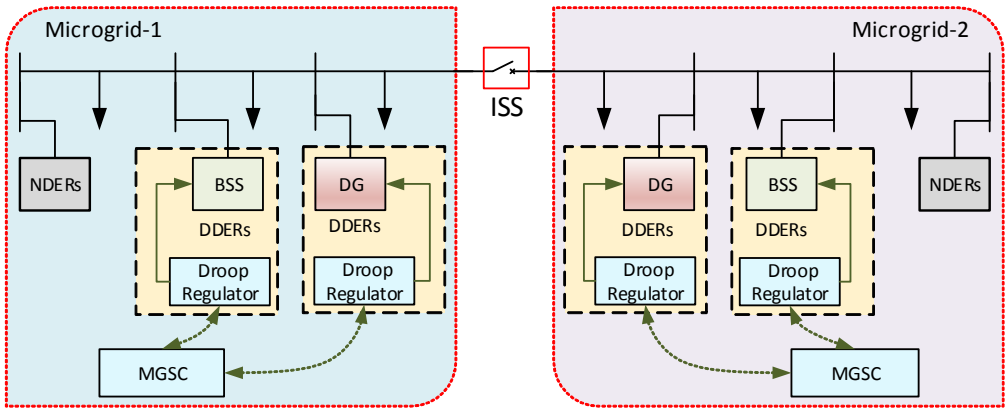

Fig 2.1 Two neighbouring microgrids, that can form a coupled microgrid, through a tie-line and ISS.

microgrids, has been introduced, with the above objectives in mind. Under this concept, two or more remote area neighbouring microgrids, can provisionally interconnect with each other, with the main aim being to provide support during sudden emergency situations [51]. For example the network in Fig. 2.1, presents two neighbouring microgrids within a remote area, connected through a tie-line and an Interconnecting Static Switch (ISS). In this scenario, the microgrid experiencing the emergency is referred to as the problem microgrid and can be provisionally supported by an available and healthy microgrid.

2.7 Energy Management in Microgrid Clusters using the Distribution Network Operator (DNO)

The structure of a modern power system may consist of multiple microgrids and Distribution Network Operators (DNOs). At this point, it is worth mentioning, that each microgrid and distribution network operator, will act as autonomous entities within the distribution system. Ref. [52-53], highlights the challenges of operating the power system, which are due to the variable NDERs generation coordination, amongst different microgrids

and between the DNO and the microgrid, as well as difficulty in optimal energy management of both entities.

The coordinated control for energy management in microgrids and DNOs, can be described as a three level, hierarchical system. The system starts with the primary local area droop based control of DERs in microgrids [54-55], followed by the secondary control of the remote area multi-microgrid [56-58] and finally, the tertiary control for optimal power flow, management [59-60]. In this hierarchical system, the third level, is important from the economic perspective of microgrid operation, which is the main focus of this research. For this purpose, a communication system is essential to ensure the transfer of data from microgrids to the DNO, from the DNO to the market and the DNO to the tertiary controller for the required action. Ref. [61-62], highlights the communication system required for the modern existing implementation of controls in microgrids system. By utilizing the communication protocols, it is possible to develop a microgrid system which involves the participation of DNOs and market participants respectively. For example, [63] proposed a multi-agent based, optimal energy management of clustered microgrids with the integration of different market entities. The coordinated operation of DNOs and clustered microgrids, is achieved by using a hierarchal, deterministic, optimization algorithm without the involvement of the market [64]. In [65], a decentralized Markov Decision Process, is used to solve the optimal control problem of clustered microgrids. The main aim was to minimize the cost of the operation of clustered microgrids, while [66-67], allows for the impact of customer participation upon the demand response of clustered microgrids. In this particular situation, optimization was achieved by MAS-based power management control. Similarly, [68] reveals that another way to control clustered microgrid operation costs is by using the cooperative power dispatching algorithm. To this end, the above references have highlighted the optimal control of clustered microgrids, by not using all features at one time. Therefore, the above studies indicate that optimal power

flow can be achieved by using either the DNO, the market, or employing the power sharing mechanism of neighbouring Microgrids.

2.8 Emergency Situations Handling

The coupling of the nearby microgrids is done by using a transformative architecture and is explained in [69]. The key focus here, is to upgrade the resiliency of the considered system, during fault conditions. In [70], a decision-making-based approach, is proposed, with the aim of identifying an overloaded problem microgrid, which can be coupled with the most suitable and healthy microgrid(s), that is available within the network. Within the coupling process, certain criteria, such as electricity cost, available surplus power, distance between the neighbouring microgrids and reliability, along with voltage/frequency deviation in the coupled microgrid, are especially taken into consideration. Ref. [71], demonstrates the technique which can be used to identify the overloading conditions experienced by a problem microgrid. Ref. [71], also provides the techniques used to identify the neighbouring healthy microgrid present, that has the availability of excess power. Interactive control to guarantee adequate load sharing in coupled microgrids is described in [72]. Ref. [73], highlights the effective operation of coupled microgrids by using DERs whereas [74], examines the powerful security management for the dynamic working of the coupled microgrids. The useful coordination of the DERs of the microgrids that is present in coupling mode, is also investigated in [75]. Ref. [76], examines the reliability factor of a coupled microgrid and indicates that their core aspects are their small signal stability, along with the controllability of the current and voltage [77-79]. Ref. [80-81] present a technique to coordinate the operation of BSS in microgrids, along with their provisional coupling. Moreover, back-to-back converters [82] or ISSs [35], can also be helpful in accomplishing the coupling of the adjacent microgrids. The key focus is to overcome the emergency situations by interconnecting a microgrid to any existing microgrid (not necessarily

an adjacent microgrid). However in doing this, it is necessary that a general physical link is available, which can act as a power exchange highway. Ref. [83-84] presents an optimisation-based technique to coordinate the microgrids whilst [85-86], discusses the calculation of achieving the least operation costs through utilising different optimisation techniques for coupled microgrids. In [87-88], it is shown that coupled microgrids can work in a cooperative mode, whilst. Providing robust distributed control, in cases where there is a high penetration of the NDERs in the network.

2.9 Optimisation Techniques for microgrids

A detailed literature review reveals that many heuristic optimisation techniques are described in the literature to solve the constrained problems, which are nonlinear. These techniques particularly focus on microgrids and also define the operational settings of the DDERs and NDERs. Ref. [89] has formulated the optimisation problem, based on the modifications in consumer demand and NDERs. This reference then uses an imperialist competitive algorithm to calculate the cost function. Ref. [90-91] has included the sizing and operational analysis of a standalone hybrid microgrid, in the formulated objective (fitness) function, which is then resolved by an ant colony, and a multi-objective algorithm. Ref. [92] overcomes the stability problem of a hybrid microgrid, with the harmony search-based hybrid firefly solver. Ref. [93-94] have employed a particle swarm-based solver to search for the setting of microgrid's control parameters. In these research works, overall power generation costs for the microgrid owner, fuel consumption by DGs, BSS life cycle characteristics and power losses, are the major factors in their formulated fitness functions [95-96]. In [97], a genetic algorithm is applied simultaneously, with the mixed integer linear programming to solve a two-stage optimisation problem, for a multi-microgrid network considering utility's profits and consumer satisfaction. On the other hand, [98] uses non-dominant sorting genetic

algorithm-II, which is a fast and elitist type of genetic algorithm, used to solve a multi-objective optimisation problem of microgrids, by controlling the load imbalance in the microgrid. In a similar way, various types of genetic algorithm, such as the real coded genetic algorithm, hybrid-Fuzzy genetic algorithm, and floating point genetic algorithm are used in [99-101] to solve the optimisation problem for standalone microgrids and power systems. In contrary to most genetic algorithm-based techniques that consider binary numbers in their genes and chromosomes, a floating-point number is used in each gene and chromosome of a floating point genetic algorithm [102]. Thus, floating point genetic algorithms have more advantages than binary genetic algorithms. The main reasons are more efficiency, less memory utilisation, and increased precision. Moreover, different operators can be utilised for greater flexibility [103].

The operation of a genetic algorithm -based solver, can be improved by considering the scaling operator, in addition to the traditionally used crossover and mutation operators [104]. The scaling operator can be applied in the form of a different function. Using an appropriate scaling function, can reduce the problem complexity and speed up the identification of a solution [105].

2.10 Optimisation Problem Formulation

Alternatively, some studies have aimed to coordinate the power exchange amongst microgrids, load curtailment and control of the power of conventional generators. As an example, [106] has considered DGs fuel consumption and emission cost, along with the power exchange with the utility grid, in the formulated objective function. Ref. [107] discusses the impact of load curtailment in microgrids, by considering the sensitivities in nodal power injection and the probabilistic uncertainties of loads and renewable sources. To this end, the cost of load curtailment, as well as the expense/revenue of exchanging power between the microgrid and a utility feeder, is considered. In these studies, the main objectives are to

maximize the footprint of renewable energies in supplying the demand and minimizing the contribution of conventional generators. However, the curtailment of renewable energy resources, is not considered, which is essential in the case of over generation.

The voltage rise problem within microgrids due to renewable energy-based DERs, is solved in [108], by curtailing their output power, using droop control. On the other hand, [109] employs an optimisation technique to maximize the lifetime characteristics of BSSs within microgrids, when compensating the variabilities of loads and renewable sources, while

Table 2.1. Comparison of the main features of the considered cost minimisation techniques, Identified in the literature and this research.

Ref.	Solver	Considered criteria in OF formulation										
		DG Fuel	DG Emission	Voltage deviation	Frequency deviation	BSS life loss	Power loss	Transaction with microgrids	NDERs curtailment	Load-shedding	Spinning reserve	Renewable penetration
[106]	[1]TLBO	✓	✓	×	×	×	×	✓	×	×	×	×
[107]	[2]SWT-PSO	✓	✓	×	×	×	×	✓	×	✓	×	×
[108]	[3]GFC	×	×	×	×	×	✓	✓	✓	×	×	×
[109]	[4]NSGA-II	✓	×	×	×	✓	×	×	✓	×	×	×
[110]	[5]NBT	×	×	×	×	✓	×	✓	×	✓	×	×
[111]	[6]SCPDA	✓	×	×	×	×	×	✓	×	×	×	×
[112]	[7]OPFA	✓	×	×	×	✓	✓	✓	×	×	×	×
[113]	[8]PL & ED	✓	×	×	×	×	×	✓	×	×	×	×
This work	Genetic algorithm	✓	✓	✓	✓	✓	✓	✓	✓	✓	✓	✓

[1]Teaching-learning based optimisation, [2]Stochastic weight trade-off particle swarm optimisation, [3]Grid forming control, [4]Non-dominated sorting Genetic Algorithm-II, [5]Nash bargaining theory, [6] Statistical cooperative power dispatching Algorithm, [7]Optimal power flow algorithm, [8]Priority list and economic dispatch.

minimizing the power generation cost of DGs. Alternatively, a bargaining technique is used in [110] ,to facilitate a proactive energy trading and fair benefit sharing, amongst remote area, interconnected microgrids, in which the main considered criterion, is the minimisation of the total operational cost. In a similar way, [111] applies demand management, in remote area microgrids, using a cooperative power dispatching algorithm, for the minimisation of a microgrid's operational cost, whilst satisfying the load demand. Ref. [112-113] has formulated an economic dispatch problem, which aims at minimizing the power loss in addition to the costs of fuel consumption, external power sharing and BSSs. A comparison of the abovementioned studies are summarised in Table 1.1. Also, the existing industrial processors by Intel® [114], National Instruments™ [115] and Analog Devices™ [116] can be effectively used, when implementing the proposed optimisation control, as they satisfy the required speed.

2.11 Research Aims in Coordination of Conducted Literature Review

In previous sections of this chapter, an in-depth literature survey related to microgrid operations has been conducted. DERs modelling and controlling, optimisation techniques, have been utilised in previous research, to develop the reliability and consistency of remote area microgrid networks. Following the survey, some technical challenges are identified, which still need significant attention. It should be noted that the technical challenges for the design of microgrids and the implementation of the optimisation technique, is not discussed in the following chapters. However, the review of the available research, which has been discussed previously, has given rise to the identification of a number of problems. These problems will be addressed, with the aim of:

- Defining and characterizing the technical parameters for modelling DERs,
- Setting up a suitable power flow study of the microgrids, so that droop control of DDERs, can be attained along with the intermittent nature of NDERs,

- Ensuring the charging and discharging of BSS, under certain operational conditions of microgrids,
- Reducing the cost of fuel of DGs, to make the system more economical,
- Maintaining the optimisation problem formulations consistency, within the required technical restrictions,
- Effectively determining the emergency situation of overloading and/or excessive generation in problem and troubled microgrids,
- Including certain technical impacts like frequency and voltage deviation, that affect the performance of microgrids, and
- Overcoming the emergency situation of overloading and excessive generation, in remote area clustered microgrids,
- Choosing the renewable curtailment for NDERs and non-essential load shedding, in emergency situations in problem microgrids,
- Developing an effective and efficient optimisation problem solver, for reaching the ultimate goal, of cost minimisation,
- Ensuring the interplay of the optimisation solver operators, for optimal solutions,
- Developing an effective supervisor control system, which can react instantly for the emergency situation handling, of remote area microgrids, and
- Proposing a new market model for optimised operation of trouble microgrids by inclusion of distribution network operator.

2.12 Summary

In this chapter, a state-of-the-art review, has been carried out, for the operation of microgrids in remote areas, wheather in they are in a standalone or coupled condition. This chapter has also discussed the literature available in the field of DERs modelling ,and other

aspects which include the optimisation problem formulation and the cost analysis, to manage an economical distribution system within emergency situations. The existing work particularly intimates that a vast amount of literature is available on the modelling of DERs and then controlling the DDERs using the droop regulated strategies. Some progress has been made in identifying the emergency situations which impact the performance of microgrids, however, comprehensive discussion about many of key research issues related to this concept, have not been fully addressed by the existing research and thus requires further improvement. Based on the presented literature review, the next coming chapters will explicitly address and outline the above research issues.

Chapter 3. The Proposed Technique

3.1 Introduction

A microgrid can function as a single controllable system, within the grid-connected or the standalone operation modes. The transition from the grid-connected mode to the standalone mode, can result in a microgrids' excessive generation or demand, which must be spilled or curtailed. To achieve the normal operation of the standalone microgrids, several challenges have been identified, which can be addressed by outlining the specific issues arising and identifying appropriate solutions. To address these issues, an optimisation-based control, has been chosen for the purpose of optimising the microgrid operations, accounting for DERs (stochastic generation and time-varying demand), as well as determining the microgrids operation constrains. The objective is to minimise the operational costs, taking into consideration, the classical generation capacities and the power exchange capacity with the neighbours, as well the operational constraints.

3.2 Challenges of this Research

Formal definition of the main challenges and core concepts are explained in this segment of chapter. The definitions and concepts will be used to explain, elaborate and characterize the key research issues in this dissertation which will be addressed. Table 3.1 precisely represents, the key challenges which will appear whilst dealing with the proposed methodology.

Table 3.1 Identified challenges within this research

Challenges	Brief description
Cost	Management of price volatility, by decreasing the cost of energy
Power Quality	Increasing power quality and reliability
Resiliency and security	Improving the power delivery, system's security and resiliency, by enhancing the availability of power resources
Environment protection	Managing the unpredictable nature of renewable energy sources and enhancing the integration, of environmentally friendly and efficient technologies
Service quality levels	Organizing the different service quality for the customers, which are present at various price points, within the network
Difference in Sources Nature	In configuration both types of NDERs and DDERs are involved with different nature in terms of their control.
Dynamic Response of sources	The DERs response can be inertial (i.e. slower) or non-inertial (i.e. faster).
Islanded microgrids	If the proposed topology, is detached from the utility, then the demand side of management, becomes a critical issue.
Operational control	During island mode the generated power of each DG unit, must be carefully controlled, to ensure reliable power distribution and modular operation.
Voltage control	Maximum and minimum voltage magnitude, of all of the buses involved in the structure of the microgrid

Frequency control	Frequency should not exceed/drop past a certain limit
Effective Response	Effective and instantaneous response of DERs, to the sudden change, on the demand side
Environmental Factors	The efficient performance of renewable sources, majorly depends upon natural resources like clouds, solar irradiance, and the average wind speed and rain etc.
Power loss estimation	For determination of proposed model efficiency, power loss estimation, is necessary
Consumer Satisfaction	Consumers on the users end, should be satisfied with both the cost and service quality
Optimisation	An act, process, or methodology of making the modelled network (in terms of low cost) as fully perfect, functional, or effective as possible; specifically: the mathematical procedures (such as finding the minimum of a cost function), involved in the problem formulation.
Objective Function	The formulated cost function for the microgrid network that is required to be minimised.
Constraints	The limitations or boundaries applied for the operation of the microgrid and they should be satisfied for the microgrid network along with feasible solution.
Power Flow Analysis	Numerical analysis of the modelled microgrid, to establish the flow of power in the lines, using the single line diagram and per unit quantities.

To address all of these challenges, it is necessary to outline the main issues, which can be addressed in appropriate stages, so as to reach the desired outcomes.

3.3 Research Issues

Applying the above knowledge and addressing these challenges has led to the identification of four problems. For all four problems, it is important to characterize the currently available technical problems and the existing methods, inherent in these solutions. These specialised methods would help to frame the premise of the proposed research problems, e.g. how they can be addressed and what will be the initial required in order to find a new solution? This section places emphasis on the research issues that should be elaborated upon, to attain any innovative outcomes. After the issues have been identified the target will be to seek solutions. This will be done in Chapter 4 onwards, where the focus will be on the research issues identified and also to address the research objectives described earlier in Chapter 1.

3.3.1 Research Issue 1

This section will explore how to identify the key parameters for the modelling of DERs and then how to implement them within the microgrid, using a strategy which is cost-effective for operation purposes?

Based on the survey of the current approaches available in the literature, about the modelling of the DERs, that has been discussed in Chapter 2, along with their characterisation

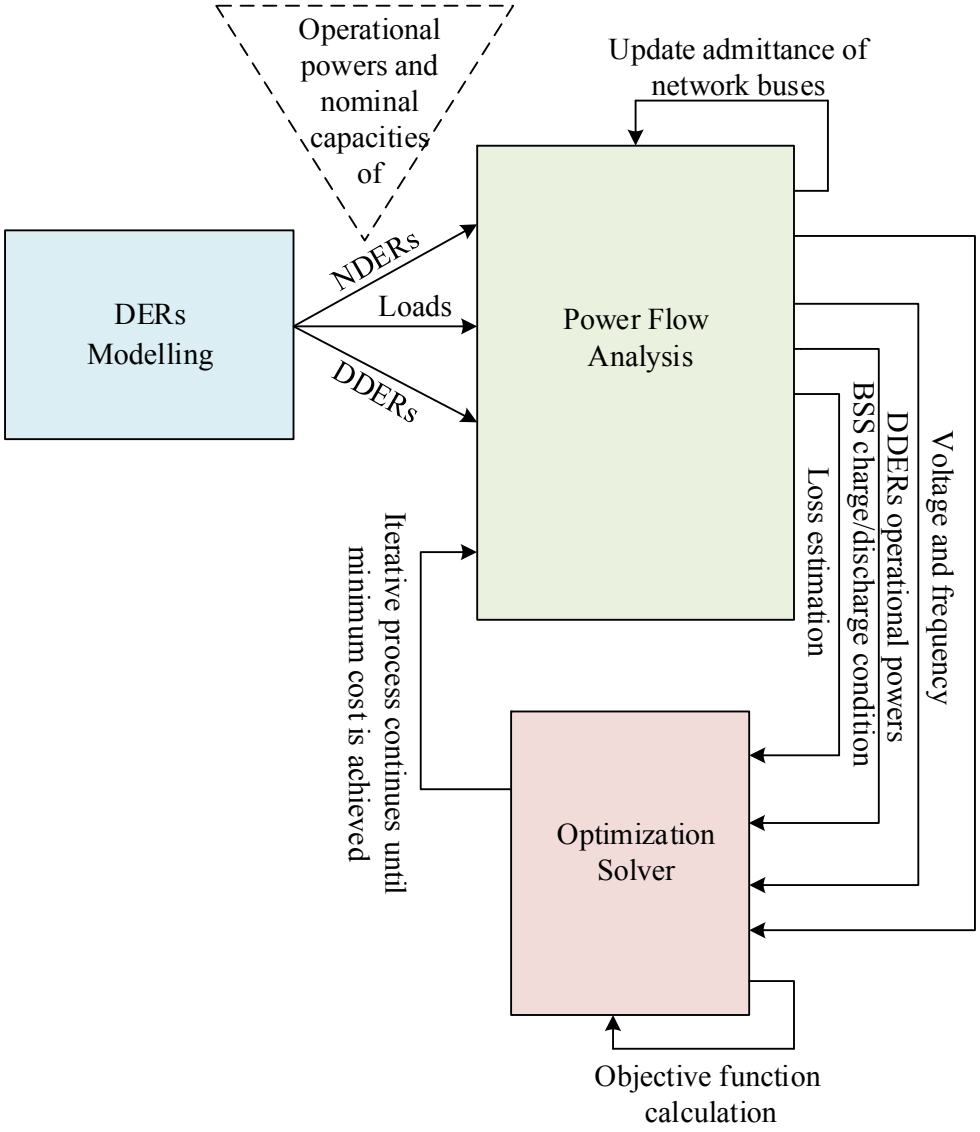

Fig 3.1 Key concept and information flow required for addressing Research Issue 1.

of the most vital parameters for designing NDERs and DDERs, but achieving the cost-effective operation of microgrid need critical inner view about the power flow analysis for the modelled load demand. Furthermore, the existing literature provides evidence for the power flow analysis, but very limited information is available on the calculation of the technical impacts such as the voltage and frequency of the microgrid network. Hence, the following questions are need addressing.

Research Question 1: What are the key factors involved in designing and determining the operational set points for DERs?

Research Question 2: What are the aspects related to reach through the safe and cost-effective operation of the microgrid?

The key factors involved in addressing this issue with defining and characterizing the most vital design and operational parameters, first a microgrid is designed with its DERs and loads, then the operational analysis will be based on the monitoring of the voltage and frequency which will finally lead to the formulation and implementation of the heuristic optimisation technique. This step by step procedure, is extensively elaborated in Chapter 4, while an overview of the issue is illustrated in Fig 3.1.

3.3.2 Research Issue 2

This section of the research will concentrate on how to develop an optimisation solver, which can be used to determine the most suitable control variables of an optimisation problem that is designed for the load balancing, of a standalone microgrid, whilst taking into account the influence of operators and their various functions within the solver? It is to be noted that this issue does not aim to compare the developed optimisation solver, e.g. the floating point genetic algorithm compared to other types of optimisation techniques that are available in the literature. The main objective is to conduct a detailed comparison of different scaling techniques when used for problem formulation and to illustrate their impact upon the optimisation outcome. To do so, the following research questions need to be considered:

Research Question 1: How to develop a technique to regulate the frequency in a standalone microgrid, using the formulated fitness function at the least cost in cases where there are sudden changes in loads?

Research Question 2: How to evaluate the interplay between different scaling techniques on an floating point genetic algorithm that are used in solving the considered fitness function?

The above research questions need to be addressed in an effective way. The methods adopted to answer the above questions will be presented in detail in Chapter 5. For addressing the above highlighted research issue, let us consider the network of Fig. 3.2, which shows a standalone remote area microgrid, composed of DGs, NDERs, BSSs and loads, operating under a microgrid secondary controller-based, centralised control. As the microgrid cannot be supported by any external entities (e.g., a utility feeder or a neighbouring microgrid), in the case of a sudden increase or decrease in demand, the microgrid's situation has to be handled by proper assessments taken of its control variables (e.g.., droop set-points of DDERs, power charge/discharge of BSSs, load-shedding, renewable curtailment of NDERs), using a suitable fitness function. A genetic algorithm-based solver, is developed to solve the formulated fitness function, as will be discussed in Chapter 5.

The NDERs are assumed to be renewable energy sources, with an intermittent nature. Due to their unpredictable output power, BSSs are used for power balancing in the microgrid, in the case of intermittencies. In comparison, DDERs are droop control based. The output power of NDERs is assumed to be controllable, based on the signal received from the microgrid secondary controller, to enable renewable curtailment. Similarly, the BSSs charging or discharging is controlled locally by a signal received from the microgrid secondary controller. The non-essential loads of the microgrid are assumed to be capable of being shedded, based on the command signal, from the microgrid secondary controller. To this end, a wireless communication system, based on IEEE 802.11n, is assumed to be available to transfer the optimal control variables from the microgrid secondary controller to the local controllers deployed at DDERs, NDERs, and non-essential loads [117-118] (see Fig. 3.2).

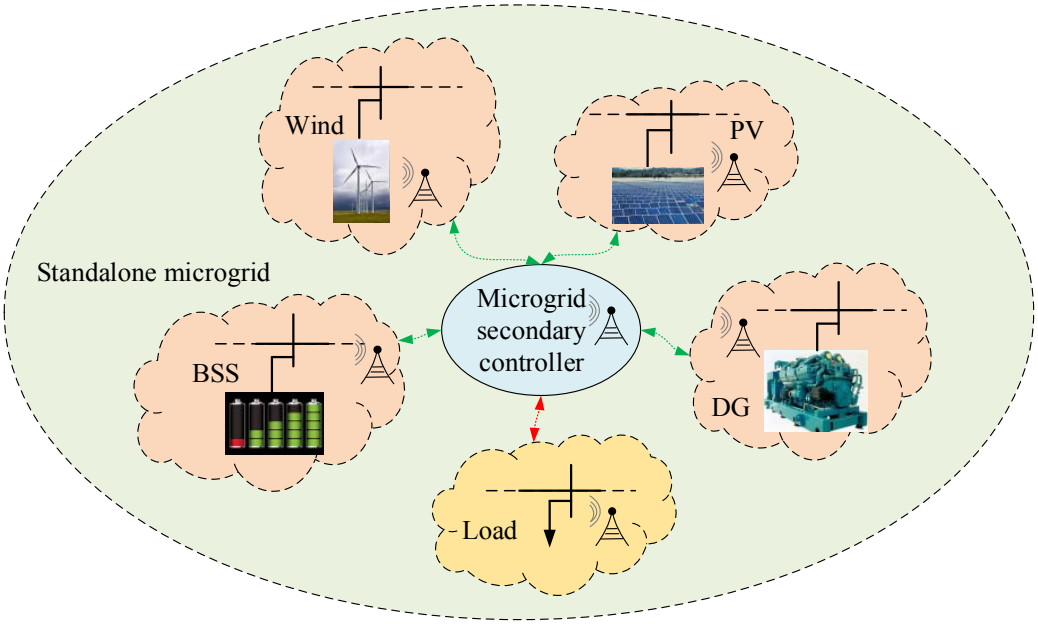

Fig 3.2 Typical illustration of a microgrid with the required communication links between the microgrid secondary controller and the local controllers.

As the microgrid is working in the standalone mode, monitoring its frequency and voltage is a critical issue, because any significant deviation in either of them, can lead to system instability. Therefore, the microgrid is desired to operate, with frequency and voltage, under permissible limits of $f_{nom} \pm f_x$ and$V_{nom} \pm V_x$. As far as the microgrid stays in the normal operating mode, no change is required. Whenever the microgrid observes a violation of either or both parameters, the microgrid secondary controller, immediately takes action to maintain them, within the desired limits. The main aim of the microgrid optimal control is to find out the most cost-effective solution, for the microgrid in cases where there may be sudden variations in demand or of the output of its NDERs.

Once the microgrid secondary controller identifies a significant voltage or frequency deviation, it determines the most suitable control variables required to maintain the demand supply balance, within the permissible limits of voltage and frequency. To this end, it uses the operational flowchart in Fig. 3.3. Identifying the most suitable options (which has the least,

overall fitness function), is achieved through an optimisation problem and solved by utilising the floating point-genetic algorithm approach, which will be discussed in Chapter 5.

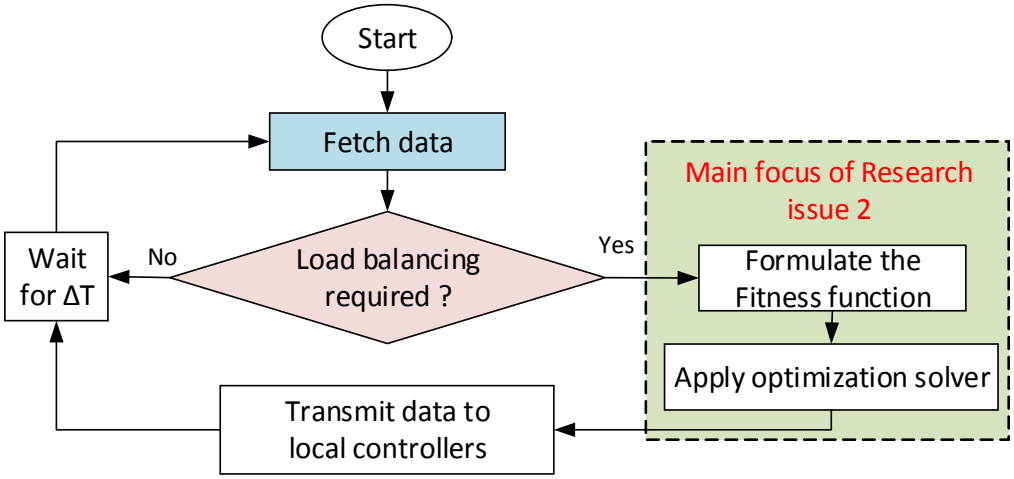

Fig 3.3 Flowchart for the proposed Research Issue 2, for load-balancing in the standalone microgrid.

3.3.3 Research Issue 3

Research Issue 3, is the question of how to develop a controller for provisionally coupled remote area microgrids, to coordinate the various options so as to yield the most suitable outcome at least cost, in situations where there sudden emergencies arise.

To achieve a centralised control, for multiple remote area microgrids, a supervisory technique is proposed. It is to be noted that the proposed supervisory emergency controller, considers the impact of voltage and/or frequency deviations on the power consumed by loads. A low-bandwidth communication is assumed to be available for the transmission of the required data, from the sensors and the microgrid secondary controller, to the supervisory emergency controller, as well as the decision variables from the supervisory emergency controller, to the microgrid secondary controller and relevant local controllers. In summary, the key advantages of using the proposed supervisory emergency controller, for these presented

research issues are:

- achieving an acceptable voltage and frequency deviation, in every microgrid of the remote area, after an emergency,
- achieving the operation of the microgrid operation for the least cost whilst also satisfying the technical constraints, and
- Minimising the rate of load-shedding and curtailment of the NDERs within the problem microgrids.

To address this problem of organising efficient working goals to cope with emergencies within the problem microgrids, the following research questions need to be considered:

Research Question 1: How to develop an optimisation-based supervisory, emergency controller for remote area problem microgrids, to address the emergencies? and,

Research Question 2: How to formulate the optimisation problem, whilst considering various system features such as control of DDERs and the curtailment of non-essential loads and NDERs, the life loss value of BSSs, spinning reserve, dependency of a microgrid to external microgrids, contribution of renewable sources and the power loss in tie lines? and,

Research Question 3: How to validate the effective operation of the proposed technique, using numerical analyses?

In exploration of this research issue, a multi-level supervisory emergency controller, that determines the answers to elaborates the above research questions, is proposed, and then comprehensively illustrated in Chapter 6. Therefore, to explain this research issue, a large remote area has been taken into consideration. So, for this purpose, let us consider Fig. 3.4 which illustrates two neighbouring microgrids that have physical links between each other, which can facilitate their temporary interconnection, during emergency conditions. A supervisory emergency controller, is considered to have the following responsibilities:

- identifying a problem microgrid,

- solving an optimisation problem, to select a suitable neighbouring healthy microgrid, to exchange power with and define the level of power transaction (import/export), and
- Transmitting the decision variables, to the microgrid secondary controller of each microgrid, of a coupled microgrid.
- receiving information, from the secondary controllers, of each microgrid,

Thus, the required communication links are illustrated schematically in Fig. 3.4.

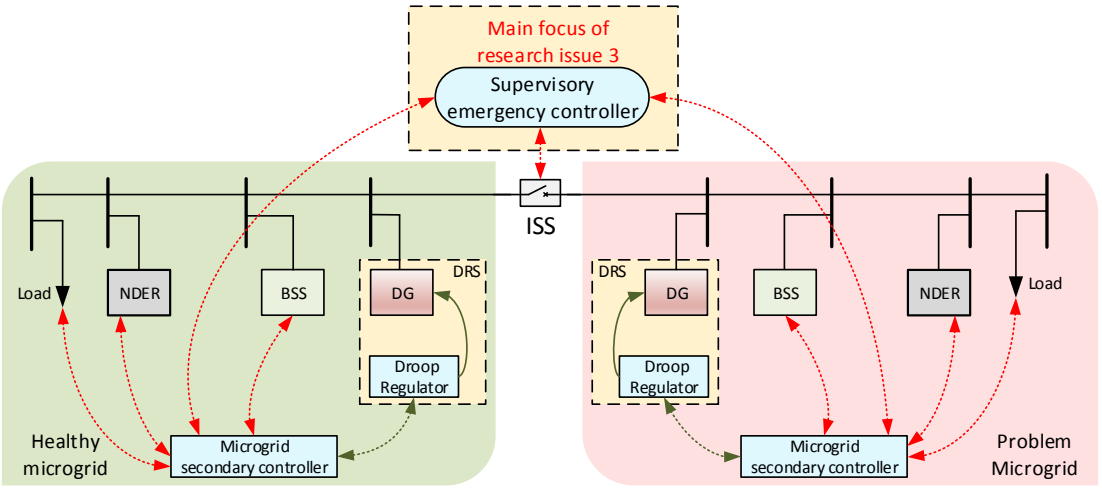

Fig 3.4 Two neighbouring microgrids, that can form a coupled microgrid,through a tie-line and the ISS, with the help of the developed supervisory emergency controller.

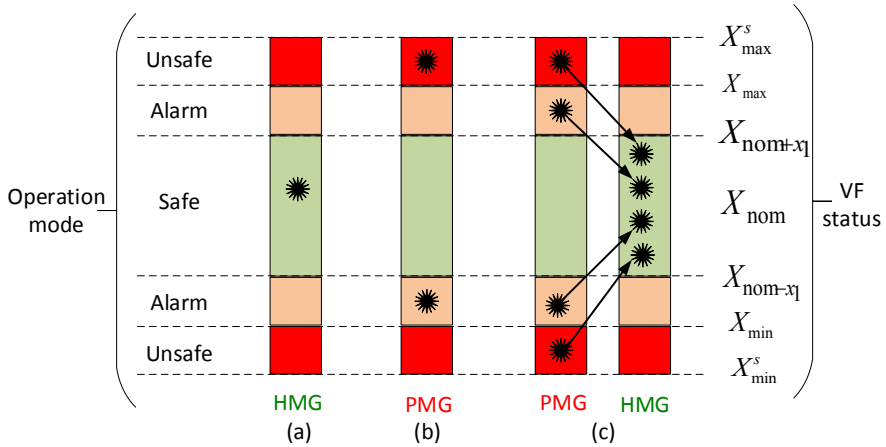

Fig 3.5 A healthy microgrid and a problem microgrid with successful and unsuccessful operations of secondary and supervisory emergency controller controllers (The operational state is denoted by✺)

To this end, a point-to-multi point, wireless communication technique, is required [119].Now, let us define both the healthy microgrid and the problem microgrid, depending upon their mode of operations (e.g. corresponding to operational VF limits) as illustrated in Fig. 3.5, where the *X* represents the VF. A healthy microgrid is the microgrid in which the frequency as well as all the bus voltages, lie in the safe mode of operation of Fig. 3.5a. However, the microgrid will be considered to be a problem microgrid if the frequency and/or the bus voltage jump into the alarm, or unsafe modes of operation (see Fig. 3.5b). In this situation, the proposed supervisory emergency controller, will take action to retain the VF limits in the safe mode (see Fig. 3.5c). The proposed supervisory emergency controller, is a multi-stage process, in which successive layers of necessary actions, are carried out to overcome the emergency, in the problem microgrid. These actions are:

- Soft actions: Adjustment of droop parameters (i.e. droop coefficients and VF set points) for droop regulated systems and power exchange with BSSs.
- Intermedial actions: Determining the required power transaction with healthy microgrid(s), and
- Hard actions: Defining the NDERs curtailment and/or load-shedding.

as portrayed schematically in Fig. 3.6a.

The proposed supervisory emergency controller, first tries to maintain the VF of the problem microgrid into safe mode, by applying soft actions, i.e., finding the most suitable droop set-points for the droop regulated systems. The operation of the droop regulated system is explained in the next chapter) and required power exchange with existing BSSs. To this end, it solves a non-linear optimisation problem for the considered microgrid, which is described in the next section. If successful, it will transmit the settings to the relevant local controllers of droop regulated systems and BSSs. However, if it is not successful in resolving the emergency in the problem microgrid, the Intermedial actions will be applied in addition to the soft actions.

Within the Intermedial action, the supervisory emergency controller, checks the availability of a neighbouring healthy microgrid. If a healthy microgrid is found available to support the problem microgrid, the supervisory emergency controller, will solve an optimisation problem so as to determine the suitable power transaction in the tie-lines, within the desired coupled microgrid in addition to the relevant control variables of the soft actions. If a healthy microgrid is not available or no feasible solution is found, through solving the optimisation problem, the supervisory emergency controller, will apply all actions, including the curtailing of either of the consumption of its non-essential loads, or the generation output of its NDERs, as a last resort. This sequential process, will guarantee that the supervisory emergency controller, will eliminate any emergency by utilising actions which are cheaper for the microgrid operator (such as adjustment of droop parameters and power exchange with BSSs or neighbouring microgrids), rather than use the hard action of load-shedding or NDER curtailment (which are very expensive for the operators). Fig. 3.6b, schematically depicts this described time sequenced operation of the supervisory emergency controller, following an event which causes a healthy microgrid, to become a problem microgrid, until it recovers. Fig. 3.6c illustrates this operational flowchart. The microgrids which are participating in the coupled microgrid, can be coupled with each other, with the help of the ISS. The principle of operation and configuration of ISS, is beyond the scope of this work and is discussed in [120]. Each ISS has its own local controller for synchronisation, before closing and coupling two neighbouring microgrids.

3.3.4 Research Issue 4

Research issue 4 will explore how to analyse the synergies between microgrids and the distribution network operator, so as to resolve emergency situations for remote area microgrids, in the grid connected mode.

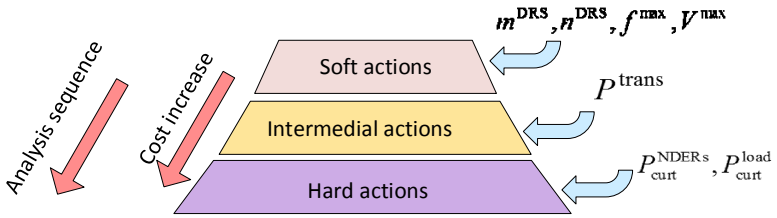

(a)

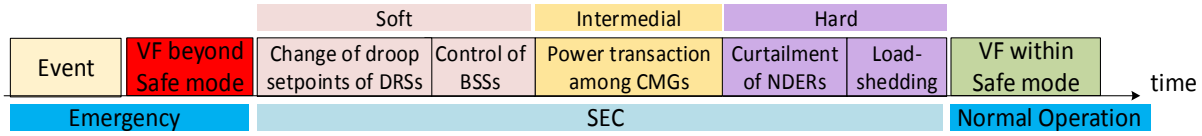

(b)

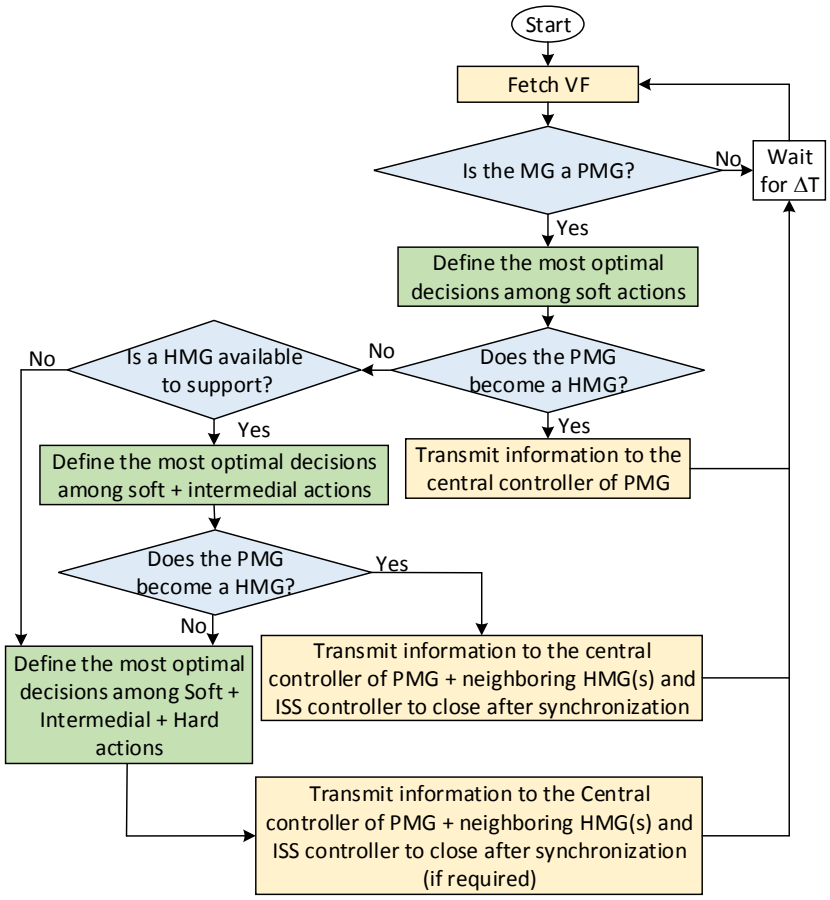

(c)

Fig 3.6 (a) Proposed multi-stage actions, for the developed supervisory, emergency controller, (b) Time-sequence of actions, from an event causing emergency, until the problem microgrid becomes a healthy microgrid, (c) Operational flowchart of the supervisory emergency controller.

To address this research issue, let us consider a large scale, multi-microgrid area, consisting of N microgrids (see Fig. 3.7). It is assumed that each microgrid has its own local primary controller. Every microgrid is composed of N DERs (including both DDERs and NDERs), N BSSs and N loads, that are connected through N buses and N lines, where $'N'$ is a variable number for each distributed entity. The NDERs are renewable based energy sources with an intermittent nature (e.g. PV, wind) unless they are accompanied by the power smoothening, BSS. Their output power is assumed to be curtailed, depending upon the command signal from microgrid's local controller. They will harvest and inject maximum possible power in market-unavailability mode. On the other hand, DDERs are assumed to be droop controlled and grid-forming when the multi-microgrid area is detached from the market. The market is assumed to be composed of a market operator which performs as the internet of energy provider, which will take consent from other microgrid clusters, to support multi-microgrid areas, in emergency situations. The communication between multi-microgrid areas and the market, will take place through the distribution network operators, where all microgrids

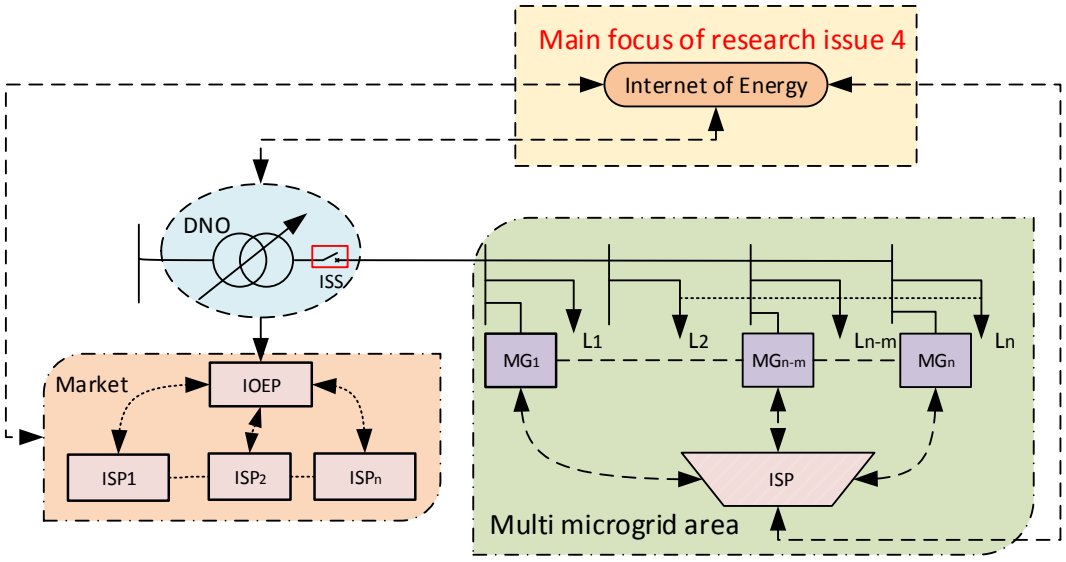

Fig 3.7 Considered large Scale multi-microgrid area

are coupled through the ISS, to exchange power amongst the neighbouring microgrids, termed as the shared service providers and internet of energy providers. Let us define a troubled microgrid, as a microgrid in which the emergency situation of over-loading or over-generation is being monitored. The secondary controller, (termed as the internal service provider i.e. the internal service provider which is present inside the multi-microgrid area) will take necessary action to retain the normal operation of troubled microgrid, by sending/receiving power to/from the shared service provider(s). If the internal service provider is successful in handling the emergency situation of the troubled microgrid, then the tertiary controller will not take any action. Here it is worth mentioning that tertiary controller, is assumed to be the internet of energy, with the ability to transfer the data, over the distribution network, operator's network. Now let us assume that the internal service provider, fails to overcome the emergency situation, and then the internet of energy, may negotiate an open access charge, with the distribution network operators. In this situation, the proposed optimization technique for the internet of energy, aims to resolve the problem for the lowest cost. The basic purpose is to combine the market to attain the maximum benefit.

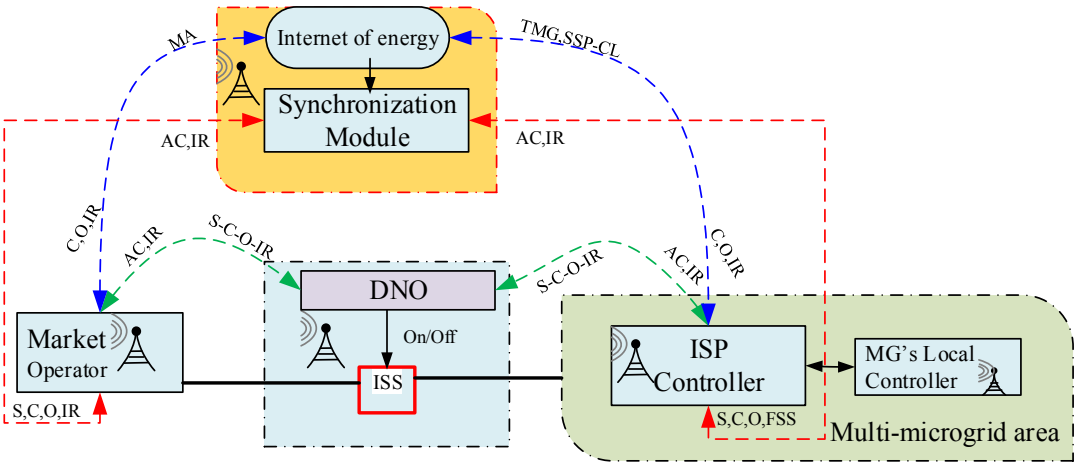

S-Synchronize, C-Close, O-Open, AC- Action Complete, IR-Information received , CL-Contribution level, MA-Market availability, FSS- Feasible solution sent

Fig 3.8 Communication Enabling Functions for the Proposed. Market Model.

To this end, an optimization problem is formulated and solved, with the use of a genetic algorithm, which is a meta-heuristic optimization technique and will be described, particularly for solving research issue 4, in the chapter 7 of this dissertation. Moreover, the assumed communication protocols, needed for the transmission of this information to all controllers is depicted in Fig. 3.8.

The proposed optimization technique will proceed in the following sequence of steps:

- the droop control or/and the BSS control will be applied with the help of microgrid's secondary controller,
- coupling amongst neighbour microgrid (s) takes place,
- power transaction with the IEOP(s),
- load shedding or the NDERs curtailment in the troubled microgrid (s).

Hence, if an emergency situation is not resolved by first step, then the proposed optimization technique will go onto the next step and so forth. However, the cost will increase proportionally, with each step taken.

To this end, the focus is to look for the most optimal solution to the problem by considering all possibilities. Once the troubled microgrid is detected within the multi-microgrid area, then internet of energy will look for the most optimal combination of service providers (SPs) and formulate a market optimization problem, therefore the corresponding distribution network operator, will respond and close the ISS on the command received from the internet of energy. In this way, the power balance of the troubled microgrid will be achieved, and if not, then optimization algorithm will again formulate the market optimization problem, until a feasible solution is found. The flow chart for this proposed methodology is shown in Fig. 3.9.

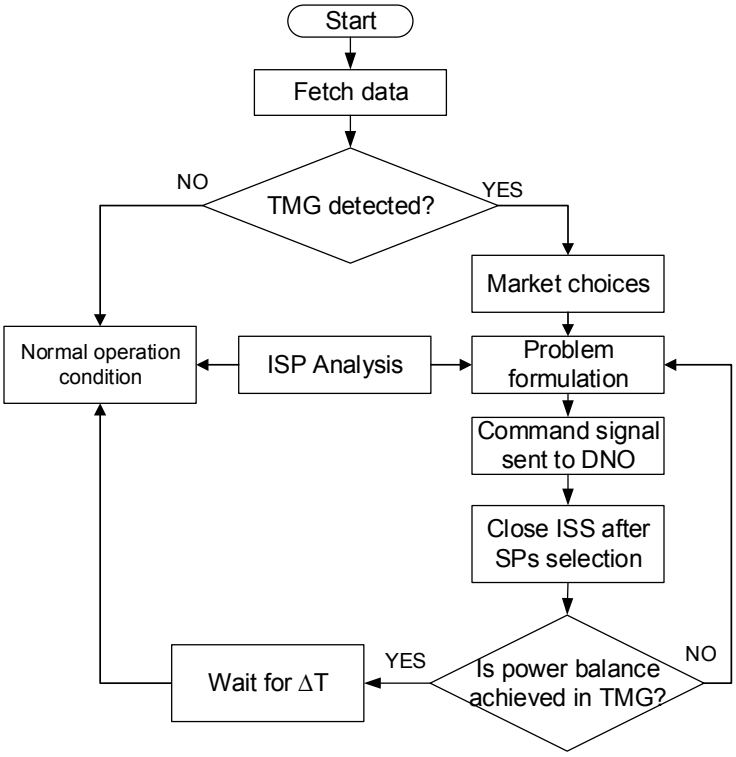

Fig 3.9 Flow chart for Research Issue 4.

3.4 Research Methodology

The research methodology related to the field of science and engineering, has been implemented into this research to solve the underlying research issues, explained in the previous section. The adopted methodology is comprised of following steps:

1. Modelling of DERs and loads,
2. checking the authenticity of developed models by performing power flow analysis,
3. Performing exhaustive simulations, accompanied by the heuristic optimisation technique, in order to reach to a feasible solution.
4. Another important aspect of this research is to perform testing of proposed models against the technical features.

In this thesis, Chapter 4 demonstrates a modelling framework for the microgrid operation, and Chapters 5–7 provide a complete formulation and solution strategy, of the proposed optimisation technique for remote area microgrids.

3.5 Summary

This chapter has provided a definition of the issues associated with organising the optimisation technique and the emergency situations impacting microgrids. By considering the socio-economic and technical issues, related to the existing solutions, research problems have been described. Additionally, the research questions that have arisen for every research problem and they should be discussed and solved for the proposed microgrid models. In order to address every predefined research problem, a conceptual procedure and framework has been proposed.

Chapter 4. Modelling and Operational Analysis of Microgrid

4.1 Introduction

Microgrids are well known for independent handling of the demand management problems. Maintaining the supply and demand balance instantaneously, has always been a crucial issue, especially in recent years, due to the high rate of the peak load growth. In the traditional way of the demand-supply match, the generation conforms to the loads consumption. However, this method is not always applicable and cost-effective. In this chapter, a stochastic based model is proposed for the microgrid applications. DERs and loads are designed and simulated in Matlab, by estimating potential outcomes from the probability distributions. Then, these recommended outcomes are structured for random variation, in inputs of one or more that correspond with the period of time. Within the historical data, fluctuations have been observed. These fluctuations provide the basis for the random variations which can occur within a selected time period, using a standard series. The simulated studies are based on the Monte Carlo principle. At first, stochastic modelling of the DERs, is done by the use of the step by step Matlab programming. Realistic climate impacts on NDERs output, is also analysed by the developed algorithms. Secondary focus will be on the power flow analysis of the modelled network that uses optimum operating, bound values for the DDERs. Features of climate scenarios, wind speed, fuel, aging, rated values and state of charge (SoC),

are taken into consideration, whilst modelling the DER components of microgrids. Finally, an explanation of an optimisation solver, is provided, alongside information on its main terminologies. The basic purpose of optimisation solver is to achieve an optimised control of the modelled microgrid network.

4.2 NDERs Modelling

PV and wind are the considered NDERs for the considered microgrid. Special focus during NDERs modelling is their unpredictable nature. The modelling is described below

4.2.1 PV Generator

The modelling of PV based NDER is described in details below:

4.2.1.1 Mathematical Modelling

The structure for modelling of PV cell is briefly explained in Fig. 4.1 [121]. Under this scheme, the current-voltage characteristic of diode can be equated as

$$I_d = I_O\left(e^{\frac{V_d}{V_T}} - 1\right) \tag{4.1}$$

$$V_T = \frac{kT}{q}.nl.N_{cell} \tag{4.2}$$

where I_O is rated current, V_d is diode voltage, V_T is the terminal voltage, k is constant value, T is the provided temperature, nl is diode ideality factor and N_{cell} are number of cells connected in PV module. The shunt and series resistors are provided in Fig. 4.1. The presence of these resistors, not only effects these characteristic of the PV cell, but also has dominant effect at the maximum value of output power [122]. Normally the in the modelled PV cell, Rs is very small as compared to R_{sh} and ranges between 0 and 1 ohm approximately. The key parameters of the PV cell are taken from the AU-Optronics PM-200 PV cell and are listed in

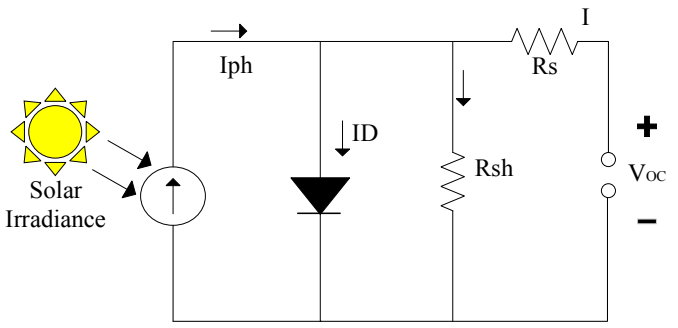

Fig 4.1 PV cell depiction by its equivalent circuit [121]

Table 4.1 [123]. To this end, probabilistic treatment of solar irradiance data, is performed and then it has been incorporated into the described PV model. In order to calculate the PV cell temperature, a linear relationship between the insolation level, ambient temperature, and the nominal temperature for the operation of the PV cell, with respect to the solar irradiance, the following equation is used:

$$T = T_{amb} + \frac{f \times (T_O - 20)}{0.8} \tag{4.3}$$

where f represents the probability density function of the beta distribution, T_{amb} is ambient temperature ($20 < T_{amb} < 48$°C) and To is nominal operating temperature (25ºC). It is used to calculate the solar radiation. Probability density function, is a function of pair of shape parameters and the considered weather condition. It is essential to select an appropriate probability distribution function. It helps to correctly represent the random phenomenon of the insolation.

Table 4.1 Numerical values of PV cell design parameters.

$\boldsymbol{V_{oc}}$	30.35 V	$\boldsymbol{k_i}$	0.078276 [A/ºC]
$\boldsymbol{V_{mpp}}$	24.14 V	I_L	8.8169 A
$\boldsymbol{k_v}$	– 0.32069 [V/ºC]	I_O	7.2566e^{-11} A
$\boldsymbol{N_{cell}}$	3000	nl	0.96434
$\boldsymbol{I_{sc}}$	8.76 A	R_{sh}	1177.4122 Ω
$\boldsymbol{I_{mpp}}$	8.38 A	R_s	0.32361 Ω

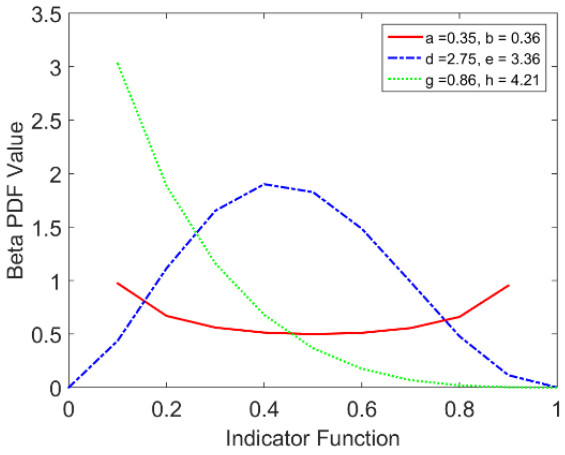

Fig 4.2 Assumed Beta distributions for the considered three climate conditions.

Although the process of selection is very difficult; there are certain possibilities to select a suitable distribution function by using empirical analyses. Several distributions can be tested so as to identify the best fit. This has been described in literature to be the normal, Weibull, and Beta distribution functions. An alternative solution, is to consider a distribution function on the basis of the observed historical data. In many situations, histograms can also provide an initial clue for the proper selection of the distribution function, as explained in [124].

In this study, Beta distribution has been selected to express the insolation level of the three conditions of sunny, cloudy, and rainy as illustrated in Fig. 4.2. Beta distribution can take a variety of shapes, depending upon the values of its pair of shape parameters; e.g. (i) Mount shape, if both parameters are bigger than one; (ii) J-shape or reverse J-shape, if one parameter is larger than one while the other parameter is smaller than one, and (iii) U-shape, if both parameters are smaller than one [125]. The data on solar exposure, shading and rainfall, can be taken from the original weather data, of the bureau of metrology. The selected Beta distribution for sunny conditions (X) is given as

$$f(X|a,b) = \frac{1}{B(a,b)} X^{a-1}(1-X^{b-1})I_{(0,1)}(X) \tag{4.4}$$

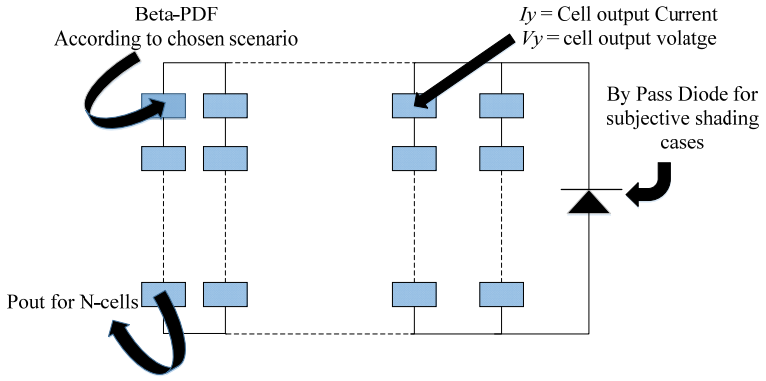

Fig 4.3 Schematic illustration of a single PV module.

where a and b are the shape parameters of the Beta distribution, and $a > 1$ and $b > 1$. The indicator function $I_{(0,1)}(x)$ ensures that values of x in the range of 0 to 1 have a nonzero probability [126]. As Beta distribution is bounded over two finite limits, it is able to replicate the random pattern of insolation levels for any given time (hour) of the day.

Shading of a PV module is a key point, as it has a great impact on the modelling parameters. For a PV system, shading is classified into objective and subjective shading. Objective shading can be formed by various weather impacts, such as clouds and haze, and will inevitably cause a reduction of the overall sunlight intensity for the PV system. On the other hand, objects near or far from the PV, can also block the sunlight and create solid shade shapes, which are considered to be subjective shading [127]. Primordial stages for estimation of irradiance on a PV generator, includes the case of subjective shading as explained in [128]. A dimensionless parameter, known as the shading factor [129], is included in the developed model, to deal with any causes of shading.

It is to be highlighted, that to minimise cracking, overheating and potentially burning due to possible hard-edged shading, bypass diodes are used in parallel, with modules that conduct when the module is shaded. It is cost-effective to provide a bypass diode, across a sub-string of cells, instead of connecting with the individual cell and each sub-string will result in one module as shown in Fig. 4.3. Bypass diodes become active only when subjective shading

effects appear in the system; otherwise, the bypass diode factor is zero. Beta distributions for cloudy and rainy conditions are given as:

$$f(C|d,e) = \frac{1}{B(d,e)}\, C^{d-1}(1-C^{e-1})I_{(0,1)}(C) \tag{4.5}$$

$$f(R|g,h) = \frac{1}{B(g,h)}\, R^{g-1}(1-R^{h-1})I_{(0,1)}(R) \tag{4.6}$$

where $d > 1$ and $e > 1$ are formed from shading factor and $g > 1$ and $h < 1$ are formed from rainfall duration and rainfall intensity components [130]. For a PV cell, the short-circuit current is calculated for the sunny, cloudy and rainy condition as

$$I_{SC}(X) = f(X|a,b)\,[I_{sco} + k_i\,(T_X - 25)] \tag{4.7}$$

$$I_{SC}(C) = I_{sc}(S)\,[1 - f(C|d,e)] \tag{4.8}$$

$$I_{SC}(R) = I_{SC}(S) f(R|g,h) - k_i\,(T_{amb} - T_O) \tag{4.9}$$

where I_{SC} denotes the short circuit current with *X, C* and *R* represents the sunny, cloudy and rainy condition respectively, I_{sco} is short-circuit current in normal conditions and $I_{sc}(S)$ is mismatched short-circuit current due to shading, k_i is Temperature coefficient of I_{sc}. Now open-circuit voltage is calculated for each condition as

$$V_{OC}(X) = V_{oc} - k_v\, T_X \tag{4.10}$$

$$V_{OC}(C) = V_{oc} + 2m\, V_t\, log[1 - f(C|d,e)] \tag{4.11}$$

$$V_{OC}(R) = \frac{KT_{amb}}{q}\, log\left(\frac{I_{SC}(S)}{I_O}\right) \tag{4.12}$$

which considers the shading factor due to the objective shading caused by clouds. Here where V_{oc} denotes the open circuit voltage, k_v is Temperature coefficient of V_{OC}, m is the bypass diode ideality factor and q is charge on electron. Thus, the voltage and current, at the maximum power point, under partial shading conditions can be calculated as: [131]

$$V_{mpp}(S) = V_{mpp} + 2c_{1m\times V_t} \log[1 - f(C|d,e)] \tag{4.13}$$

$$I_{mpp}(S) = I_{mpp}[1 - f(C|d,e)] \tag{4.14}$$

From (4.7)-(4.14), the deviation of the current-voltage characteristic of a PV cell with respect to the ideal condition, denoted by the fill factor, is determined as:

$$Fill\ Factor = \frac{V_{mpp}\, I_{mpp}}{V_{oc}\, I_{sc}} \tag{4.15}$$

In the above equations, V_{mpp} and I_{mpp} are the voltage and current at maximum power point respectively. Thus, the output voltage and current of a PV module, consisting of a strings of cells as shown in Fig. 4.3, can be calculated under all condition as:

$$I_{out} = f(s|a,b)\,[I_{sc} + k_i\,(T-25)] \tag{4.16}$$

$$V_{out} = V_{oc} - k_v\,T \tag{4.17}$$

Thereby, the total output power of a PV module, under any condition, can be defined as

$$P_{PV} = I_{out} \times V_{out} \times fill\ factor \tag{4.18}$$

4.2.1.2 Developed Algorithm for PV Generator

The major purpose of the developed algorithm (shown schematically in Fig. 4.4), is to calculate the weather-based output power of the PV system. A stochastic modelling approach, which is a useful tool for estimations of the probability distributions, has been used here, as the simulation technique. The potential outcomes, taken from the Beta probability density function, are allowed for random variation of one or more inputs, based on historical data for selected intervals, using metrological year data. To this end, a typical metrological data of one month, has been captured for a site (e.g. Sydney, Australia). Multiple trial runs are performed in Matlab, using random variables, specified earlier in the stochastic modelling stage. It is assumed that a sunny condition does not have any clouds; light clouding is considered for cloudy conditions, and heavy clouding is considered for rainy conditions. Thus, it is thought that a sunny condition does have 0% shading, a cloudy condition has 15-40% shading, while 45-75% shading is considered for rainy conditions

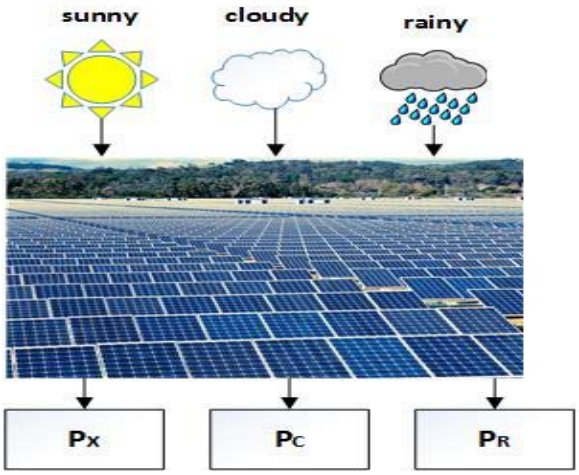

Fig 4.4 Assumed PV System topology.

The required computational procedure is as follows:

- Step-1: Select the month for which the expected output power is needed.
- Step-2: Perform statistical analysis, to determine Beta probability density function, from the input metrological data.
- Step-3: Compute the ambient and cell temperature, for that particular time of the day.
- Step-4: Solve equations of current and voltage for the PV module under consideration (Objective shading assumptions made earlier should be taken into account).
- Step-5: Calculate the fill factor, to see the deviation from the original voltage-current characteristics.
- Step-6: Calculate the output power of the PV system, for a sunny, cloudy and rainy condition.

The flow chart of Fig. 4.5, illustrates schematically the computational procedure in more detail.

4.2.2 Wind Generator

The horizontal axis wind turbine, is used as the model for the wind generator. The

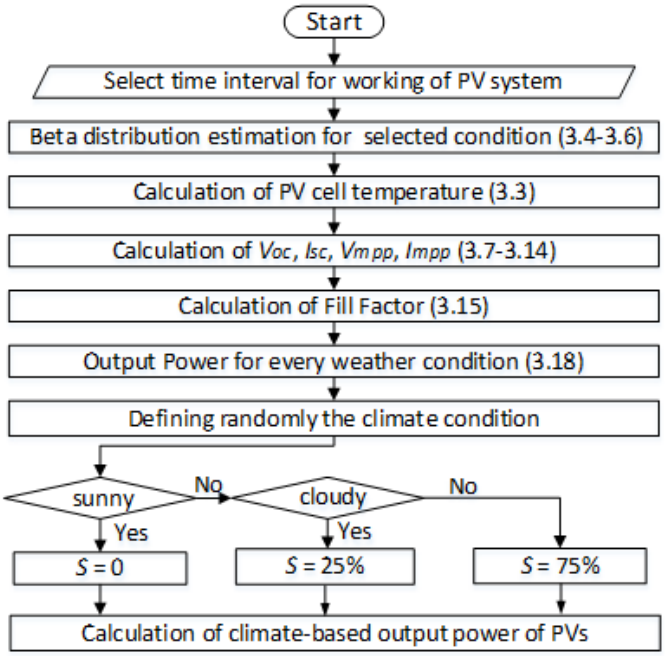

Fig 4.5 The PV generator algorithm flowchart.

operating machine is assumed to be an upwind machine e.g. the rotor in the modelled scheme is assumed to be facing the wind direction, to capture the maximum wind for utilisation. The induction generator is selected for the conversion of the mechanical input power to the electrical output. Stochastic analysis for the annual energy produced by wind speed, is done by using the weibull distribution function, where scale and shape factors are the parameters of weibull distribution function. Monte-Carlo Simulations, show that the final output from the induction generator can be approximately 15MW maximum at 15m/sec wind speed. Now for the wind generator, the calculation of the wind speed *(V)* is done by the probability density function, utilising shape (β), scale (η) and location (γ) parameters [132]. While the location parameter is set to the zero value for the purpose of the calculations, the wind generator's basic block diagram representing its functions, is shown in Fig. 4.6. The expected output from power generator is calculated after the determination of speed. It includes the following equations

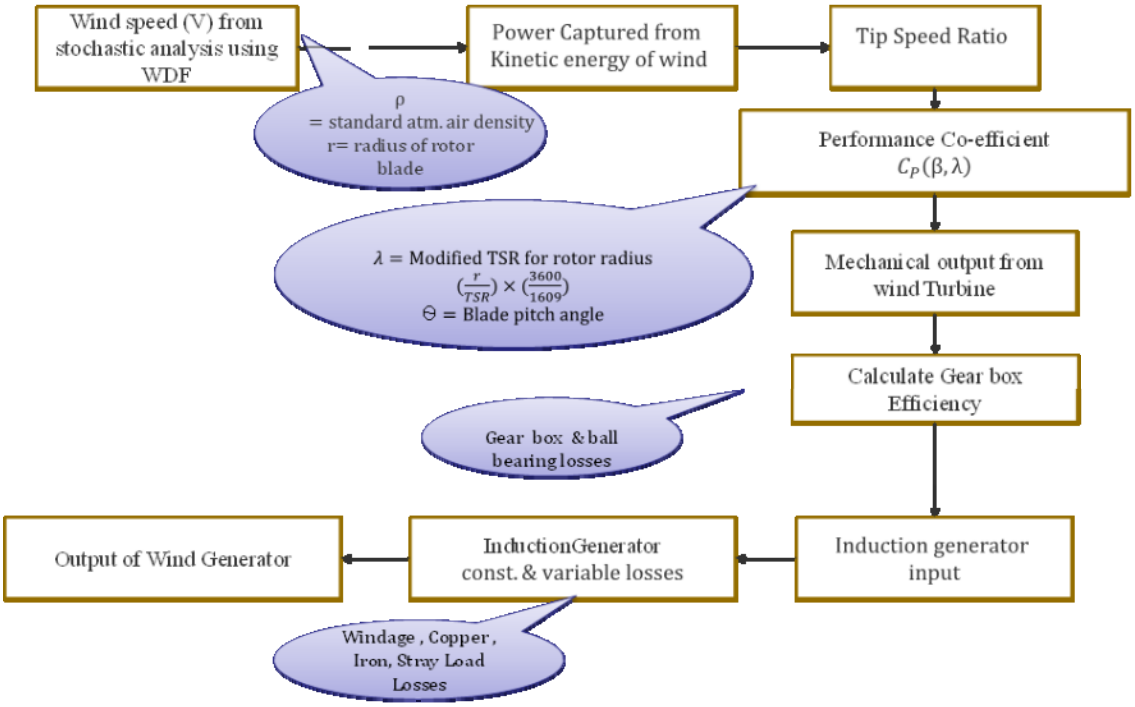

Fig 4.6 Functional block diagram of the wind generator.

$$P_{KE} = 0.5 \times \rho \times A \times V^3 \tag{4.19}$$

Equation (4.19) is utilised for measuring the kinetic energy of wind and then calculating the total power captured. Here A is the area of rotor and ρ is the standard atmosphere air density.

$$TSR = \frac{\omega \times r}{V} \tag{4.20}$$

In (4.20) TSR is the Tip speed ratio and it is defined as, the ratio between tangential speed and the real wind velocity.

$$C_P(\beta,\lambda) = 0.5 \times \left[(\lambda - 0.22) \times \Theta^2 - 5.6) \times e^{-0.17/\lambda}\right] \tag{4.21}$$

While C_P is the coefficient of performance. Then by using $(\frac{r}{TSR}) \times (\frac{3600}{1609})$, the actual TSR is calculated where Θ is the blade pitch angle.

$$P_{mech} = 0.5 \times \rho \times A \times V^3 \times C_P \tag{4.22}$$

$$\eta_{gear} = \frac{\left[P_{mech} - \{0.01 \times (q_{step} \times P_{rated})\}\right]}{P_{mech}} \tag{4.23}$$

$$IG_{input} = P_{mech} \times \eta_{gear} \tag{4.24}$$

$$P_{Wind} = IG_{input} - losses \tag{4.25}$$

Conversion of mechanical output from the wind turbine to an electrical output is done through the use of the induction generator. The wind generator's Computational block diagram, is shown in Fig. 4.7 and the design parameters of the induction generator used for energy conversion, are described in Table 4.2.

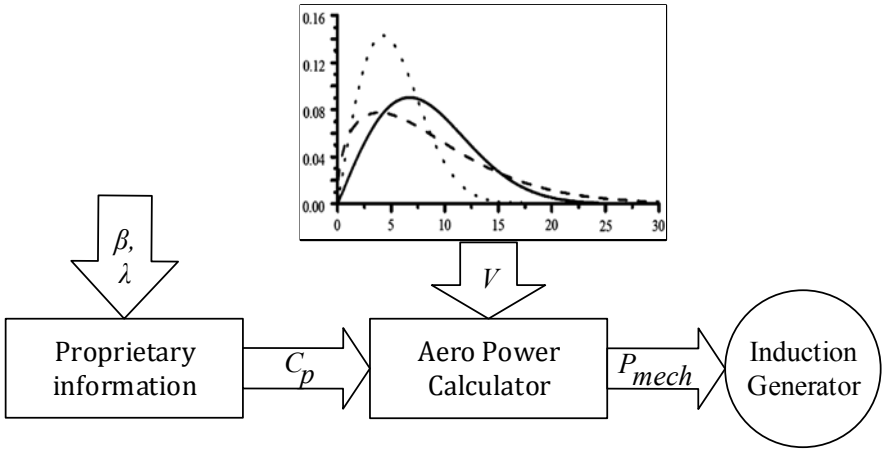

Fig 4.7 Wind Generator computational block diagram.

Table 4.2 Design Specifications of Induction Generator.

Rated Power	16 MVA	Rated Voltage	6600 V
Frequency	50 Hz	Poles	6
Stator Resistance	0.0052 pu	Staor leakage reactance	0.089 pu
Rotor Resistance	0.0092 pu	Rotor leakage reactance	0.13 pu
Iron loss resistance	135 pu	Magnetizing reactance	4.8 pu

4.3 DDERs Modelling

The DGs are assumed as synchronous generators, in which their output power can vary between the minimum loading limit and their nominal capacity. The nominal capacity of the DGs is decided on the basis of the nominal capacity of the load or microgrid's demand at that time. The auto-synchronizer module, is used for this purpose and it serves better results. The reason being, that the synchronisation of frequency, phase and voltage can be done automatically [133]. Light load conditions, in terms of the DGs operation and for extended hours, can increase the risk of premature ageing and engine failure. Studies show that if the loading level is as low as 25%, in comparison to the rated output, then the fuel consumption of the DGs, can increase tremendously [134]. It is assumed for the sake of this work that

$$P_{DG}^{cap} = P_{DG}^{UB} = selected\ percentage \times P_{load}^{cap} \tag{4.26}$$

where P_{DG}^{cap} is set by stochastic modelling. For economic benefit, it is assumed that DG will not be turned off completely. Therefore, for DGs the starting and Shutdown costs are set to zero. Another aim is to achieve the long life of the machine. Therefore, restrictions are put on a lower operational bound P_{DG}^{LB} and are taken as a necessary operational constraint. Thus, the operational power from the DG, should remain higher than P_{DG}^{LB} i.e. $P_{DG} \geq P_{DG}^{LB}$.

The safe operation of BSS, is ensured by adopting a battery management system. The key advantage in doing so, is the responsibility for monitoring many core parameters for the case temperature range and the limits of voltage and currents etc. [135]. It is also critical to consider the BSS lifetime and it is necessity for accurate calculation of the operating cost of the microgrid. This is achieved by assuming that the lifetime of the BSS, is the time equal to

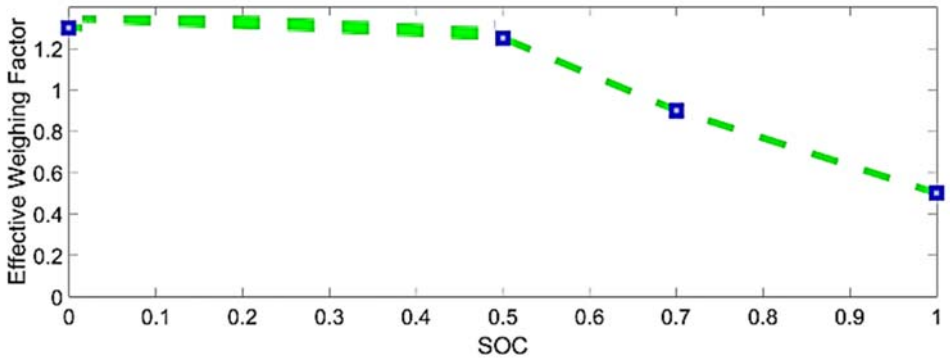

Fig 4.8 SoC profile for BSS [136].

the total ampere-hour (Ah) throughput and it is similar to the measured Ah throughput. Care is taken in that that low SoC, can stress the BSS, as compared to the high SoC values. Hence it is important to compare any Ah in case of charge/discharge, with a weighing factor. This factor should be higher or lower than the SoC. It is a fact that an effective cumulative lifetime of considered BSS, is coorelated to operating SoC values, as described in [136-137] and shown in Fig. 4.8. The following limits are considered for SoC of BSS.

$$SOC^{LB} < SOC < SOC^{UB} \tag{4.27}$$

While nominal capacityP_{cap}^{BSS} of BSS is taken from the aforementioned stochastic modelling.

4.4 Load Modelling

The loads are assumed time-varying and their nominal capacity (P_{cap}^{load}), is determined randomly while the instantaneous power demand of the loads are between zero and their nominal values. It is assumed that all considered loads are constant-impedance. Therefore, both of the active and reactive load demands, will consequently dependent upon the frequency and voltage magnitude, given at their corresponding connection bus [138]. A sample of the load profile of 24 hours, generated for the purpose of analysis, is presented in Fig. 4.9.

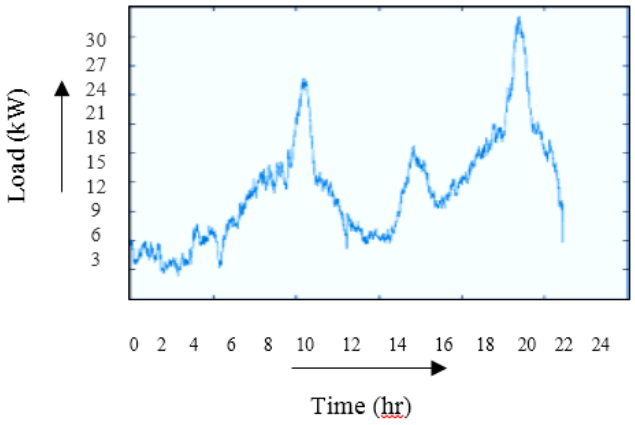

Fig 4.9 A sample of load profile generated for analysis

4.5 Microgrid Topology and its Components

The considered topology of a microgrid is shown in Fig. 4.10 and it is assumed that microgrid is composed of a total of six buses. Out of which the PV generator is connected to bus-1, wind generator to bus-2, BSS with bus-3, load on bus-4, DG on bus-5 and bus-6 will be assumed to be connected with an ISS, for the purpose of connectivity with other neighbour microgrid(s). It is essential to do demand supply analysis of the considered system. Therefore, after modelling, it is important to do a power flow analysis for the microgrid, which is described in detail in the next section.

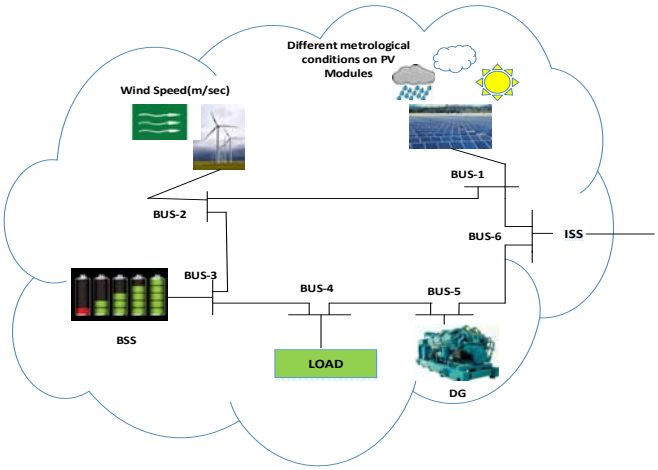

Fig 4.10 Topology of modelled microgrid.

4.6 Power Flow Analysis for Modelled Microgrid

To analyse the microgrid performance, when solving the optimisation problem, a load flow analysis is required to reveal the deviation of voltages and the frequency in the microgrid. This research uses a modified Gauss-Seidel type algorithm, for this purpose. In this work, it is assumed that DDERs (i.e., DGs, BSSs, as well as BSS-coupled NDERs) are droop controlled i.e., they regulate the voltage magnitude and frequency, at their point of connection, using the droop equations of

$$f = f^{max} - m^{DDER}\, P^{DDER} \tag{4.28}$$

$$|V|^{DDER} = V^{max} - n^{DDER}\, Q^{DDER} \tag{4.29}$$

where m^{DDER} and n^{DDER} are the droop coefficients (see Fig. 4.11).

In the first iteration, using the instantaneous power of BSS, NDERs and load, the output power of DDERs are approximated. Then, using the droop equation of (4.28), the microgrid's frequency, is calculated in this iteration from which the microgrid's Y-bus and the new active and reactive power consumption of each load, is updated by

$$Y^{bus} = \begin{bmatrix} Y_{11}(f) & Y_{12}(f) & \dots & Y_{1N}(f) \\ Y_{21}(f) & Y_{22}(f) & \cdots & Y_{2N}(f) \\ \vdots & \vdots & \ddots & \vdots \\ Y_{N1}(f) & Y_{N2}(f) & \cdots & Y_{NN}(f) \end{bmatrix} \tag{4.30}$$

$$P^{load} = P^{nom}(1 + k_1 \Delta f)(V/V^{nom})^{k_2} \tag{4.31}$$

$$Q^{load} = Q^{nom}(1 + k_3 \Delta f)(V/V^{nom})^{k_4} \tag{4.32}$$

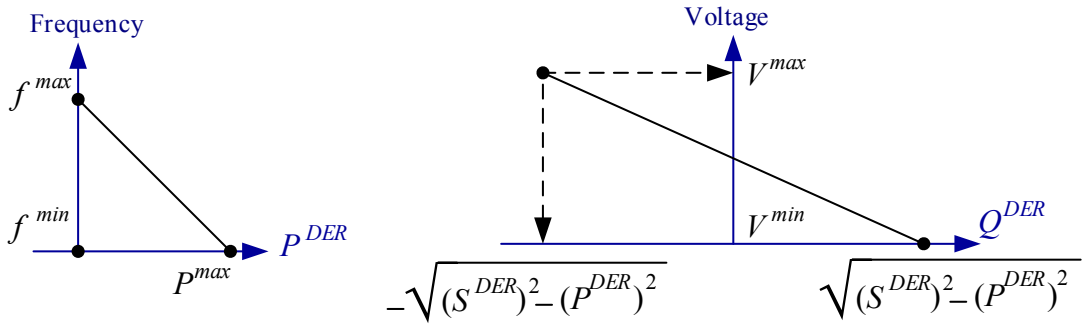

Fig 4.11 Droop Regulated control illustration for microgrid network.

in which $\Delta f = f - f^{nom}$ represents the deviation of microgrid's frequency from the nominal frequency (e.g. 50 Hz) whereas V^{nom} is the nominal voltage magnitude in the microgrid (i.e., 1 pu) and P^{nom} and Q^{nom} denote the instantaneous power of the load at nominal frequency. In (4.31)-(4.32), k_1, k_2, k_3 and k_4 are constants (their numerical values are described in the next Chapter) [53].

Assuming a set of initial values for voltages of all buses (e.g., $1\angle 0^{o}$ pu), the current drawn by each load can be calculated. Then, the Gauss-Seidel algorithm is applied to determine the voltage V_x^j of all buses [103]. Then, the acceleration factor (μ) is applied to slightly modify the bus voltages to define new voltages, for the next iteration in the form of

$$V_x^{j+1} = V_x^{j-1} + \mu\left(V_x^j - V_x^{j-1}\right) \tag{4.33}$$

At this stage, the power consumed in the lines of the microgrid can be calculated as:

$$S^{line} = \sum_{x=1}^{N_{bus}} \sum_{y=x}^{N_{bus}} -Y_{x,y}^{bus}\left(V_x - V_y\right)^2 \tag{4.34}$$

where N_{bus} denotes the number of buses in the microgrid. Hence, the total output power from DDERs ($\sum S^{DDER}$) will be:

$$\sum S^{DDER} = \sum S^{load} + S^{line} - \sum S^{NDER} + \delta \sum S^{BSS} \tag{4.35}$$

in which $\delta = +1$ if the BSS is charging; $\delta = -1$ when discharging and $\delta = 0$ when the BSS

is not in operation.

Now, the active and reactive power of DDERs, can be distinguished on the basis of their droop ratios by:

$$P_x^{DDER} = \mathrm{Re}\left(\sum S^{DDER}\right) Ratio^{DDER} \tag{4.36}$$

$$Q_x^{DDER} = \mathrm{Im}\left(\sum S^{DDER}\right) Ratio^{DDER} \tag{4.37}$$

where $\mathrm{Re}(.)$ and $\mathrm{Im}(.)$ are respectively the real and imaginary functions and $Ratio^{DDER}$ shows the ratio of the output power of DDERs, correlated to their droop coefficient m^{DDER}. Replacing (15) in (7), reveals the voltage magnitude at the DDER buses which will be updated by the angles given by the corresponding values in (12). Likewise, replacing (15) in (6) will determine the new frequency for the next iteration. The above-discussed iterative technique will be continued until the numerical analysis converges. At this stage, the frequency deviation and voltage magnitude deviation (i.e.,$\Delta V = \max(|V_x - V^{nom}|)$ in the microgrid, can be determined in which $\max(.)$ is the maximum operator.

Due to the absence of a slack bus, one of the buses in the microgrid (e.g., the bus connected to the first DDER, is assumed to be the reference bus, that has an angle of 0º. Thus, all other angles are calculated with respect to this reference bus.

4.7 Optimisation Solver

In this study, a genetic algorithm, based upon optimisation techniques is used to find the most suitable control variables (i.e., the output power of DGs and BSSs, as well as the level of load-shedding and renewable curtailment in NDERs) that result in the least fitness or objective function value, amongst any other variables. Floating point-genetic algorithm, is a special type of genetic algorithm which uses floating-point numbers, instead of binary numbers, which is

common in traditional genetic algorithms. Thus, it is more advantageous in terms of efficiency, memory utilisation, and precision [103]. Moreover, there is greater flexibility in using different operators. To this end, floating point-genetic algorithms, generates a series of output powers for every control variable, in the form of floating-point numbers, which are referred to as genes (*gene*). Each combination of these genes form a vector, referred to as chromosome. While a group of chromosomes, constitute the population. Floating point-genetic algorithm, includes an iterative mechanism of population initialisation, calculating the developed fitness function, for each chromosome of the population, applying different operators on a specific or suitable portion of the population, to generate a new population until fulfilling the stopping criteria. This optimisation solver, is explained in more detail with its operators, in the next coming chapter of this work. However, the different terminologies of the floating point-genetic algorithm-based solver, are shown in Table 4.3.

Table 4.3 Floating point genetic algorithm terminologies.

Terms	Explanation
Gene or individual *(ind)*	Each control variable
Chromosome	The vector consisting of all *ind*s
Population	The set of all chromosomes
Fitness value	Quality of a chromosome
$\boldsymbol{Rank}$	Order of a chromosomes when sorted from least to highest number
$\boldsymbol{N_c}$	Position of an *ind* within a chromosome for crossover
$\boldsymbol{N_{ind}}$	Number of *ind*s in a chromosome
$\boldsymbol{Per_c}$	Percentage of *ind*s for which crossover is applied
$\boldsymbol{Per_m}$	Percentage of *ind*s for which mutation is applied

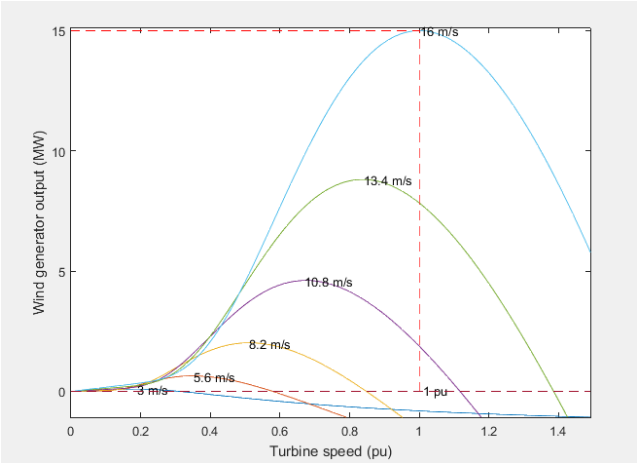

Fig 4.12 Wind based NDERs output

4.8 Simulation Results

The simulation studies have been completed for the considered microgrid topology which was shown previously in Fig. 4.10. In this chapter only those simulation studies, related to the NDERs and DDERs, are presented. While power flow analysis and floating point-genetic algorithm solver implementations will be discussed later in Chapter 5, 6 and 7 respectively.

4.8.1 NDERs Numerical Analysis

Monte-Carlo Simulations show that nominal capacities of NDERs, can be approximately 18MW (out of which P_{cap}^{PV} is 3MW and P_{cap}^{wind} is 15MW with corresponding maximum 15m/sec wind speed). The units of DERs powers can be changed according to the considered microgrid system (for example in coming Chapters, the units are kW instead of MW for the standalone and clustered microgrid systems). Wind based NDERs output analysis is depicted in Fig. 4.12. The performance of a PV System, with the developed algorithm, is evaluated by considering one year's data, and is tabulated in Table 4.4. First, $f(X)$ has been computed using (4.4) where parameters a, $b < 1$, so the beta probability density function obtained for sunny conditions is U-shaped as demonstrated previously in Fig. 4.2. After this, the corresponding temperature is

Table 4.4 Comparisons amongst the assumed three weather conditions and their expected output power for the months of a year

Month	$f(X)$	P_X [MW]	$f(C)$	P_C [MW]	$f(R)$	P_R [MW]
January	0.301	4.713	0.391	2.923	0.771	1.723
February	0.422	8.922	0.232	4.902	0.992	1.122
March	0.324	5.131	0.673	2.481	0.513	1.831
April	0.321	5.349	0.534	2.509	0.904	1.309
May	0.311	4.358	0.215	4.08	0.795	1.708
June	0.292	4.667	0.546	2.487	0.786	1.717
July	0.403	7.276	0.697	2.156	0.947	1.856
August	0.325	5.185	0.228	4.075	0.818	1.225
September	0.392	7.794	0.399	2.804	0.719	1.914
October	0.351	5.903	0.351	3.253	0.961	1.183
November	0.313	4.312	0.542	2.592	0.672	1.962
December	0.406	7.721	0.173	5.871	0.613	2.161

calculated while the normal operating temperature is set at 25ºC. The short circuit current obtained using (3.7) for 12 months, is in the range of 1.05 to 1.28 A, while the open circuit voltage is in the range of 22.04 to 22.08 V. The fill factor value is 0.7 for sunny weather. Finally, P_X values are calculated and indicate that the expected output power is the maximum (approximately 8.9 MW) for February, due to the highest expected insolation level, while lower values of 4.3 MW, are expected for May and November, because of the lower expected exposure to sunlight.

When the evaluation is carried out for cloudy weather, the shading factor is involved in the composition of $f(C)$,so a high value of shading will create a lower power output, and the probability density function has a mount-curve shape. The expected output power of the

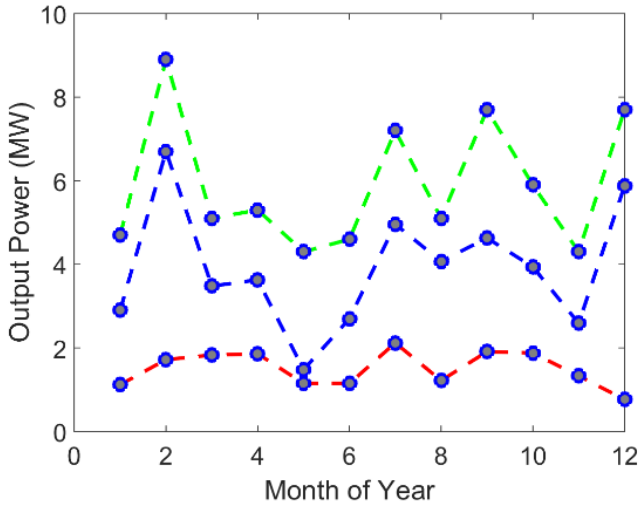

Fig 4.13 Graphical representation of the expected output power of the considered PV system under sunny, cloudy and rainy conditions.

considered PV system in rainy conditions (P_C) is 5.87 MW for December, while it reduces to 2.15 MW in July, because of the larger expected shadings. Beta probability density function for rainy conditions is made from the rainfall duration and rainfall intensity factors and inclusion of shading effects is obvious in this case. The probability density function has a J-shaped curve. The expected output power, of the considered PV system, in this condition (P_R), is expected to generate 1.85 and 1.22 MW, for July and August. Fig. 4.13 illustrates the expected output power of the considered PV system, in these three conditions, throughout the year.

The stochastic analysis shows a reduction of respectively 25-40 % and 60-70 %, in the expected output power of the considered PV system, for cloudy and rainy conditions in comparison to sunny conditions.

4.8.2 Numerical Analysis with Droop Control

For stochastic modelling of DG, ramp up and down limits, fuel and aging, rating and overloading limits, are important features. The ramp up and ramp down limit of DG are considered as 95%P_{cap}^{DG} and 30%P_{cap}^{DG} respectively. In the same manner, battery operation is bounded by charging/ discharging times, SoC limits, Battery capacity etc. So the SoC^{LB} is set at 20% and $SoC^{UB}$is 90% respectively.

Exhaustive simulations are carried out for finding the minimum effective values of DDERs, using droop regulated based control algorithms, developed in Matlab. The purpose is to look at the feasible DERs values to ensure all modelling parameters are satisfied. Values should be satisfying the demand, at that particular time of the planning horizon. First the demand supply analysis is necessary when the DDERs are operating at their rated capacities. Table 4.5 explains the situation when the NDERs are generating their powers and the climate situation, is also taken into account. The solar irradiance level and wind speeds have predominant influence on the generation levels of the NDERs. Load patterns are also randomly generated, with the help of historical data. When the DDERs are operating at their maximum available capacity, it can then create a power overload, so in order to create an optimum scenario, it is necessary to identify the preferable values that can provide maximum benefit. Fig 4.14 (a) shows the demand supply analysis without including the DDERs and it is clear that scenario (3, 4, 6, 7, 8, 9, and 10) are suffering from a power deficiency. While (1, 2) are experiencing a power overload, only 5 is ideal one with the power balance. When the system is solved to meet the modelling constraints of the DDERs, then we can attain the power balance of the microgrid network. So firstly, the NDERs generation will be monitored in relation to its accommodation of the required load.

If the NDERs generation meets the load demand, then the excessive power from DG can be utilised to charge BSS (with the condition that SoC of BSS should not be reached on maximum limit). On the other hand, if the NDERs, is not enough to meet the load demand, then power will be taken from the DG (with the condition that the DG will not operate at the maximum limit).For making the modelled DERs, more economical for microgrid operation, effort is made to operate the DGs at their minimum possible level and the rest of power (if desired) is fetched from BSS discharging. In an ideal and of course rare situation, in which the NDERs are producing accurate amounts of power as the load demands, then the DG will operate at the lower limit and the DG power can be transmitted to BSS (so that SoC limit is not violated). More explanations about the developed function for the demand supply analysis, as well the three related situations are presented in Table 4.5, while the graphical depiction is provided in Fig. 4.14 (b).

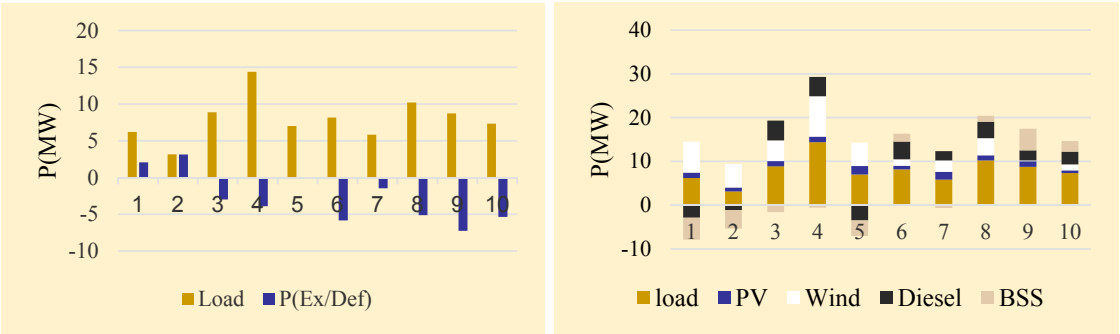

(a) (b)

Fig 4.14 Demand/supply analysis of microgrid (a) without droop control (b) with droop control

Table 4.5 Simulation results for the considered microgrid demand and supply analysis.

Scenario	PV		Wind		Load	$P^{PV} + P^{Wind} - P^{Load}$	P^{DG}_{cap}	P^{DG}	P^{BSS}_{cap}	P^{BSS}
	Climate Scenario	P^{PV} (MW)	Speed (m/s)	P^{Wind} (MW)	P^{Load} (MW)	(MW)	(MW)	(MW)	(MW)	(MW)
1.	cloudy	1.24	12	7.03	6.2	2.07	9.67	2.9	5.2	-4.97
2.	rainy	0.89	10	5.37	3.14	3.12	3.79	1.13	9.38	-4.25
3.	cloudy	1.19	9.8	4.71	8.88	-2.97	15.17	4.55	8.61	-1.58
4.	cloudy	1.26	13	9.23	14.39	-3.89	14.77	4.43	6.95	-0.54
5.	sunny	1.92	13	5.58	7.02	0	11.73	3.52	12.38	-3.52
6.	cloudy	0.83	6.5	1.5	8.17	-5.84	13.52	4.05	12.52	1.79
7.	sunny	1.79	7	2.57	5.84	-1.47	7.12	2.13	8.93	-0.66
8.	cloudy	1.15	8.5	3.95	10.22	-5.11	12.40	3.72	12.75	1.39
9.	cloudy	1.29	3	0.2	8.74	-7.25	7.65	2.29	6.94	4.96
10.	rainy	0.62	5.6	1.34	7.33	-5.36	9.84	2.95	9.75	2.41

4.9 Summary

In this chapter, the modelling of DERs, for microgrid operations followed by the power flow analysis is discussed. Here, the NDERs model includes the environmental aspects. The unpredicted nature of the NDERs is embedded by the use of different probability density functions, and then the stochastic modelling is applied to replicate the phenomenon of random variables. DDERs have operational limits due to their controllable nature and loads are assumed to be a constant impedance time in the considered time horizon. The demand supply analysis, of the considered microgrid topology, has shown that within a certain time frame, the load can be accommodated by the combination of the NDERs output at that time, adjustment of operational limits for DGs, as well as the BSS conditions of charge and discharge.

Chapter 5. Optimisation Technique for Standalone Microgrid

5.1 Introduction

The standalone hybrid remote area power systems, also known as microgrids, can provide reasonable priced electricity in geographically isolated and edge of grid locations, for their operators. To achieve the reliable operation of microgrids along with minimal consumption of fossil fuels and maximum penetration of renewables, the frequency and voltage, should be maintained within acceptable limits. This can be realised by solving an optimisation problem. The floating point-genetic algorithm, is a heuristic technique that has been strongly proven to find feasible/optimal solutions. This solver requires a fitness function, to extract the most suitable, as well as optimal control variables, for the microgrid. And it is done on top of the selection of the appropriate operators. At first, a suitable fitness function, is formulated in this chapter and it is done by including the operational, interruption and technical costs, which are then solved with a floating point-genetic algorithm, using different operators. The considered operators along with the developed fitness functions are testified to have a non-linear optimisation algorithm of a 38-bus microgrid. Detailed discussions are provided, on the impact of which different operators have on the outcomes of the fitness function.

5.2 Optimisation Formulation

This section presents the formulated fitness function and the considered constraints for addressing Research Issue 1, described earlier in Chapter 3.

5.2.1 Formulated Fitness Function and Technical Constraints

As mentioned above, the main aims are to minimise the overall cost of electricity generation in the microgrid, losses, interruption to loads and renewable curtailment, and enhance the lifecycle of BSSs. Thus, a fitness function can be defined as a mixed integer nonlinear optimisation problem and formulated as

$$FF = FF_{op} + FF_{int} + FF_{vf} \tag{5.1}$$

where FF_{op}, FF_{int} and FF_{vf} are respectively the microgrid's operational costs, interruption costs because of load-shedding or curtailment of NDERs, and the equivalent cost of voltage and frequency deviation. FF_{op} is defined as

$$FF_{op} = cost_{DG} + cost_{BSS} + cost_{loss} \tag{5.2}$$

where $cost_{DG}$ is the cost of power generation by DGs, $cost_{BSS}$ is the life loss cost of BSS because of charging/discharging, and $cost_{loss}$ is the cost of power loss in the microgrid lines. $cost_{DG}$ is calculated as

$$cost_{DG} = \Delta T \sum P^{DG}(cost_{\text{fuel}} + cost_{\text{em}}) \tag{5.3}$$

where ΔT is the period for which the new actions will be applied in the system (see Fig. 3.2 of Chapter 3), P^{DG} is the output power of DGs (in kW), $cost_{\text{fuel}}$,is the cost of fuel used in the DGs (in \$/liter) and $cost_{\text{em}}$, is their greenhouse emission cost (in \$/kg). The fuel expenditure

is taken as a quadratic function and expressed as:

$$cost_{\text{fuel}} = \psi\ (\gamma_{11} + \gamma_{12}\ P^{DG} + \gamma_{13}(P^{DG})^2) \tag{5.4}$$

where γ is a constant, and $\psi = 0$ when the DG is not operating; otherwise, it is unity. In a similar way, $cost_{BSS}$ and $cost_{loss}$ are defined as

$$cost_{BSS} = \psi\ (\gamma_{21} + \gamma_{22}\ |P^{BSS}| + \gamma_{23}\ (P^{BSS})^2) \tag{5.5}$$

$$cost_{loss} = \gamma_{31} P^{loss} + \gamma_{32}\ (P^{loss})^2 \tag{5.6}$$

In (5.5), $\psi = 1$ if the BSS is in operation; otherwise, it is zero. Also, the absolute operator of $|.|$ is used in (5.5) because P^{BSS} can be positive and negative.

In (5.1), FF_{int} is formulated as

$$FF_{int} = \Delta T \left(\sum P_{shed}^{load} cost_{shed} + \sum P_{curt}^{NDER} cost_{curt} \right) \tag{5.7}$$

in which P_{shed}^{load} and P_{curt}^{NDER} are respectively the amount of load-shedding and renewable curtailment (in kW) whilst $cost_{shed}$ and $cost_{curt}$ are respectively, their corresponding costs (in \$/kWh).

Similarly, FF_{vf} is derived as

$$FF_{vf} = \max(\Delta V_x) + |\Delta f| + PF \tag{5.8}$$

Where *PF* is penalty factor and $PF = 0$ unless one of the following technical constraints is not satisfied:

$$\sum S^{DDER} + \sum S^{NDER} = \sum S^{BSS} + \sum S^{load} + \sum S^{loss} \tag{5.9a}$$

$$-P_{cap}^{BSS} \leq P^{BSS} \leq +P_{cap}^{BSS} \quad (5.9b)$$

$$SoC^{min} \leq SoC \leq SoC^{max} \quad (5.9c)$$

$$P_{LB}^{DG} \leq P^{DG} \leq P_{cap}^{DG} \quad (5.9d)$$

$$-\sqrt{\left(S_{cap}^{DDER}\right)^2 - \left(P^{DDER}\right)^2} \leq Q^{DDER} \leq \sqrt{\left(S_{cap}^{DDER}\right)^2 - \left(P^{DDER}\right)^2} \quad (5.9e)$$

$$P_{shed}^{load} \leq P^{load} \quad (5.9f)$$

$$P_{curt}^{NDER} \leq P^{NDER} \quad (5.9g)$$

$$V^{min} \leq |V_x| \leq V^{max} \quad (5.9h)$$

$$f^{min} \leq f \leq f^{max} \quad (5.9i)$$

$$I_l \leq (I_l)^{max} \quad (5.9j)$$

$$P^{loss} < (P^{loss})^{max} \quad (5.9k)$$

Eq. (5.9a), represent the power balance within the microgrid while (5.9b-c), show the limitation in power exchange and the SoC of the BSS. The lower and upper bounds of the output power of a DG and a DDER are given by (5.9d-e). The maximum load-shedding limit and curtailment of the NDERs are defined in (5.9f-g). Eq. (5.9h-k) show the permissible variation in voltage and frequency in the buses of the microgrid, as well as the thermal limits of the current and the power loss in the network lines.

5.3 Floating Point Genetic Algorithm Solver

The floating point-genetic algorithm operation, includes an iterative mechanism of population initialisation, calculating the developed fitness function for each chromosome of

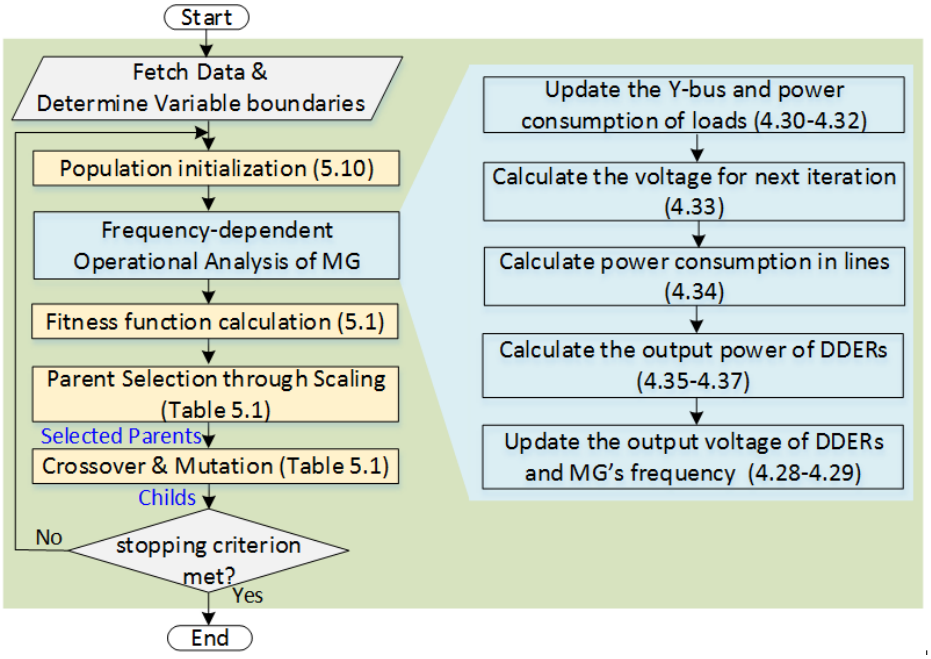

Fig 5.1 Flowchart of the floating point-genetic algorithm-based optimisation including the frequency-dependent analysis of the microgrid.

the population, applying different operators on a specific or suitable portion of the population, to generate a new population, until fulfilling the stopping criteria. The different stages of the floating point-genetic algorithm-based solution and frequency dependent power flow analysis (as described in Chapter 4), is depicted in Fig. 5.1.

5.3.1 Population Initialisation

In this study, the first population is created randomly; however, it is to be noted that under some situations, a randomly generated initial population, can restrict the considered solutions in the zone of local minima [139]. Alternatively, other techniques such as full load average production, cost-based priority order, and adapted priority list, can be used [140-141]. Considering the control variables for this study as being the output power of the DGs, the BSSs, load-shedding and the NDERs curtailment (i.e., $P^{DG}, P^{BSS}, P_{shed}^{load}$ and P_{curt}^{NDER}), a population

with *N* chromosomes, can be formed and represented by a matrix in the form of (5.10), in which each *gene* takes a floating-point number. Thus, the population is a double vector, considering both the integer and decimal numbers of the *gene*s [142].

$$pop = \begin{matrix} chrm\text{-}1 \\ chrm\text{-}2 \\ \vdots \\ chrm\text{-}N \end{matrix} \begin{bmatrix} P_1^{DDER} & \dots & P_{N_{DDER}}^{DDER} & P_{shed,1}^{load} & \dots & P_{shed,N_{load}}^{load} & P_{curt,1}^{NDER} & \dots & P_{curt,N_{NDER}}^{NDER} \\ P_2^{DDER} & \dots & P_{N_{DDER}}^{DDER} & P_{shed,2}^{load} & \dots & P_{shed,N_{load}}^{load} & P_{NDER,2}^{curt} & \dots & P_{curt,N_{NDER}}^{NDER} \\ \vdots & & \vdots & & & & \vdots & & \\ P_N^{DDER} & \dots & P_{N_{DDER}}^{DDER} & P_{shed,3}^{load} & \dots & P_{shed,N_{load}}^{load} & P_{NDER,N}^{curt} & \dots & P_{curt,N_{NDER}}^{NDER} \end{bmatrix} \quad (5.10)$$

5.3.2 Floating Point Genetic Algorithm Operators

Three operators of scaling, crossover and mutation, are used here to define the optimal solution. They are discussed briefly below, while their characteristics are summarised in Table 5.1.

In each iteration of the floating point-genetic algorithm, the scaling operator makes copies of solutions that pose the best values of the fitness function in the previous iteration. If for some solutions, the considered technical constraints are not met, the scaling operator will try to scale them in a range that is suitable for the mutation and cross over operations. Otherwise, if the solution does not seem to be feasible, it will eliminate them from the solution pool. This operator affects the performance of the floating point-genetic algorithm, by selecting a suitable range for the scaled values. For instance, if the scaled values vary too widely, the *gene* with the highest scaled values, reproduce too rapidly, taking over the solution pool too quickly, and preventing the floating point-genetic algorithm, from searching other areas of the solution space. On the other hand, if the scaled values vary only a little, all *gene*s will have approximately the same chance of reproduction, and thereby, the search will progress very slowly. The sum of the scaled values, over the entire population, equals the number of parents needed to create the next population.

The scaling operator can be used in either of the Rank, Proportional, Top and Shift-linear functions. The Rank function, scales the solutions based on the rank (*Rank*) of each *gene* (i.e., the order of a chromosome within a population, when sorted from least to highest fitness function value). This function scales down each chromosome by $1/\sqrt{Rank}$ of that chromosome. On the other hand, the Proportional function distributes proportionately, between the unscaled and scaled *gene*s. This function forms a new population, with all chromosomes in the previous population, after sorting them in proportional to their *Rank*. The Top function forms a new population by a process in which a specific percentage of chromosomes with the best *Rank,* are selected and then multiplied with a constant number to equalize them. Thus, only a certain percentage of the fittest *gene* is selected as parents, for the next population. Hence, the Top function restricts parents to the fittest *gene* and creates less diverse populations, than other functions. In case of Shift-linear function, a new population is formed by adding and multiplying a constant number to each chromosome

Table 5.1 Floating Point-Genetic Algorithm Operators Characteristics.

Operator	Function	Characteristics
Scaling [143-145]	Rank	• All chromosomes of the population are selected, however, each chromosome is scaled down by $1/\sqrt{Rank}$ of that chromosome.
	Proportional	• New population is formed by all chromosomes in the previous population after being sorted proportional to their *Rank*.
	Top	• New population *is* formed by a process in which a specific percentage of chromosomes with best *Rank* are selected and then multiplied with a constant number to equalize them.
	Shift-linear	• New population is formed by adding and multiplying a constant number to each chromosome.
Crossover	Constraint-	• Crossover of chromosome is applied such that the corresponding

[146-147]	dependent	constraints of *gene*s are satisfied.
	1-point	• Forming a child by selecting the first portion of *gene*s from parent-1 and the second portion from parent-2 based on the assumed position of a *gene* within a chromosome and a specific percentage of chromosomes.
	2-point	• Forming a child by selecting the first portion of *gene*s from parent-1, the second portion from parent-2 and the third portion from parent-1 based on the assumed position of two *gene*s within a chromosome and a specific percentage of chromosomes.
	Scattered	• Creating a random binary vector (with a size equal to that of a parent) and forming a child by selecting *gene* from parent-1 when the random number is unity and from parent-2 when the random number is zero.
	Intermediate	• Forming a child by adding one of the parents with the difference between two parents after being multiplied by a random number.
	Heuristic	• Forming a child by adding the parent with the higher *Rank* to the absolute of the difference between two parents after being multiplied by a random number.
	Arithmetic	• Forming a child by averaging each *gene* of two parents.
Mutation [148-149]	Constraint-dependent	• Mutation of the chromosome is applied so that the corresponding constraints of the *gene*s are satisfied.
	Gaussian	• Adding a random number (taken from a Gaussian distribution curve with a zero mean value) to each *gene*.
	Uniform	• Adding a random number to a specific percentage of *gene*s
	Feasible	• Adding or subtracting a random number to each *gene* to result in feasible values for each decision variable.

The crossover operator, aims to recombine different solutions whilst serving two main roles: providing new chromosomes for the next iteration from the current population, and provides unique and new hyperplanes for the existing new chromosomes, which were not presented by the parent chromosomes. Thus, there will be a chance that the probability of the better performing child will increase. This operator can be applied using different methods such as the well-known 1-point, 2-point, scattered techniques, or the newly proposed ones such as the constrained-dependent, intermediate, heuristic and arithmetic [143] (see Table 5.1).

The mutation operator is used,, to visit, some untouched points, in the search space. To this end, a random number can be added to the existing population. Low probability is assigned to this operator, to avoid the increase of randomness. This operator can be applied, using different functions, such as constrained-dependent, Gaussian, uniform and the adaptive feasible functions [143] (see Table 5.1).

Along with the abovementioned operators, there are two variables that should be selected carefully for the reproduction of *genes* for the next population. These variables are elite count and crossover fractions. The elite count determines the number of *genes* that are sure to survive in the next population and its value is less than or equal to the population size. On the other hand, the crossover fraction, varying between 0 and 1, determines the proportion of the *genes* that the crossover operator is applied to.

5.3.3 Stopping Criterion

The iterative procedure of generating new populations from an existing one, continues until defining the optimal solution. The stopping criterion achieves an acceptable convergence for the fitness function with a confidence level of 95%. This is deemed to be true when no significant improvement is observed in the progressive solution; e.g.., the mean and variance

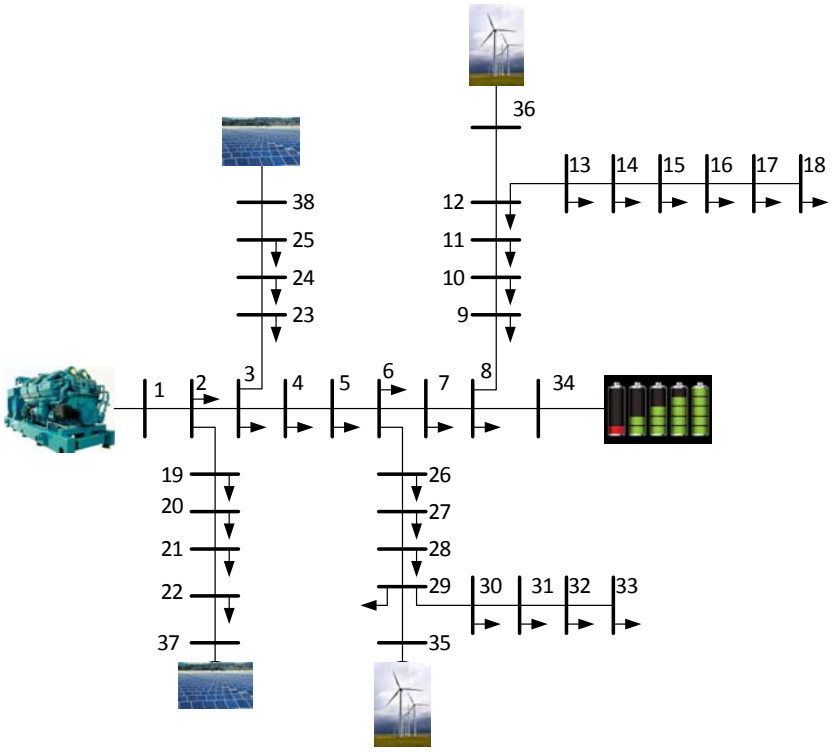

Fig 5.2 Considered 38-bus system microgrid system.

of the fitness functions' optimal value obtained in each trial remains almost unchanged, with respect to the number of iterations. Additionally, to prevent immature results, a minimum number of iterations have to be applied. Moreover, a maximum number of iterations are also assumed to reduce the simulation time.

5.4 Performance Evaluation

A floating point-genetic algorithm, is applied to yield the most optimal performance of the considered 38-bus microgrid of Fig. 5.2, to solve the formulated fitness function of (5.1). In the considered microgrid, it is assumed that x NDERs and 2 x DDERs (composed of one DG and one BSS) are connected to the network, as seen in the following figure. Table 5.2 lists their assumed nominal capacities, as well as the nominal and permissible limits of variation, for the voltage and frequency in the microgrid, along with the assumed costs for the different

Table 5.2 Considered parameters for numerical analyses.

Parameters used in (4.19)-(4.25) for power calculation of wind-based NDERs

$\boldsymbol{\lambda = 8.1}$; $\rho = \mathbf{1.225\ Kg/m^3}$; $\boldsymbol{\eta = 0.75}$; $\theta = \mathbf{0.2}°$; $\boldsymbol{A = 7.254\ m^2}$;

$\boldsymbol{q_{step} = 0.73}$; $\boldsymbol{P_{cap}^{wind} = 60\ kW}$

Weibull probability density function parameters: shape =0-2; scale=0-1; location=0

Nominal Capacities of demand, supply and storage system

P_{cap}^{PV} [kW]	P_{cap}^{wind} [kW]	P_{cap}^{load} [kW]	P_{LB}^{DG} [kW]	P_{cap}^{DG} [kW]	P_{cap}^{BSS} [kW]	SoC (%)	$P_{ch,max}^{BSS}$ [kW]	$P_{Dch,min}^{BSS}$ [kW]
50	60	850	70	650	200	20-100	20	190

Technical permissible limits

$\boldsymbol{f^{nom} = 50\ Hz}$; $\boldsymbol{f^{min} = 49.5\ Hz}$; $\boldsymbol{f^{max} = 50.5\ Hz}$

$\boldsymbol{V^{nom} = 1pu}$; $\boldsymbol{V^{min} = 0.975\ pu}$; $\boldsymbol{V^{max} = 1.025\ pu}$

Costs and parameters values for fitness function calculation

$\boldsymbol{cost_{fuel} = 5}$ \$/kWh; $\boldsymbol{cost_{em} = 2}$ \$/kg; $\boldsymbol{cost_{loss} = 0.8}$ \$/kWh;

$\boldsymbol{cost_{curt} = 25}$ \$/kWh; $\boldsymbol{cost_{shed} = 5.5}$ \$/kWh;

$\boldsymbol{\gamma_{11} = 2.438}$, $\boldsymbol{\gamma_{12} = 2.554}$; $\boldsymbol{\gamma_{13} = 0.0025}$; $\boldsymbol{\gamma_{21} = 3.01}$; $\boldsymbol{\gamma_{22} = 0.08}$;

$\boldsymbol{\gamma_{23} = 0.0025}$; $\boldsymbol{\gamma_{31} = 1.8}$; $\boldsymbol{\gamma_{32} = 0.00876}$, $\boldsymbol{k_1}$= 2.7; $\boldsymbol{k_2}$= 1; $\boldsymbol{k_3}$= 1.3; $\boldsymbol{k_4}$= 1.

criteria in (5.2)-(5.8) and the limits of the technical constraints of (5.9). The considered network topology and impedances are taken from [150].

The microgrid of Fig. 5.2, is analysed under two events. In Event-1, it is assumed that the total demand of the microgrid increases from 651 to 675 kW (i.e., 6% increase). Following this demand increase, the maximum voltage and frequency of the system respectively drops to 0.92 pu and 49.23 Hz (both below the permissible limits of 0.95 pu and 49.5 Hz, respectively).

Table 5.3 Considered events and their optimal solutions.

Initial status						
	P^{load}	P^{DG}	$\max(\lvert V_x \rvert)$	$\min(\lvert V_x \rvert)$	f	P^{NDER}
	[kW]	[kW]	[pu]	[pu]	[Hz]	[kW]
Event-1	675	636.2	0.994	0.923	49.23	38.8
Event-2	450	392.7	1.046	1.039	50.2	57.8

Optimal solution								
	P^{DG}	$\max(\lvert V_x \rvert)$	$\min(\lvert V_x \rvert)$	f	P^{BSS}	P^{loss}	P^{NDER}_{curt}	P^{load}_{shed}
	[kW]	[pu]	[pu]	[Hz]	[kW]	[kW]	[kW]	[kW]
Event-1	623.3	1.034	0.986	49.82	13.5	1.6	0	1.3
Event-2	411.2	1.022	0.991	50.12	-15	0.2	4	0

At this time, the DG is supplying 636.2 kW, while the NDERs' overall contribution is 38.8 kW. In Event-2, it is assumed that the total demand of the microgrid, decreases from 500 to 450 kW while the DG is supplying 392.7 kW along with a 57.8 kW contribution from NDERs. As a result, the frequency and the maximum voltage across the microgrid, are respectively 50.2 Hz and 1.046 pu (i.e., voltage exceeds the permissible limit of 1.025 pu, while frequency is within the range). Table 5.3 summarizes these events.

When applying the floating point-genetic algorithm, to determine the optimal control variables for the microgrid, under consideration in each of the above two events, it is assumed that the size of the population is 100 and that the initialisation of the first population is random. Based on (5.10), each chromosome in this study is composed of 38 *gene*s (i.e., one P_{DG}, one P_{BSS}, 32 P^{shed}_{load} and 4 P^{curt}_{NDER}). The elite count for *gene* reproduction in the next iteration is thought to be 5% of the population size (i.e., 5) while the crossover fraction is 0.5. When using the Top function as the scaling operator, 40% of the fittest *gene*s are scaled to the same value.

The minimum number of iterations needed to prevent an immature solution is assumed to be 50 while the maximum number of iterations are set to be 150. Also, the confidence level for the convergence of the analysis, is assumed to be 95%.

For the given assumptions, the fitness function of (5.1), is solved several times for each event in Matlab. In each study, the type of the function of one of the operators is varied. Considering the 4 functions for scaling, 6 functions for crossover and 4 functions for mutation (see Table 5.1), overall, the system can be analysed under $44 \times 6 \times 4 = 96$ scenarios. It is noteworthy that the actual number can be infinite, considering the continuous range of numerical variations that some functions have. Also, as the considered microgrid has technical constraints to satisfy, at least one of the operators of the crossover or mutation should be constraint-dependent; otherwise, all constraints will not be satisfied and the results will be unacceptable.

From this perspective, Table 5.4 lists only those analysis results in which a constraint-dependent function is used. The analyses are referred to as R1 to R10, P1 to P10, T1 to T10 and S1 to S10 so as to respectively denote those analyses that the scaling operator is using including Rank, Proportional, Top and Shift-linear functions whereas numbers 1 to 10 illustrate different combinations of crossover and mutation functions. For any of these scenarios, the best (optimal) solution is presented, for both of the considered events. The number of iterations in which the best solution is defined, is also given. The scenario that has yielded the lowest fitness function value is highlighted for each group of the scaling functions (i.e., scenario-R4, P3, T9 and S3 for Event-1, and R9, P5, T1 and S9 for Event-2).

The convergence of the fitness function value for each of these scenarios, is depicted in Fig. 6. Comparing these scenarios between Event-1 and Event-2, illustrates no consistency on the combination type of the crossover and mutation functions for each scaling function. However, it can be seen that the Top function of the scaling operator, yields the most feasible

solution (i.e., the solution with the least fitness function at the least number of iterations) for both events (i.e., scenario-T9 and T1 for Event-1 and 2, respectively). This is in line with the findings of [147] because this function restricts parents to the fittest gene and creates less diverse populations than other functions. The study further continues to analyse 1,000+ different events in a Monte Carlo analysis and the above conclusion was observed for those events as well.

Table 5.4 Different combinations of the operators for solving the microgrid optimisation problem using an floating point-genetic algorithm.

Scenario	Scaling Function	Mutation	Crossover	Optimal Solution			
				Event-1		Event-2	
				Iteration number	Fitness function [$]	Iteration number	Fitness function [$]
R1	Rank	Constraint-dependent	Constraint-dependent	93	102.26	150	96.67
R2		Gaussian		89	Infeasible	150	Infeasible
R3		Uniform		150	95.01	141	94.36
R4		Adaptive Feasible		91	93.48	150	95.34
R5			Scattered	134	94.34	142	92.81
R6			1-point	79	113.02	150	94.65
R7		Constraint-dependent	2- point	150	98.14	150	92.88
R8			Intermediate	150	94.04	148	95.20
R9			Heuristic	125	115.21	141	94.59
R10			Arithmetic	144	96.19	143	92.93

P1	Proportional	Constraint-dependent	Constraint-dependent	95	96.68	150	99.23
P2		Gaussian		150	Infeasible	150	Infeasible
P3		Uniform		141	96.13	147	92.44
P4		Adaptive Feasible		150	92.15	146	95.39
P5		Constraint-dependent	Scattered	150	96.87	142	92.86
P6			1-point	150	98.43	150	92.94
P7			2- point	150	94.92	136	96.33
P8			Intermediate	68	99.19	150	97.41
P9			Heuristic	150	92.11	150	93.05
P10			Arithmetic	131	97.91	119	94.34
T1	Top	Constraint-dependent	Constraint-dependent	133	94.91	138	90.16
T2		Gaussian		150	Infeasible	89	Infeasible
T3		Uniform		144	94.77	150	96.45
T4		Adaptive Feasible		150	96.01	150	94.66
T5		Constraint-dependent	Scattered	150	97.15	134	96.23
T6			1-point	150	92.23	79	95.46
T7			2- point	150	97.78	150	97.03
T8			Intermediate	150	98.97	150	96.56
T9			Heuristic	150	92.15	138	97.32
T10			Arithmetic	64	102.25	144	94.80
S1	Shift-linear	Constraint-dependent	Constraint-dependent	101	96.54	93	93.29
S2		Gaussian		150	Infeasible	89	Infeasible
S3		Uniform		125	93.22	150	94.35
S4		Adaptive		70	97.35	150	95.01

	Feasible					
S5		Scattered	150	93.87	134	94.66
S6		1-point	150		79	93.23
S7	Constraint-	2- point	122	101.05	150	92.69
S8	dependent	Intermediate	150	93.64	150	92.84
S9		Heuristic	150	94.66	139	92.20
S10		Arithmetic	66	97.27	144	94.38

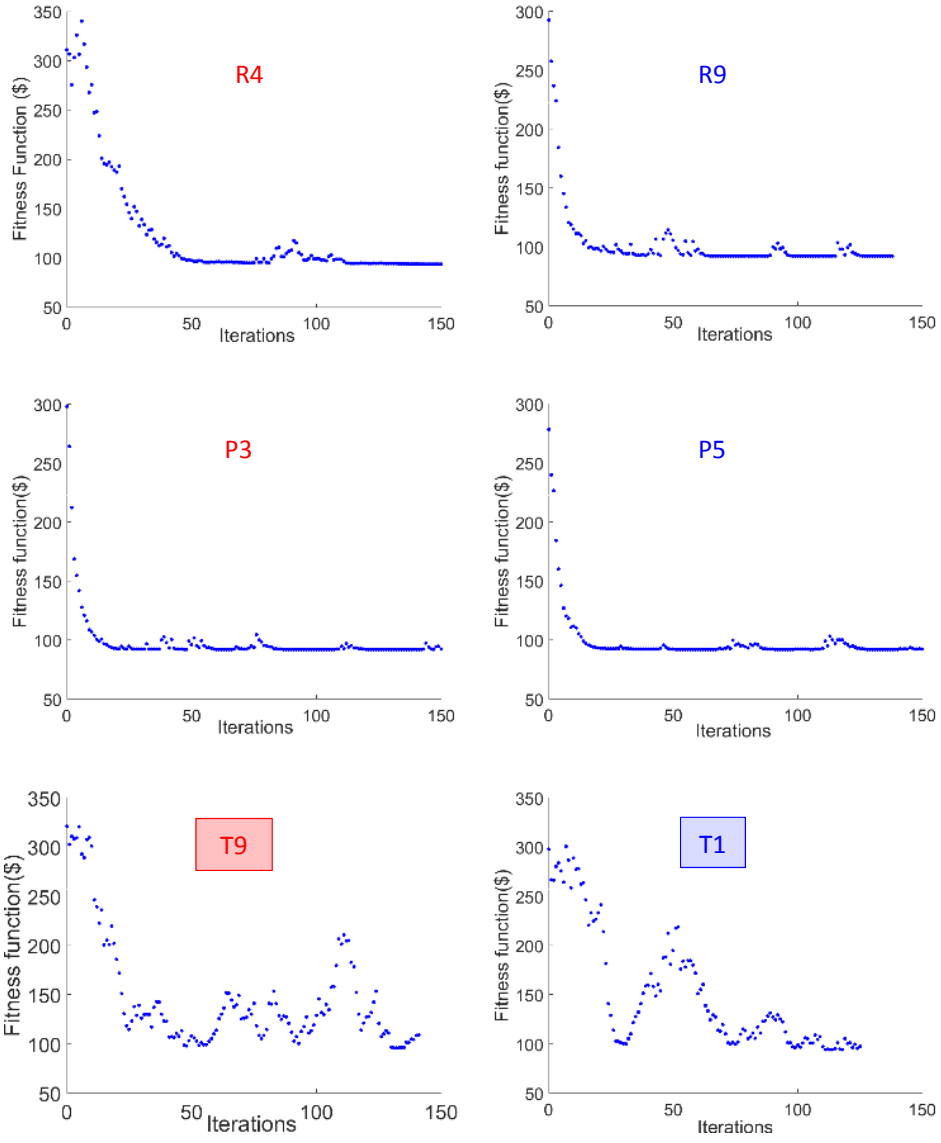

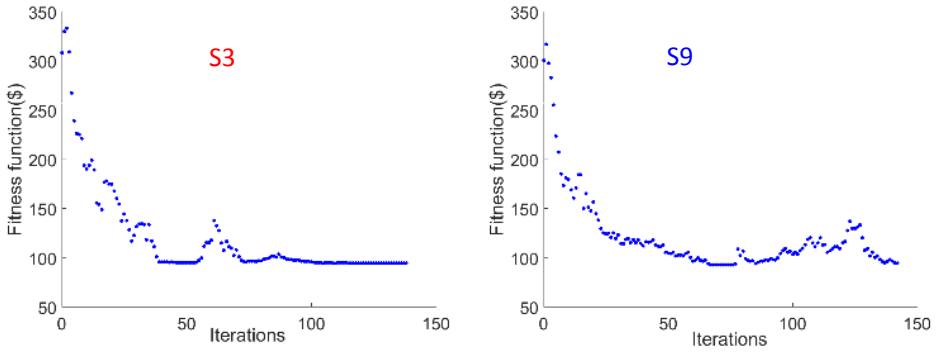

Fig 5.3 Comparison of potential results of all case studies of observed events.

As seen from Table 5.4, the best value of the fitness function in Scenario-T9 versus those of R4, P3 and S3 is 1-5% lower for Event-1. This is similar, when comparing the fitness function of Scenario-T1 versus those of R9, P5 and S9. The values of the control variables defined by scenario-T9 and T1 (for Event-1 and 2 respectively) are listed in Table 5.3. As seen from this Table, in Event-1, before applying the optimisation technique, the microgrid had to apply a load-shedding of 13.4 kW to maintain the frequency within the desired limit. However, the developed fitness function proposes to reduce the output power of the DG from 636.2 to 623.3 kW on top of discharging the BSS by 13.5 kW and a load-shedding of 1.3 kW. Thus, the microgrid frequency increases from 49.23 to 49.82 Hz (above the minimum allowed level of 49.5 Hz) whilst the minimum observed voltage magnitude of the microgrid, increases from 0.923 to 0.986 pu (above the minimum allowed level of 0.975 pu). Similarly, in Event-2, before applying the optimisation technique, the microgrid had to apply a RC of 19 kW to maintain the voltage to within the desired limits. However, the developed fitness function proposes to charge the BSS by 15 kW and a RC of 4 kW. Thus, the maximum observed voltage magnitude of the microgrid reduces from 1.046 to 1.022 pu (below the maximum allowed level of 1.025 pu).

5.5 Summary

A floating point-genetic algorithm-based solver, is used in this chapter to determine the optimal control variables in a standalone microgrid, under emergencies such as overloading and excessive generations of the NDERs that has led to unacceptable voltage and/or frequency deviation. The formulated fitness function, considers the operational cost of the DDERs, the interruption cost to loads and the NDERs, as well as the voltage and frequency deviation from their nominal values. The study has focused on the impact of the scaling operator for the floating point-genetic algorithm solver, when forming new populations within the optimisation algorithm, along with different combinations of the crossover and mutation functions. The efficacy of a scaling operator in combination with other operators is already proven in the literature; thus, this chapter only focused on the interplay of various functions of the scaling operator. Through numerous analyses over a considered microgrid network, realised in Matlab, it is seen that the Top function of the scaling operator helps the solver to yield a 1-5% lower value for the best fitness function, in comparison to the other scaling functions. The results were validated by a Monte Carlo study.

It is to be noted that scaled fitness functions can also be applied for solving optimisation problems of large interconnected systems within a floating point-genetic algorithm solver; however, a standalone hybrid microgrid, was considered as the non-linear test case in this research, because it can observe larger deviations in its voltage and frequency, due to the variability of its loads and the NDERs.

Chapter 6. Supervisory Emergency Control for Microgrid Clusters

6.1 Introduction

Remote and regional areas are usually supplied by isolated and self-sufficient, electricity supply systems. These systems, often referred to as microgrids, rely on renewable energy-based NDERs, to reduce the overall cost of electricity production. Emergencies, such as overloading and excessive generation by renewables sources, can lead to significant voltage or frequency deviation in these systems. As a result, protective relays trip some of the sources or loads, to prevent system instability. This chapter presents a multi-stage, supervisory emergency controller, for microgrids in such emergencies so as to provisionally manage them. The proposed controller, includes different layers of actions. These actions include, soft actions, such as adjustments of the droop control parameters of the sources and charging/discharging the control of the existing battery energy storage systems Other actions are the intermedial actions, which include the power exchanges within a group of neighbouring microgrids (which is highly probable in the case of large remote areas), as well as the hard actions, such as the curtailment of the loads or renewable sources (as the last resort). Other objectives, include the minimizing of the power loss in the tie-lines between the microgrids as well as minimising the dependency of a microgrid upon the external microgrids, Another focus includes maximizing the contribution of renewable sources to the generation of electricity, whilst minimizing the

fuel consumption and greenhouse gas emissions from the conventional generators, along with frequency and voltage deviations. To this end, a suitable optimisation problem is formulated and solved, identifying the most suitable actions and their level of contribution, to producing the least cost for the operator. The performance of this proposal, is evaluated by several numerical analyses carried out in Matlab.

6.2 Problem Formulation

The optimisation problem has been formed to determine the most economical solution to overcoming the overloading or over-generation issue. This issue subsequently causes under-voltage/frequency and over-voltage/frequency, in the problem microgrid(s), under the proposed power transaction strategy, described above. This is formulated as an objective function (OF), which is solved by the supervisory emergency controller, to yield the most feasible solution whilst minimizing the overall operational costs and maximizing the footprint of renewables and the spinning reserve in them as well as satisfying the considered technical constraints. It is formulated as a multi-objective problem, with an OF in the form of

$$OF = w_1 OF_{\text{tech}} + w_2 OF_{\text{oper}} + w_3 OF_{\text{cont}} \tag{6.1}$$

where OF_{tech}, OF_{oper} and OF_{cont} are respectively the OFs denoting the technical, operational and desirable conditions in the coupled microgrid and the isolated problem microgrid(s). In (6.1), w_1 to w_3 are the weightings of the considered OFs. The calculated *OF*, highly depends upon the assumed weightings, related to each OF; therefore, it is important to carefully select them. In power systems that have complex configurations, there is no systematic method to define these weightings; however, an acceptable method is to conduct a survey with field experts' to gather their opinions regarding the importance and impact of each OF [53]. These experts may express the importance either n numerical terms (e.g., 0 to 100%) or linguistic terms (e.g. extremely/very/little big/small or neutral). These responses can then be mapped into

a digit, in the range of [0, 1] and then normalised. At the end, the weighting of each OF, they will be expressed as the average of all normalised values as:

$$w = \sum_k w_k \ /N_{\text{exp}} \tag{6.2}$$

where N_{exp} is the number of experts that participated in the survey. In this work, for the purpose of simplicity, it is assumed that $w_1 = w_2 = w_3$ (e.g., each OF is assumed to be of equal importance).

In (6.1), the OF_{tech} aims to selecting those sets of decision variables (actions) that will yield the minimum voltage and frequency deviation, in the coupled microgrid and the isolated, problem microgrid. It is expressed as,

$$OF_{\text{tech}} = |\Delta f| + \max(|\Delta V|) + Violation \times Penalty \tag{6.3}$$

in which $|\Delta V|$ and $|\Delta f|$ represents respectively, the level of voltage magnitude deviation, in all the buses of the microgrids; within the coupled microgrid and the isolated problem microgrid(s) and the corresponding frequency deviation (in pu). $Penalty$ is selected as a large value (e.g., 10^8), to eliminate those sets of decisions (conditions), that yield unacceptable voltage or frequency deviation, in the coupled microgrid and the isolated problem microgrid(s), or overloading of microgrid lines. Thus, $violation$ is defined as:

$$Violation = V_{\text{vio}} + I_{\text{vio}} + f_{\text{vio}} + Constraint_{\text{vio}} \tag{6.4}$$

where

$$\begin{aligned}
V_{\text{vio}} &= \begin{cases} 1 & \exists|\Delta V_i| > \Delta V^{\max}, i \in \textbf{bus} \\ 0 & \text{otherwise} \end{cases} \\
I_{\text{vio}} &= \begin{cases} 1 & \exists|I_i| > I^{\max}, i \in \textbf{line} \\ 0 & \text{otherwise} \end{cases} \\
f_{\text{vio}} &= \begin{cases} 1 & |\Delta f| > \Delta f^{\max} \\ 0 & \text{otherwise} \end{cases}
\end{aligned} \tag{6.5}$$

$$Constraint_{\text{vio}} = \begin{cases} 1 & \text{if a considered constraint is not met} \\ 0 & \text{otherwise} \end{cases}$$

in which $\Delta V^{\max}$, $\Delta f^{\max}$ and $I^{\max}$ are respectively the permissible limits for the voltage

deviation, frequency deviation and the maximum line loading limit. Also, **bus** and **line** , are two vectors, representing the number of the buses and the lines, of the coupled microgrid and the isolated problem microgrid(s). These parameters are calculated from the power flow analysis, for clustered microgrids, which are described in next section of this chapter.

The OF_{oper} in (6.1), aims at minimising the overall operational cost of the coupled microgrid and the isolated problem microgrid(s), which includes those of the DGs, the BSSs, the power loss and the power transaction, along with the penalties because of the curtailing of the NDERs or non-essential loads and emitting greenhouse gases. It is formulated as:

$$OF_{\text{oper}} = \sum_{k} (\alpha_1 OF_{\text{DG}} + \alpha_2 OF_{\text{BSS}} + \alpha_3 OF_{\text{curt}} + \alpha_4 OF_{\text{trans}} + \alpha_5 OF_{\text{loss}}) Time \qquad \forall k \in \mathbf{MG} \tag{6.6}$$

where $OF_{\text{DG}}, OF_{\text{BSS}}$ and OF_{curt} are respectively the OFs, denoting the running cost of the DG(s), life loss cost of the BSS(s), and the penalty cost of curtailing the NDER(s) and/or non-essential load(s) of all microgrids, within the coupled microgrid and the isolated problem microgrid(s). OF_{trans} denotes the power transaction costs, for selected healthy microgrid(s) within the coupled microgrid, while OF_{loss} represents the corresponding cost of the power loss in the tie-line(s) between the microgrids of the coupled microgrid. The vector **MG** includes, the number of microgrids within the coupled microgrid and the isolated problem microgrid(s) while $Time$, is the total time required for the system to operate under the new condition (which is equal to ΔT of Fig. 3.6c in Chapter 3). In (6.6), α_1 to α_5 be coefficients to equalize the impact of the abovementioned OFs, which are derived respectively as:

$$OF_{\text{DG}} = \sum_{k} \left(C^{\text{fuel}} + C^{\text{cfp}} \partial_k\right) P_k^{\text{DG}} \qquad \forall k \in \mathbf{DG} \tag{6.6a}$$

$$OF_{\text{BSS}} = \sum_{k} C^{\text{BSS}} \left| P_k^{\text{BSS}} \right| \qquad \forall k \in \mathbf{BSS} \tag{6.6b}$$

$$OF_{\text{curt}} = \sum_{k} C_{\text{curt}}^{\text{NDERs}} P_{\text{curt}}^{\text{NDERs}} + \sum_{l} C_{\text{curt}}^{\text{load}} P_{\text{curt}}^{\text{load}} \qquad \forall k \in \mathbf{NDER}, l \in \mathbf{load} \tag{6.6c}$$

$$OF_{\text{trans}} = \sum_k C^{\text{trans}} |P_k^{\text{trans}}| \qquad \forall k \in \mathbf{MG} \tag{6.6d}$$

$$OF_{\text{loss}} = \sum_k C^{\text{loss}} P_k^{\text{loss}} \qquad \forall k \in \mathbf{line} \tag{6.6e}$$

In (6.6a), OF_{DG} , aims to minimise the running cost the power generation by the DGs (denoted by C in \$/kWh) which includes the cost for fuel consumption and the corresponding carbon footprints (respectively denoted by $^{\text{fuel}}$ and $^{\text{cfp}}$) where ∂_k is the emission ratio (in kg/kWh). As the BSS does not have any ongoing operational costs, only the cost of its life loss is considered in OF_{BSS} in (6.6b). Similarly, the corresponding cost of curtailing the output power of NDERs by $P_{\text{curt}}^{\text{NDERs}}$ and the non-essential loads by $P_{\text{curt}}^{\text{load}}$ (respectively denoted by $C_{\text{curt}}^{\text{NDERs}}$ and $C_{\text{curt}}^{\text{load}}$ in \$/kWh) is used in (6.6c) to determine OF_{curt}. The corresponding cost of power transaction ($|P^{\text{trans}}|$ in kW) over the tielines between the microgrids of the coupled microgrid (denoted by C^{trans} in \$/kWh) is used in (6d) to define OF_{trans}. Eq. (6.6e), aims at minimising the power loss in the tie-lines between the microgrids of the coupled microgrid (P^{loss} in kW) when calculating OF_{loss} while C^{loss} is the associated power loss cost (in \$/kWh). In (6.6), $\mathbf{DG}, \mathbf{BSS}, \mathbf{NDER}, \mathbf{load}$ and $\mathbf{line}$ are vectors respectively representing the number of the DGs, the BSSs, the NDERs ,the loads and lines (including tie-lines between microgrids) in the microgrids within the coupled microgrid and the isolated problem microgrid(s).

The OF_{cont} in (6.1) aims at maximising the contribution of NDERs in the overall demand supply as well as maximising the spinning reserve of the coupled microgrid and the isolated problem microgrid(s). It is formulated as:

$$OF_{\text{cont}} = (1 - RPL) + (1 - SRI) \tag{6.7}$$

in which $RPL \in [0, 1]$, represents the renewable penetration level of the coupled microgrid or the isolated problem microgrid, and is defined from:

$$RPL = \frac{\sum_{k_1} P^{\text{NDER}}}{\sum_{k_2} P^{\text{load}}} \qquad \forall k_1 \in \mathbf{NDER};\ \forall k_2 \in \mathbf{load} \tag{6.8}$$

to maximise the footprint of renewables, at the system for any given demand, while $SRI \in [0, 1]$ is the spinning reserve index of the microgrid, derived from:

$$SRI = \sum_k 1 - \frac{P_k^{\mathrm{DG}}}{\left(P_k^{\mathrm{DG}}\right)^{\max}} \qquad \forall k \in \mathbf{DG} \tag{6.9}$$

to have enough capacity in the system to respond appropriately and without being overloaded by a sudden increase in demand or an unexpected drop in the output power of the NDERs.

The OF of (6.1), is then solved by a genetic algorithm solver, with different composition of chromosome (described in next section), while considering the constraints of:

$$\sum_{k_1} S^{\mathrm{DG}} + \sum_{k_2} S^{\mathrm{NDER}} + \sum_{k_3} \beta S^{\mathrm{BSS}} + \sum_{k_4} S^{\mathrm{trans}} = \sum_{k_5} S^{\mathrm{load}} \sum_{k_6} S^{\mathrm{line}} \tag{6.10a}$$

$$\forall k_1 \in \mathbf{DG};\ \forall k_2 \in \mathbf{NDER};\ \forall k_3 \in \mathbf{BESS};\ \forall k_4 \in \mathbf{MG};\forall k_5 \in \mathbf{load};\ \forall k_6 \in \mathbf{line}$$

$$\begin{cases} \left(P_k^{\mathrm{DG}}\right)^{\min} \le P_k^{\mathrm{DG}} \le \left(P_k^{\mathrm{DG}}\right)^{\max} \\ \left|Q_k^{\mathrm{DG}}\right| \le \sqrt{\left(\left(S_k^{\mathrm{DG}}\right)^{\max}\right)^2 - \left(Q_k^{\mathrm{DG}}\right)^2} \end{cases} \qquad \forall k \in \mathbf{DG} \tag{6.10b}$$

$$\begin{cases} -\left(P_k^{\mathrm{BSS}}\right)^{\max} \le P_k^{\mathrm{BSS}} \le \left(P_k^{\mathrm{BSS}}\right)^{\max} \\ SoC^{\min} \le SoC^k \le SoC^{\max} \end{cases} \qquad \forall k \in \mathbf{BSS} \tag{6.10c}$$

$$V^{\min} \le |V^k| \le V^{\max} \qquad \forall k \in \mathbf{bus} \tag{6.10d}$$

$$f^{\min} \le f \le f^{\max} \tag{6.10e}$$

$$I_k \le I_k^{\max} \qquad \forall k \in \mathbf{line} \tag{6.10f}$$

Constraint (6.10a) shows the apparent power balance equation within the coupled microgrid and the isolated problem microgrid(s)in which β is respectively +1 and –1 for the discharging and charging BSSs. Constraint (6.10b) denotes the active and reactive power loading of DGs. Likewise, the active power loading and SoC limits of BSSs are given by (6.10c). The variation limits of the voltage magnitude at all buses of the coupled microgrid or isolated problem microgrid(s) are given by (6.10d-e) whereas (6.10f) shows the current loading of each line in those systems.

6.3 Optimisation of Clustered microgrids using Genetic Algorithm

Genetic algorithm, is the solver used for finding the best optimal solution for the proposed supervisory emergency controller that has a proven record of accomplishment in solving optimisation problems of electrical distribution networks, including their planning and operational analysis [103]. In each iteration of the genetic algorithm, first a population is initialised, which is made of multiple chromosomes. The considered chromosome structure, for the purpose of this research, is illustrated schematically in Fig. 6.1 and includes respectively the droop set-points of $f^{\max}$ and $V^{\max}$, the droop coefficients of m^{DRS} and n^{DRS} for every droop regulated system, the power exchange between the microgrid and its BSSs, the power transaction between the microgrid and its neighbouring microgrids, the level of power curtailed from the NDERs and the load-shedding.

Next, the considered problem microgrid or the coupled microgrid, is analysed using the assumed control variables in each chromosome to find the corresponding OF of (1). Following this, the heuristic crossover, adaptive feasible mutation, and the Top scaling function are used to produce new chromosomes for the next iteration of the optimisation, until achieving a suitable convergence of the optimal OF value, with a confidence level of 95% and a maximum number of 200 iterations, while a minimum of 50 iterations are assumed to prevent immature convergence.

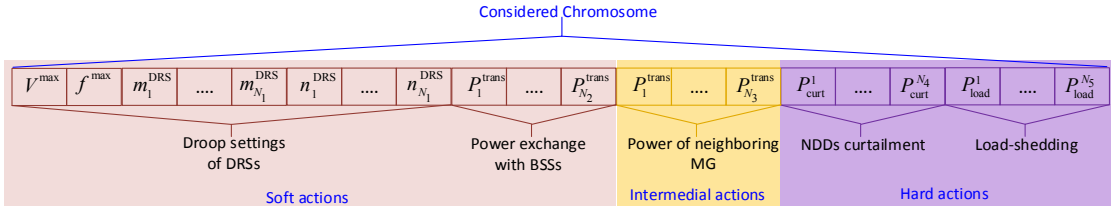

Fig 6.1 Considered structure of the chromosome in the genetic algorithm solver.

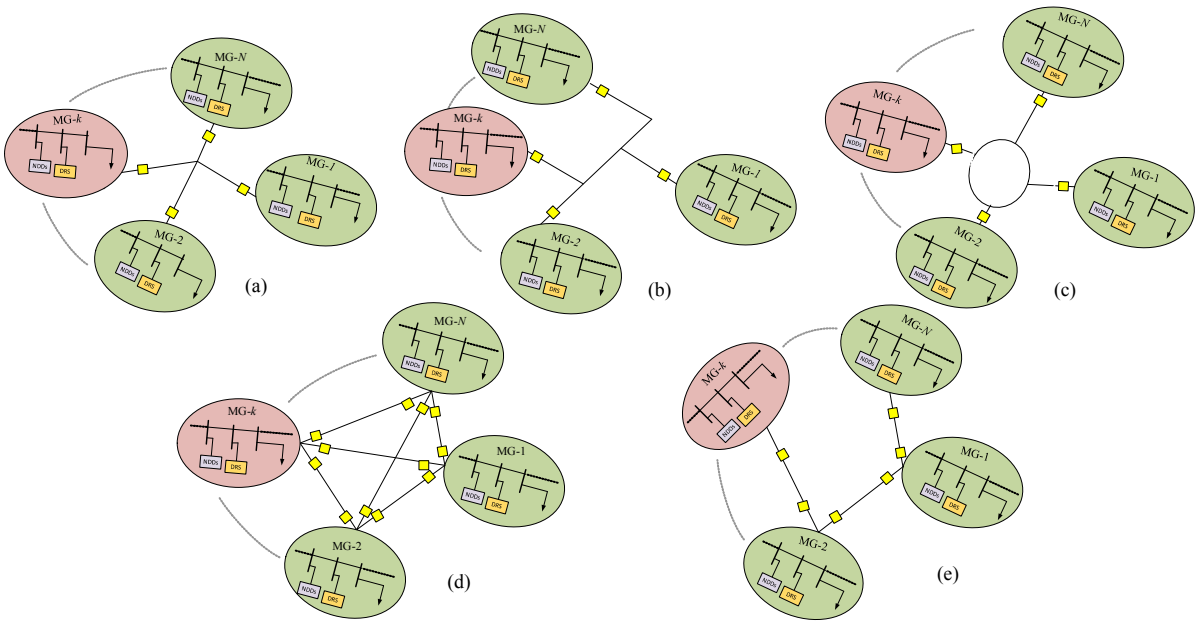

Fig 6.2 Possible physical communication links between microgrid(s) participating in coupled microgrids

6.4 Performance Evaluation

To evaluate the performance of the developed supervisory emergency controller, in sucessfully eleminating the emergency condition of a remote area microgrid, a Monte Carlo analysis is conducted in Matlab. Numerous random study cases have been produced, for some of which, an emergency condition of overloading, or excessive NDER generation, has been observed. The studies demonstrate that the developed supervisory emergency controller, can effectively address the emergency of a problem microgrid and can convert it to a healthy microgrid, by finding optimal values for the assumed soft, Intermedial and hard actions. A few of these study cases are described below:

First, let us consider a large remote area with 6 microgrids (named as microgrid-1 to microgrid-6) that are connected through a common central node (similar to the topology of Fig.

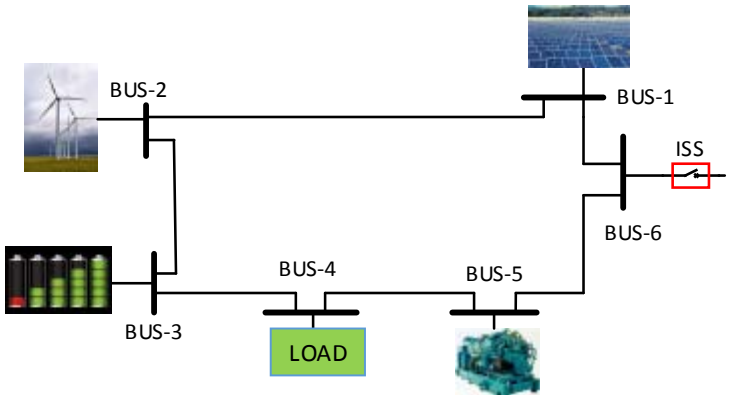

Fig 6.3 Topology of the considered microgrids for performance evaluation.

6.2a). For simplicity, all microgrids are assumed to have the same topology as of Fig. 6.3 because the performance of the developed supervisory emergency controller, is independent upon the internal topology of the microgrids, as well as their internal components and ratings. As seen from this figure, each microgrid is presumed to have two PV and wind-based NDERs, one BSS and one droop regulated system. All loads are connected to bus-4 of the microgrids,

Table 6.1 Considered nominal capacities for components of each microgrid in the numerical analysis.

	NDERs	Load	**DG**		**BSS**			
	$P_{\text{cap}}^{\text{NDERs}}$ (kW)	$P_{\text{cap}}^{\text{load}}$ (kW)	$(P^{\text{DG}})^{\min}$ (kW)	$(P^{\text{DG}})^{\max}$ (kW)	P^{BSS} (kWh)	$SOC^{\min}$ (%)	$SOC^{\max}$ (%)	$(P^{\text{BSS}})^{\max}$ (kW)
MG-1	25	65	12	40	10	20	100	9
MG-2	25	60	13.5	45	10	20	100	9
MG-3	35	85	15	50	12	20	100	11
MG-4	20	45	9	30	8	20	100	7
MG-5	30	80	16.5	55	14	20	100	12
MG-6	25	65	12	40	10	20	100	9

Table 6.2 Assumed distance between each microgrid of Fig. 4a from the central common point.

	MG-1	MG-2	MG-3	MG-4	MG-5	MG-6
Distance (km)	4	6	2	7	5	5

while the microgrids can couple with a neighbouring microgrid, through an ISS and a tie line at bus-6. The assumed nominal capacities of the loads, NDERs, DGs and BSSs of each microgrids are provided in Table 6.1, while the impedance data for all buses of the microgrids, is taken from [70]. Table 6.2, lists the distance between the microgrids, while Table 6.3 and 6.4 summarize the presumed different costs required, in calculating the OF of (6.1) and the important terminologies used in the numerical analysis. It is worth mentioning here that in all case studies the values of powers are normalize as pu values by using same base value.

Table 6.3 Considered costs data for the numerical analyses.

$\boldsymbol{C}^{\text{fuel}}$	0.31$/kWh	$\boldsymbol{C}^{\text{load}}_{\text{curt}}$	0.15 $/kWh
$\boldsymbol{C}^{\text{cfp}}$	0.02 $/kg	C^{BSS}	0.98 $/kWh
$\boldsymbol{C}^{\text{loss}}$	0.04 $/kWh	$C^{\text{NDERs}}_{\text{curt}}$	0.3 $/kWh
∂	0.003 kg/kWh	C^{trans}	0.4 $/kWh

Table 6.4 Important terminologies used in Case Studies for the proposed network

Terms	Explanation
PMG^{OL}	Problem Microgrid experiencing overloading
PMG^{OG}	Problem microgrid experiencing excessive generation by NDERs
PMGI	Problem Microgrid is left isolated
HMGA	Healthy Microgrid available
CMGF	Coupled Microgrid is formed
+	Power exported/discharged
-	Power exported/discharged
ACS	All constraints satisfied after actions

6.4.1 An overloaded Problem Microgrid

Consider study case-I (see Fig. 6.3a), in which microgrid-3 is detected as a PMG^{OL} (with a frequency of 49.38 Hz and a minimum voltage of 0.912 pu, both beyond the safe mode). As seen from Table 6.5, this microgrid has a load demand of 0.738 pu, an SRI of below 1% and an RPL of 34%). The developed supervisory emergency controller, proposes only soft action as the most optimal solution (with an OF value of 5.26$), to address the emergency of this microgrid. The supervisory emergency controller does not use any Intermedial and hard actions for this study case. As a result, a 0.034 pu support from the BSS reduces the output power of the droop regulated system from 0.498 to 0.446 pu, which will subsequently increase the observed minimum voltage and frequency to 0.963 pu and 49.71 Hz, respectively.

Now, let us consider study case-II, in which microgrid-5, is defined as an overloaded problem microgrid (denoted by PMG^{OL}) because of its operation within the unsafe mode (i.e., a frequency drop to 49.29 Hz and a voltage drop to 0.923 pu, both below the acceptable limits). At this condition, as seen from Table 6.5, the microgrid load demand is 0.782 pu, its RPL is 30% and its droop regulated system supplies 0.548 pu (nearly equal to its nominal capacity of 0.55 pu, as seen from Table 6.5), assuming a base power of 100kVA. Thereby, the SRI of the microgrid is almost zero. Without the developed supervisory emergency controller, the only possibility of recovering the microgrid into the safe mode, is a load-shedding of 0.1 pu. Assuming the implementation of the developed supervisory emergency controller, it takes action immediately when the voltage and frequency drop beyond the safe zone and solves this problem using a combination of soft and intermedial actions. As a result, microgrid-2 (a healthy microgrid with a load demand of 0.233 pu, an RPL of 23%, a minimum voltage of 1.039 pu, a frequency of 50.39 Hz and an SRI of 60%) along with microgrid-4 (A healthy microgrid with a load demand of 0.135 pu, an RPL of 8.9%, operating at 50.41 Hz and observing a minimum voltage of 1.034 pu and an SRI of 58.6%), are coupled with microgrid-5. This is the most

optimal solution with an OF value of 9$. As a result, microgrid-5 imports a total of 0.096 pu (i.e., 0.067 pu from microgrid-2 and 0.039 pu from microgrid-4 after a 0.01 pu loss in the tie lines) (see Fig. 6.4b). In addition, the droop regulated system of microgrid-2 and microgrid-4, supply 0.224 and 0.163 pu, respectively, which results in the droop regulated system of microgrid-5, to reduce its output to 0.452 pu. Additionally, the BSS of microgrid-2, will discharges 0.023 pu. As expected, the coupled microgrid formation increases the bus voltages in microgrid-5, while they decrease in microgrid-2 and microgrid-4. Consequently, the coupled microgrid frequency settles at 50.21 Hz and a minimum voltage of 0.989 pu, is observed throughout the coupled microgrid. As a result, the coupled microgrid's SRI becomes 35% while its overall RPL is 26%.

Now, let us consider case study-III, in which microgrid-3 is detected as the problem microgrid^{OL}, as shown in Fig. 6.4c and Table 6.5 (with a frequency of 49.69 Hz which is within the permissible range, but a minimum voltage of 0.937 pu, which is below the minimum allowed limit). Microgrid-3 has a load demand of 0.82 pu, an RPL of 39% and an SRI of only 1%. The developed supervisory emergency controller, proposes a combination of soft, intermedial and hard actions as none of the soft or intermedial actions alone can reach a feasible solution. The supervisory emergency controller proposes coupling of microgrid-1 (a healthy microgrid with a load demand of 0.206 pu, an SRI of 52% and an RPL of 8%, and operating at a frequency of 50.32 Hz and a minimum voltage of 1.024 pu) with the problem microgrid, as the most economical solution which results in the optimal OF value of 8.7$. Therefore, the output power of the droop regulated system of microgrid-1, increases from 0.192 to 0.232 pu, from which 0.056 pu is exported to the problem microgrid, while its BSS discharges by 0.016 pu, along with a load-shedding of 0.008 pu, in the problem microgrid. Thereby, microgrid-3 lowers down the output of its droop regulated system to 0.434 pu. Thus, the formed coupled microgrid, will observe a minimum voltage of 0.987 pu, and a frequency of 49.87 Hz along

Table 6.5 Case studies results for overloaded problem microgrids

Case Study	I	II			III		IV
Observed MGs	MG-3	MG-2	MG-4	MG-5	MG-3	MG-1	MG-2
MG's State	PMG^{OL}	HMG	HMG	PMG^{OL}	PMG^{OL}	HMG	PMG^{OL}
MG Parameters under Emergency							
P^{load} (pu)	0.738	0.233	0.135	0.782	0.82	0.206	0.57
P^{NDERs} (pu)	0.260	0.055	0.012	0.236	0.326	0.017	0.128
P^{DG} (pu)	0.498	0.18	0.124	0.548	0.494	0.192	0.446
max (V) (pu)	0.998	1.045	1.057	0.994	0.990	1.045	0.991
min (V) (pu)	0.912	1.039	1.034	0.923	0.937	1.024	0.910
f (Hz)	49.38	50.39	50.41	49.29	49.69	50.32	49.46
Mode	Unsafe	Safe	Safe	Unsafe	Alarm	Safe	Unsafe
SRI (%)	0.65	60	58.6	0.3	1.2	52	0.8
RPL (%)	34.21	23.6	8.9	30.17	39.7	8.2	22.4
CMG(s) Parameters after SEC's performance							
HMGA	no	yes			yes		no
CMGF	no	yes			yes		no
PMGI	yes	no			no		yes
ACS	yes	yes			yes		yes
P^{trans} (pu)		0.067	0.039	–0.096	–0.052	0.056	
$\boldsymbol{P^{NDER_s}_{curt}}$ (pu)							
$\boldsymbol{P^{load}_{curt}}$ (pu)					0.008		0.006
P^{BSS} (pu)	0.034	0.023				0.016	0.008
P^{DG} (pu)	0.446	0.224	0.163	0.452	0.434	0.232	0.428
CMG max (V) (pu)	1.041	1.034			1.039		1.004
CMG min (V) (pu)	0.963	0.989			0.987		0.955
$\boldsymbol{f}$ (Hz)	49.71	50.21			49.87		49.61
CMG Mode	Safe	Safe			Safe		Safe
P^{loss} (pu)	0.002	0.01			0.004		
CMG SRI (%)		35			74		
CMG RPL (%)		26.34			33.4		
OF ($)	5.26	9.00			8.70		12.23

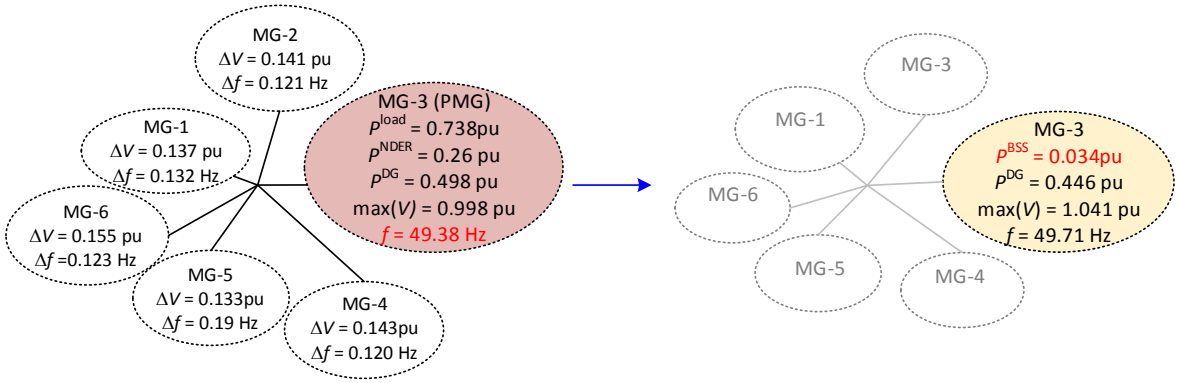
MG-2
ΔV = 0.141 pu
Δf = 0.121 Hz
MG-1
ΔV = 0.137 pu
Δf = 0.132 Hz
MG-3 (PMG)
P^load = 0.738pu
P^NDER = 0.26 pu
P^DG = 0.498 pu
max(V) = 0.998 pu
f = 49.38 Hz
MG-6
ΔV = 0.155 pu
Δf =0.123 Hz
MG-5
ΔV = 0.133pu
Δf = 0.19 Hz
MG-4
ΔV = 0.143pu
Δf = 0.120 Hz
MG-3
MG-1
MG-6
MG-5
MG-4
MG-3
P^BSS = 0.034pu
P^DG = 0.446 pu
max(V) = 1.041 pu
f = 49.71 Hz

(a)

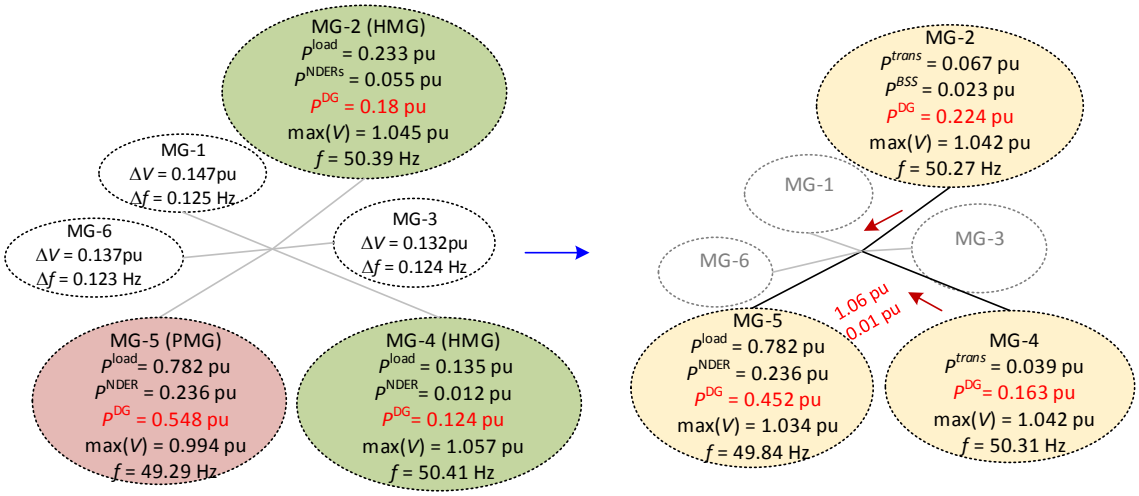
MG-2 (HMG)
P^load = 0.233 pu
P^NDERs = 0.055 pu
P^DG = 0.18 pu
max(V) = 1.045 pu
f = 50.39 Hz
MG-1
ΔV = 0.147pu
Δf = 0.125 Hz
MG-6
ΔV = 0.137pu
Δf = 0.123 Hz
MG-3
ΔV = 0.132pu
Δf = 0.124 Hz
MG-5 (PMG)
P^load= 0.782 pu
P^NDER = 0.236 pu
P^DG = 0.548 pu
max(V) = 0.994 pu
f = 49.29 Hz
MG-4 (HMG)
P^load = 0.135 pu
P^NDER= 0.012 pu
P^DG= 0.124 pu
max(V) = 1.057 pu
f = 50.41 Hz
MG-2
P^trans = 0.067 pu
P^BSS = 0.023 pu
P^DG = 0.224 pu
max(V) = 1.042 pu
f = 50.27 Hz
MG-1
MG-3
MG-6
1.06 pu
0.01 pu
MG-5
P^load = 0.782 pu
P^NDER = 0.236 pu
P^DG = 0.452 pu
max(V) = 1.034 pu
f = 49.84 Hz
MG-4
P^trans = 0.039 pu
P^DG= 0.163 pu
max(V) = 1.042 pu
f = 50.31 Hz

(b)

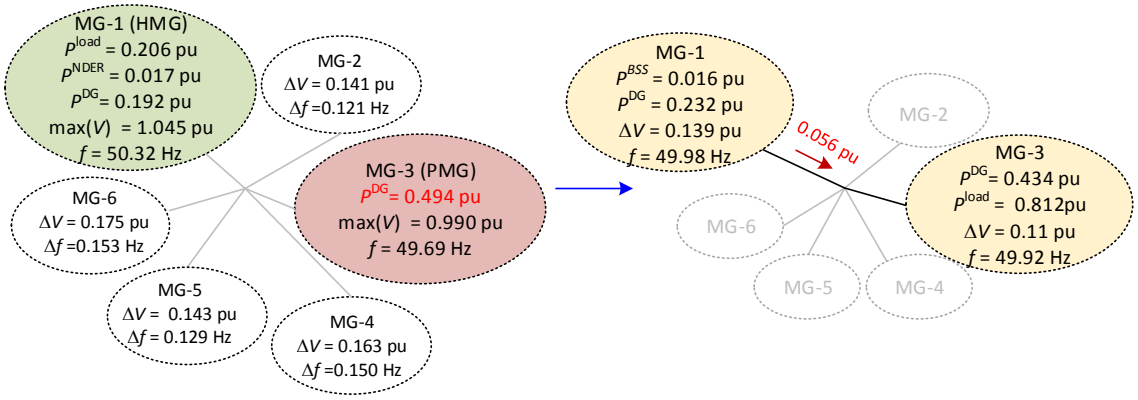
MG-1 (HMG)
P^load = 0.206 pu
P^NDER = 0.017 pu
P^DG= 0.192 pu
max(V) = 1.045 pu
f = 50.32 Hz
MG-2
ΔV = 0.141 pu
Δf =0.121 Hz
MG-3 (PMG)
P^DG= 0.494 pu
max(V) = 0.990 pu
f = 49.69 Hz
MG-6
ΔV = 0.175 pu
Δf =0.153 Hz
MG-5
ΔV = 0.143 pu
Δf = 0.129 Hz
MG-4
ΔV = 0.163 pu
Δf =0.150 Hz
MG-1
P^BSS = 0.016 pu
P^DG = 0.232 pu
ΔV = 0.139 pu
f = 49.98 Hz
0.056 pu
MG-2
MG-3
P^DG= 0.434 pu
P^load = 0.812pu
ΔV = 0.11 pu
f = 49.92 Hz
MG-6
MG-5
MG-4

(c)

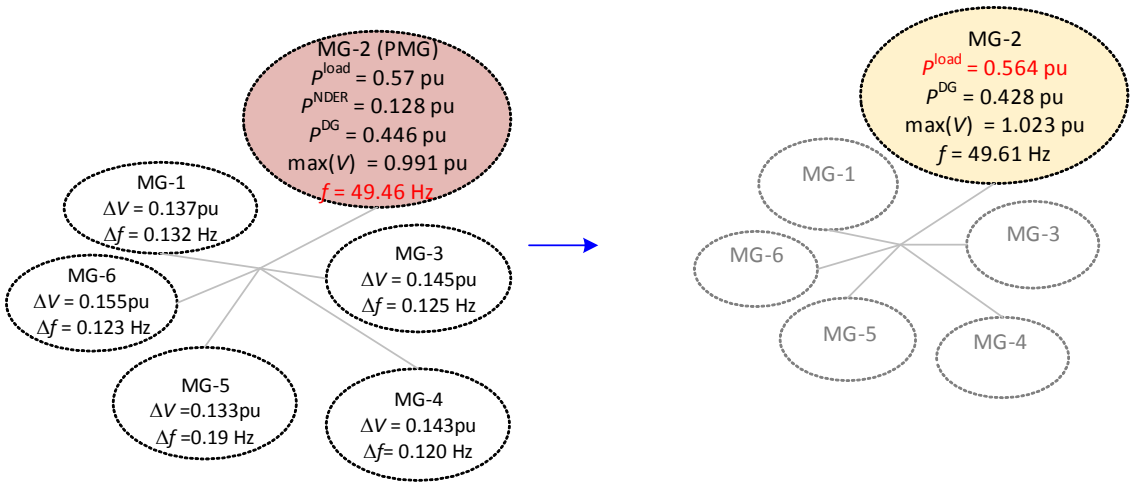

(d)

Fig 6.4 Schematic illustration of study case-I to IV for overloaded PMG.

with an SRI of 74% and an RPL of 33.4%. Now, let us consider study case-IV (see Fig. 6.4d), in which microgrid-2 is detected as a PMG^{OL} (with a frequency of 49.46 Hz and a minimum voltage of 0.91 pu, both beyond the safe mode). As seen from Table 6.4, this microgrid has a load demand of 0.57 pu, an SRI of below 1% and an RPL of 22%). The developed supervisory emergency controller proposes a combination of soft and hard actions, as the most optimal solution (with an OF value of 12.23$) to address the emergency of this microgrid. The supervisory emergency controller, does not use any intermedial actions for this study case. As a result, a load curtailment of 0.006 pu, along with a 0.008 pu support from the BSS ,reduces the output power of the droop regulated system from 0.446 to 0.428 pu, which will subsequently increase the observed minimum voltage and frequency to 0.955 pu and 49.61 Hz, respectively.

6.4.2 A Problem Microgrid Experiencing Excessive Generation

Consider case study-V (see Fig. 6.5a) in which microgrid-5 is detected as a problem microgrid, observing excessive generation from its NDERs (referred to as PMG^{OG}) and

experiencing a maximum voltage and a frequency of 1.056 pu and 50.6 Hz, respectively, both beyond the safe mode limits). As seen from Table 6.6, microgrid-5, has a load demand of 0.251 pu, an SRI of 67% and an RPL of 29%. Without the application of the proposed supervisory emergency controller, a renewable curtailment of 0.03 pu, is needed to retain this microgrid in the safe mode. The supervisory emergency controller finds a combination of soft and Intermedial actions, as the most optimal solution to address this emergency (with an OF value of 7.29$). To this end, the supervisory emergency controller, proposes the coupling of microgrid-5 to microgrid-6 (a healthy microgrid with a load demand of 0.153 pu, an SRI of 66.5% and an RPL of 12%, operating at a frequency of 49.7 Hz and a maximum voltage of 1.036 pu). As a result, microgrid-5 exports 0.032 pu, out of which 0.026 pu, is received by microgrid-6, considering the losses in the tie line and all this power is charged into the BSS of microgrid-6. Thereby, the coupled microgrid operates at a new frequency of 50.26 Hz, and will observe a maximum voltage of 1.05 pu, an SRI of 36% and an RPL of 23%.

Now, let us consider case studyVI (see Fig. 6.5b), in which the microgrid-4 is detected as problem microgrid^{OG} (operating in the unsafe mode, with a load demand of 0.20 pu, an SRI of 44% and an RPL of 12%, with a frequency of 50.53 Hz and a maximum voltage of 1.061 pu, both beyond the permissible limits). Without the proposed supervisory emergency controller, a renewable curtailment of 0.04 pu, is required to eliminate the emergency. The proposed supervisory emergency controller, determines a combination of soft, intermedial and hard actions, as the most suitable solution to address the emergency (with an OF value of $10). As a result, the supervisory emergency controller, proposes to couple microgrid-1 (a healthy microgrid with a load demand of 0.32 pu, an SRI of 26% and an RPL of 7%, operating at a frequency of 49.9 Hz and observing a maximum voltage of 1.018 pu) and microgrid-6 (A healthy microgrid with a load demand of 0.305 pu, an SRI of 32% and an RPL of 12% operating at a frequency of 50.19 Hz and a maximum voltage of 1.036 pu) with microgrid-4. Thereby,

Table 6.6 Case studies results for problem microgrids with excessive generation

Case Study	V		VI			VII
Observed MG(s)	MG-5	MG-6	MG-1	MG-4	MG-6	MG-1
MG's State	PMG^{OG}	HMG	HMG	PMG^{OG}	HMG	PMG^{OG}
MG Parameters under Emergency						
P^{load} (pu)	0.251	0.153	0.32	0.2	0.305	0.346
P^{NDERs} (pu)	0.074	0.019	0.023	0.037	0.038	0.012
P^{DG} (pu)	0.182	0.134	0.294	0.168	0.272	0.334
max (V) (pu)	1.056	1.036	1.018	1.061	1.036	1.072
min (V) (pu)	1.034	1.008	0.988	1.026	1.024	1.040
f (Hz)	50.6	49.7	49.9	50.53	50.19	50.48
Mode	Unsafe	Safe	Safe	Unsafe	Safe	Alarm
SRI (%)	66.9	66.5	26.5	44	32	74.22
RPL (%)	29.48	12.41	7.18	12.45	12.4	3.46
CMG(s) Parameters after SEC's performance						
HMGA	yes		yes			no
CMGF	yes		yes			no
PMGI	no		no			yes
ACS	yes		yes			yes
P^{trans} (pu)	0.032	–0.026	–0.019	0.045	–0.023	
$\boldsymbol{P}_{\mathbf{curt}}^{\mathbf{NDER_s}}$ (pu)				0.008		0.009
$\boldsymbol{P}_{\mathbf{curt}}^{\mathbf{load}}$ (pu)						
P^{BSS} (pu)		–0.026	–0.016		–0.022	–0.013
P^{DG} (pu)	0.214	0.134	0.297	0.205	0.272	0.356
CMG max (V) (pu)	1.050		1.039			1.032
CMG min (V) (pu)	0.993		1.017			0.998
$\boldsymbol{f}$ (Hz)	50.26		49.88			50.21
CMG Mode	Safe		Safe			Safe
P^{loss} (pu)	0.006		0.003			0.002
CMG SRI (%)	36.63		29.63			
CMG RPL (%)	23.01		9.45			
OF ($)	7.29		10.00			6.32

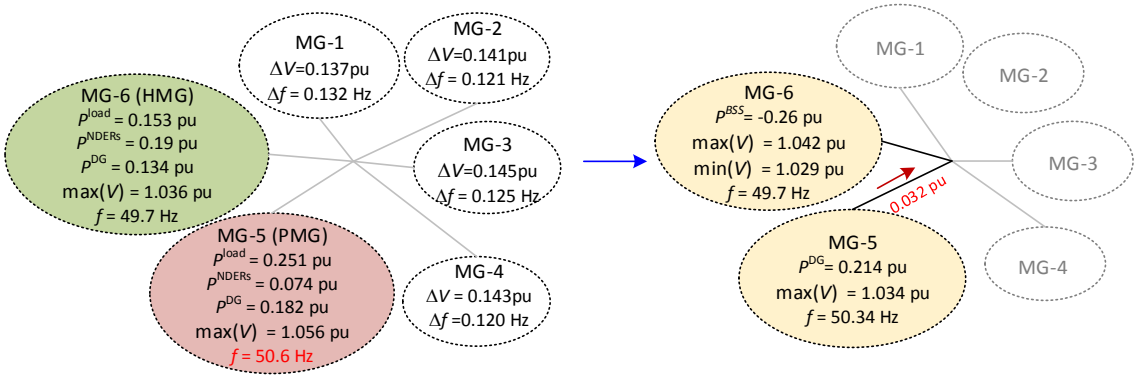

(a)

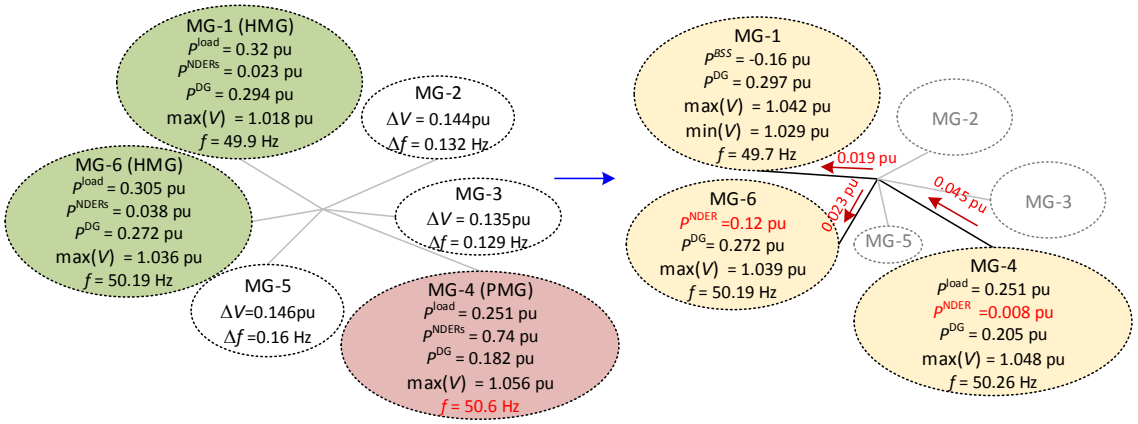

(b)

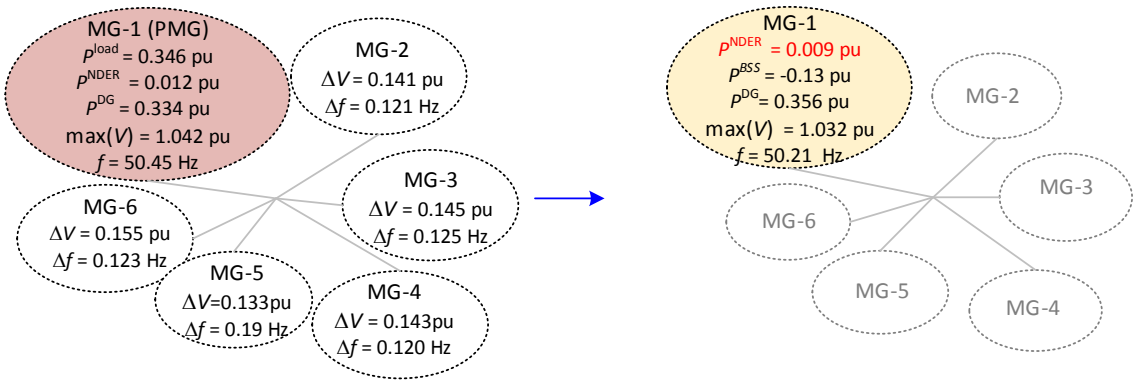

(c)

Fig 6.5 Schematic illustration of study case-V to VII.

microgrid-4 exports 0.045 pu (out of which 0.019 pu is imported by microgrid-1 and 0.023 pu is imported by microgrid-6 after a total loss of 0.003 pu). In this period, the output power of the droop regulated system of microgrid-4, increases from 0.168 to 0.205 pu, whilst this value

almost remains unchanged, for microgrid-1 and microgrid-6. The imported power by these microgrids is charged by their BSSs. Thus, the frequency in the formed, coupled microgrid reaches up to 49.88 Hz, while a maximum voltage of 1.039 pu, is observed. Also, the coupled microgrid observes an SRI of 29% and an RPL of 9%.

Consider case study VII (see Fig. 6.5c) in which microgrid-1, is detected as a PMG^{OG} (observing a maximum voltage of 1.071 pu, which is higher than the acceptable permissible limi,t whereas its frequency is 50.48 Hz and within the safe mode range). This microgrid has a load demand of 0.346 pu, an SRI of 74% and an RPL of 3%. The supervisory emergency controller defines a combination of soft and hard actions, as the most suitable solution for this emergency (with an OF value of 6.32$). As seen from Table 6.6, the supervisory emergency controller, proposes a renewable curtailment of 0.009 pu and a BSS charging by 0.013 pu, which will reduce the output power of the DG from 35.6 to 0.334 pu. Thus, the microgrid will have operated at a frequency of 50.21 Hz and will observe a maximum voltage of 1.032 pu.

6.4.3 Multiple Problem Microgrids

Consider case study VIII (see Fig. 6.6), in which microgrid-1 is defined as a problem $microgrid^{OG}$ (observing a maximum voltage of 1.054pu and a frequency of 50.61 Hz, both are beyond the permissible limits of the safe mode, with a load demand of 0.132 pu, an SRI of 67% and an RPL of 3%), while microgrid-4 is defined as a problem $microgrid^{OL}$ (observing a minimum voltage of 0.937 pu and a frequency of 49.23Hz, both beyond the permissible limits of the safe mode, with a load demand of 0.43 pu, an SRI of almost zero and an RPL of 30%). The supervisory emergency controller, finds a combination of soft, intermedial and hard actions when addressing this concurrent emergency in two of the considered microgrids. To this end, the supervisory emergency controller, proposes coupling of microgrid-3 (a healthy microgrid with a load demand of 0.468 pu, an SRI of 29% and an RPL of 24%, operating at a

Table 6.7 Case studies result for multiple problem microgrids

Case Study	VIII			
Observed MG(s)	MG-1	MG-3	MG-4	MG-5
Observed MG(s) State	PMG^{OG}	HMG	PMG^{OL}	HMG
	MG Parameters under Emergency			
P^{load} (pu)	0.132	0.468	0.43	0.296
P^{NDERs} (pu)	0.004	0.116	0.132	0.004
P^{DG} (pu)	0.129	0.354	0.298	0.292
max (V) (pu)	1.054	1.016	0.991	1.038
min (V) (pu)	1.032	0.980	0.937	1.025
f (Hz)	50.61	51.28	49.23	49.59
Mode	Alarm	Safe	Unsafe	Safe
SRI (%)	67.7	29.2	0.66	46.90
RPL (%)	3.03	24.8	30.69	1.35
	CMG(s) Parameters after SEC's performance			
HMGA	yes			
CMGF	yes			
PMGI	no			
ACS	yes			
P^{trans} (pu)	0.074	–0.070	–0.063	0.065
$\boldsymbol{P}_{\mathbf{curt}}^{\mathbf{NDD_s}}$ (pu)		0.033		
$\boldsymbol{P}_{\mathbf{curt}}^{\mathbf{load}}$ (pu)			0.012	
P^{BSS} (pu)	–0.031	–0.037		0.04
P^{DG} (pu)	0.234	0.387	0.223	0.32
CMG max (V) (pu)	1.039			
CMG min (V) (pu)	0.987			
$\boldsymbol{f}$ (Hz)	49.77			
CMG Mode	Safe			
P^{loss} (pu)	0.007			
CMG SRI (%)	66.51			
CMG RPL (%)	16.8			
OF ($)	11.45			

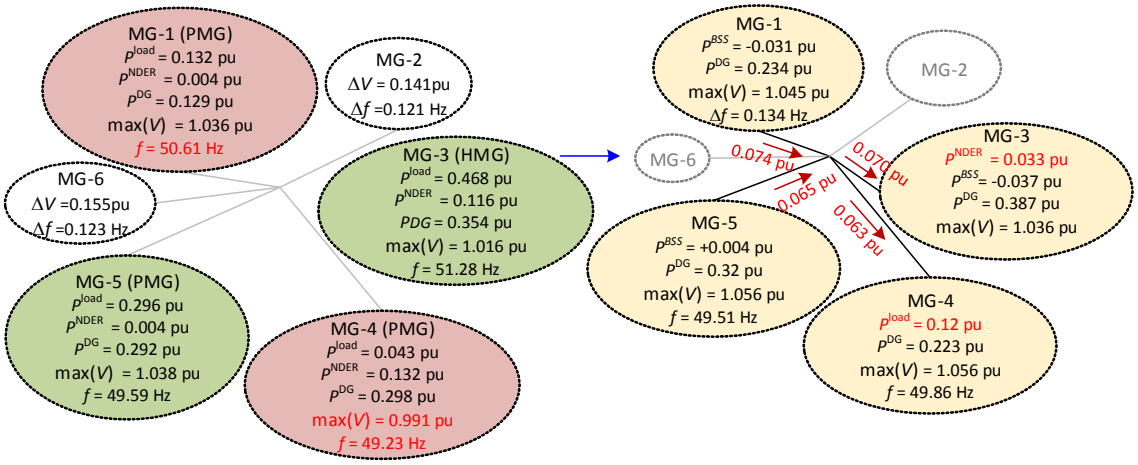

Fig 6.6 Schematic illustration of study case-VIII.

frequency of 51.28 Hz, and a minimum and maximum voltages of respectively 0.98 and 1.016 pu) with microgrid-5 (a healthy microgrid with a load demand of 0.296 pu, an SRI of 46% and an RPL of 1%, observing a frequency of 49.59 Hz, and a minimum and maximum voltages of respectively 1.025 and 1.038 pu), with both problem microgrids, as the most optimal solution (with an OF value of 11.45$). Therefore, microgrid-1 and microgrid-5 export respectively 0.074 and 0.065 pu, whilst microgrid-3 and microgrid-4 import respectively 0.07 and 0.063 pu. The BSS of microgrid-1 and microgrid-3 charges by 0.031 and 0.037 pu, respectively while the BSS of microgrid-5 discharges by 0.04 pu. Thereby, the output power of the droop regulated system of microgrid-1, microgrid-3 and microgrid-5, increases from 12.9, 35.4 and 29.2 to respectively 0.234, 0.387 and 0.32 pu, while this figure decreases from 0.298 to 0.223 pu for microgrid-4. Thereby, the frequency of the coupled microgrid reaches 49.77 Hz and observes a minimum and maximum voltages of respectively 0.987 and 1.039 pu. It also has an SRI of 66% and an RPL of 16%.

6.5 Summary

This chapter has presented a multi-stage supervisory emergency controller, for

eliminating the overloading and excessive generation emergencies, of remote area microgrids. Supervisory emergency controller is activated as soon as the voltage and frequency of the microgrid drops beyond the safe mode and determines a set of actions, to eliminate the emergency and recover the microgrid to the safe mode of operation. The considered actions are soft actions, such as the adjustment of the droop parameters of the droop regulated systems and the charging/discharging control of the BSSs, intermedial actions, such as power exchange with one or more neighbouring microgrids. Additionally there are also the hard actions taken which have included load-shedding or renewable curtailment which are considered in a sequential basis. The aim of the formulated objective function is to reduce the operational cost of conventional diesel generators, whilst maximizing the RPL and SRI along with minimising the power loss in the tie-lines amongst the microgrids and the frequency and voltage deviation. The successful operation of the proposed technique is validated, through the numerical analysis performed in Matlab.

Chapter 7. Market Model for Clustered Microgrid Optimisation

7.1 Introduction

This chapter proposes a new market model, to enable the optimisation of clustered microgrids that are connected by distribution networks, in conditions of energy balance, and emergency situations i.e. overloading or over-generations within the cluster. The proposed structure, enables the integration of the internet of energy providers within the networked microgrids. The microgrids, internal service providers, internet of energy providers and distribution network operators, are present as distinct entities, with individual objectives of minimum operational cost. Each MG is assumed to be composed of the NDERs and the DDERs with a commitment to service its own loads prior to exportation. To this end, an optimization problem is formulated, with the core objective being the minimum cost of operation, reduced network loss and least distribution network operator charges. A novel control strategy, is proposed for the coordinated operation of the microgrids by introducing the internal service providers, whose objective is formulated as a bi-level stochastic problem. The first level relates to determine the generation level of DERs in emergency situations and the second level is to adjust the generation, based upon the optimization constraints. The problem formulated in this way is then solved by using a genetic algorithm. Case studies are carried out on a distribution system, with multiple microgrids, internal

service providers and internet of energy providers, which illustrates the effectiveness of the proposed market, optimization strategy.

7.2 Market Optimisation Problem Formulation

Market optimization goal is formulated as

$$OF = min\left[K_1.\sum_{MG=1}^{n} OF_{ISP} + K_2\sum_{ESP=1}^{N} OF_{IOEP} + K_3\sum_{IOEP=1}^{N}\sum_{SSP=1}^{N}\sum_{State=1}^{n} OF_{DNO}\right]\times \Delta T \quad (7.1)$$

The main objective for the optimal choice selection, from the internet of energy, depends upon three factors these include the cost of the operation of the internal service provider e.g.. OF_{ISP}, cost of economic efficiency loss i.e. OF_{EEL} and the cost of the operation of the distribution network operatorOF_{DNO}. Multipliers K_1, K_2 and K_3 are the weightings assigned to each OF, such that sum of all multipliers will be unity e.g.$\sum_{i=1}^{n} K_i = 1$ and ΔT is the time taken by the internet of energy, to re-evaluates the systems' condition. Each part of (7.1) is described in detail, with constraints in the subsections *A, B* and *C,* as given below.

7.2.1 Internal Service Provider Operation

For the internal service provider OF formulation, the rolling horizon optimization approach [151], is used (see Fig. 7.1.). Therefore, (t+T_p) is the total time considered for the optimization window of the internal service provider, where T_p is the time taken by the internal service provider to implement necessary changes, according to internet of energy optimization decision. Scenarios *i* and *p* are related to the rolling horizon time *t* and T_p respectively. The operation of the internal service provider is assumed to be a bi-level stochastic process [152], so decision variables are divided into

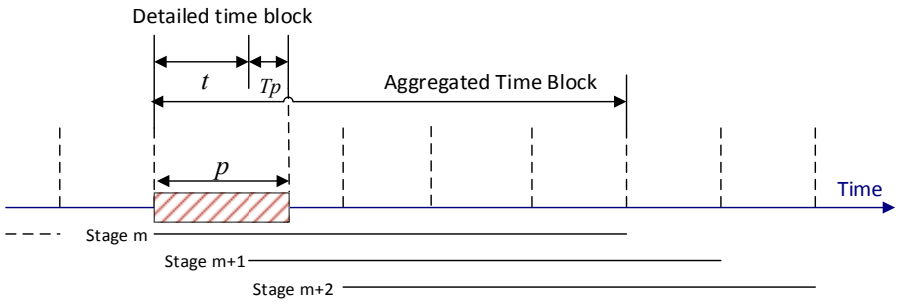

Fig 7.1. Pictorial representation of rolling-horizon approach for internal service provider

two groups. At first, the actual realization of supply and demand, is done using the power flow analysis based on the modified Guass-Siedel iterative technique [153]. Once the uncertain scenarios have unfolded, further operational adjustments can made, according to the internet of energy decision. Hence, the OF for the internal service provider, is the combination of the sum of the operational costs of the troubled microgrid, both in emergency *(i)* and adjustment of emergency *(p)* scenarios as under:

$$OF_{ISP} = min \sum_{TMG=1}^{N} \left(\sum_{i} Cost_{t}^{S1} + \sum_{p} Cost_{T_p}^{S2} \right) \forall \text{ ISP} \in \text{MMA} \tag{7.2}$$

Eq (7.2) is the desired OF for the internal service provider operation and it consists of two parts: first is related with the cost analysis of the troubled microgrids, during emergency conditions, while the second describes the adjustments of operational costs, proposed by the internet of energy as the optimal solution. For scenario *i*, the internet of energy providers cannot be included in the optimization horizon. It typically relates with to the demand/supply analysis of the troubled microgrid(s).

$$\sum_{i} Cost_{t}^{S1} = \sum_{t}\left(\sum_{i} C^{DG} P_{i,t,n}^{DG} + \sum_{i} C^{emi}\partial_{i} P_{i,t,n}^{DG} + C_{inturruption}^{NDERs,load} P_{i,t,n}^{load,NDERs} + C_{lifeloss}^{BSS} P_{i,t,n}^{BSS} + \left(C_{SSP}^{imp}\alpha_{j,t}^{imp} - C_{SSP}^{expo}\beta_{j,t}^{expo}\right)\right) \quad (7.3)$$

Eq (7.3) is associated with level one of the bi-level stochastic programming, in which the internal service provider will describe the demand supply situation of the troubled microgrids and possible shared service provider(s) contributions to overcoming the power deficiency situation. Internal service providers will make a demand/supply analysis at this stage and the cost analysis will indicate the existing economics of the troubled microgrids.

$$\sum_{p} Cost_{T_p}^{S2} = \sum_{T_p}\left(\left(\gamma_{p,DG,n}\sum_{p}(C_{i,p,T_p,}^{adj} + \Delta\partial_{i} C_{emi,p,T_p}^{adj})\Delta P_{i,p,T_p,n}^{DG}\right) + \gamma_{p,BSS} C^{BSS}\Delta P_{i,t,T_p,n}^{BSS} + \gamma_{\gamma_{p,load/NDERs}}^{curtailment} + \gamma_{p,IOEP}\left(C_{IEOP}^{imp}\alpha_{j,T_p}^{imp} - C_{IEOP}^{expo}\beta_{j,T_p}^{expo}\right)\right) \quad (7.4)$$

Part two e.g. Eq (7.4), is related to the second level of the bi level stochastic program. Part two describes the adjustments of the operation costs to overcome the emergency situation, following the internet of energy optimal analysis, which is described in the coming section of this paper. The cost of the import/export power from the internet of energy providers, is also included in the predictive horizon. This decision directly effects the connect/disconnect condition of ISS. The first item in (7.3), represents the generation cost of all diesel generators present within the troubled microgrids. The next item is the estimated cost of diesel generator emissions. The NDERs (WT, PV) and the

BSS have zero fuel costs, but costs due to the unpredictable changes in the output of the NDERs and the load are included here. The fourth and fifth item represents the BSS life loss cost, as well as the import/export energy cost, amongst the shared service providers, respectively. Following on from the internet of energy optimization solution, adjustment of the costs described in (7.3), is required. These adjustment costs not only play a role in the demand management, but also give an idea as to whether V/f controls are achieved or not. For example, if demand management is not possible by the shared service providers' adjustment, as shown in (7.3), then a request will be sent to the internal service provider. The proposed control action between the internal service provider and multi-microgrid area -microgrids, is based on the master-slave control strategy. The DG or the BSS inside the troubled microgrids, which adopt constant V/f control, could serve as the master control unit [154]. All of the other DGs will adopt P/Q control for certain active and reactive power outputs. These DG or BSS will provide a local reference voltage in microgrids. It is obvious that frequency adjustment, is not needed if multi-microgrid area is working in connection with the internet of energy providers. Moreover for the connect/disconnect purposes of ISS, it is assumed that only the low bandwidth communications are needed to control the microgrid power flow and synchronization with the internet of energy providers. There are two possibilities in this situation: 1) importing energy from SPs or 2) exporting energy to the SPs. Hence the fourth item of objective function, represents the adjustment cost for the import/export power between the internet of energy providers and the internal service providers with the intermediate connection of the internet of energy.

Now the constraints related to the described OF are listed below:

$$P_{SSP} = \alpha_{j,t}^{SSP} - \beta_{j,t}^{SSP} \qquad , \alpha, \beta = \begin{cases} 0 \\ 1 \end{cases}, \forall i \in t \tag{7.5}$$

Constraint (7.5), represents the power exchange between the shared service providers. As it is assumed that during level one of bi level stochastic programming, internet of energy providers, cannot participate in the planning horizon because of the V/f control, so the parameters (α, β) are set equal to 0 or 1. This means that the troubled microgrid can or cannot import/export power from/to a certain shared service provider.

$$SOC_{k,i,min} \leq SOC_{k,i} \leq SOC_{k,i,max}, \forall\, k, i \in t \tag{7.6}$$

$$SOC_{k,i,t} = SOC + \int \frac{P_{BSS,rate} P_{BSS_{i,t}}}{V_{dc} I_{dc,rate} C_{BSS,rate}} dt, \forall\, k, i \in t \tag{7.7}$$

$$-P_{BSS,k,i}^{ch,max} \gamma_{k,i,t} \leq P_{BSS,k,i} \leq P_{BSS,k,i}^{dch,max} \lambda_{k,i,t}, \forall\, k, i \in t \tag{7.8}$$

$$\gamma_{k,i,t} + \lambda_{k,i,t} \leq 1 \quad , \quad \forall\, i, k \in t \tag{7.9}$$

Constraint (7.6), represents the state of charge (SOC) limits for BSS Constraint (7.7), is related to the SOC value available, in existing in time *t*. Constraint (7.8), represents the charge/discharge limit for the BSS. Constraint (7.9), shows that the charging and discharging of the BSS cannot take place at the same time, this means that either γ or λ , will be equal to zero during the operation of the network.

$$P_{i,t} = \sum_{i=1}^{N} |V_I|\,|V_l|(G_{Il} Cos\emptyset_{Il} + B_{Il} Sin\emptyset_{Il})\,, \forall I, l \in t \tag{7.10}$$

$$Q_{i,t} = \sum_{i=1}^{N} |V_I|\,|V_l|(G_{Il} Cos\emptyset_{Il} + B_{Il} Sin\emptyset_{Il})\,, \forall I, l \in t \tag{7.11}$$

$$\emptyset_{Il} = \delta_I - \delta_l \tag{7.12}$$

$$1 - \varepsilon \leq V_{i,t} \leq 1 + \varepsilon\,, \forall i \in t \tag{7.13}$$

Constraints (7.10-7.11), are the power flow equations of the network. Constraint (7.12) is the difference in the voltage angles between two nodes of the distribution system. Constraint (7.13), signifies the voltage deviation at each bus of the system will have voltage deviations that are within permissible limits. ε is a constant that is applied to guarantee the

voltage deviation. Its value can be set between 0.05 to 0.08.

$$P_{i,t}^{exp.out} \leq P_{i,t}^{DG} + \sigma_{k,t} P_{k,t}^{BSS} - P_{i,t}^{loss} + \sum_{i,n,t} P_{i,t}^{NDERs} \ , \forall i \in t \tag{7.14}$$

$$Q_{i,t}^{exp.out} \leq Q_{i,t}^{DG} + \sum_{i,n,t} Q_{i,t}^{NDERs} \ , \forall i \in t \tag{7.15}$$

Constraint (7.14-7.15), are the expected active/reactive power outputs from the troubled microgrids following the first level of stochastic programming. Active power losses, which is are a substantial issue arising in the distribution system, are also included.

$$P_{i,t}^{DG} + P_{k,t}^{BSS} + \sum_{i,n,t} P_{i,t}^{NDERs} \leq \sum_{i,t} P_{i,t}^{load} \ , \forall i \in t \tag{7.16}$$

$$P_{i,l,t}^{loss,min} mp_{i,l,t} \leq \sum_{i=1}^{N} P_{i,l,t}^{loss} \leq P_{i,l,t}^{loss,max}, mp_{i,l,t} \geq 0, \forall i \in t \tag{7.17}$$

$$C_{p,T_p}^{\gamma_p} \geq (C^{DG} + C^{emi} + C^{imp} + C^{exp}) \ , \forall i \in t, p \in T_p \tag{7.18}$$

Constraint (7.17), shows that the first stage of the load, can or cannot be equal to the generation from the DGs. Constraint (7.18), shows the permissible limit of the system losses, so that the power factor cannot drop to a minimum range. Constraint (7.19), assumes that cost of the adjustment for the second leve,l can be equal or greater than first level costs of the operation.

Constraints (7.19-7.31), represents the adjustment scenarios, applied for overcoming emergency situation. p is chosen as the probability and T_p is the time in which the adjustment takes place. It is to be noted here that i is also included in some constraints, because the total the time of the optimization window is (t+T_p) , therefore some constraints can be effected by stage one variables also. Constraint (7.19), represents the adjustment of the power needed upstream from the network, following the P/Q control. Due to the power

emergency of the troubled microgrid(s), the power transaction will be carried out. Therefore import/export parameters are set as $\Delta\alpha \geq 0, \Delta\beta \geq 0$.

$$\Delta P_{IOEP} = \Delta\alpha_{j,T_p}^{IOEP} - \Delta\beta_{j,T_p}^{IOEP} \quad , \Delta\alpha \geq 0, \Delta\beta = 0, \forall p \in T_p \tag{7.19}$$

Constraint (7.21-7.23), represents adjustments of BSS second stage variables i.e. $\Delta SOC, \Delta P_{BSS}$.

$$SOC_{k,p,min} \leq SOC_{k,i} + \Delta SOC_{k,T_p} \leq SOC_{k,p,max} \, , \forall \, k, p \in T_p \tag{7.20}$$

$$SOC_{k,p,T_p} = SOC + \Delta SOC_{k,p,T_p} + \int \frac{P_{BSS,rate}\Delta P_{BSS_{i,p}}}{V_{dc} I_{dc,rate} C_{BSS,rate}} dt, \forall \, k, p \in T_p \tag{7.21}$$

$$-P_{BSS,k,p}^{ch,max} \gamma_{k,p,T_p} \leq P_{BSS,k,p,T_p} + \Delta P_{BSS,k,p,T_p} \leq P_{BSS,k,i}^{dch,max} \lambda_{k,p,T_p} \qquad \forall \, k, p \in T_p \tag{7.22}$$

$$\gamma_{k,p,T_p}^{adj} + \lambda_{k,p,T_p}^{adj} \leq 1, \forall \, k, p \in T_p \tag{7.23}$$

Constraint (7.24-7.26), are power flow equations representated for the scenario p with adjustment variables $\Delta P_{i,p,T_p}, \Delta Q_{i,p,T_p}$ and $\Delta\emptyset_{Il}$ respectively.

$$\Delta P_{i,p,T_p} = \sum_{i=1}^{N} |\Delta V_I| \, |\Delta V_l| G_{Il} \mathrm{Cos}(\emptyset_{Il} + \Delta\emptyset_{Il}) + B_{Il} Sin(\emptyset_{Il} + \Delta\emptyset_{Il}) \, , \forall I, l \in T_p \tag{7.24}$$

$$\Delta Q_{i,p,T_p} = \sum_{i=1}^{N} |\Delta V_I| \, |\Delta V_l| G_{Il} \mathrm{Cos}(\emptyset_{Il} + \Delta\emptyset_{Il}) + B_{Il} Sin(\emptyset_{Il} + \Delta\emptyset_{Il}) \, , \forall I, l \in T_p \tag{7.25}$$

$$\Delta\emptyset_{Il} = \Delta\delta_I - \Delta\delta_l \tag{7.26}$$

Constraint (7.28), guarantees that the voltage at each bus of the network, will not deviate from its permissible limits, when the supply adjustment takes place. Variable $\Delta V_{p,T_p}$ is the voltage adjustment variable.

$$1 - \varepsilon \leq V_{i,t} + \Delta V_{p,T_p} \leq 1 + \varepsilon \, , \forall i \in \, T_p \tag{7.27}$$

Constraint (7.28-7.29) are the expected active/reactive power outputs following the second stage of stochastic programming. $\Delta P_{i,p,T_p}^{DG} / \Delta Q_{i,p,T_p}^{DG}, \Delta P_{k,p,T_p}^{BSS}$, are adjustments made to the active/reactive powers of the master control unit operators.

$$\Delta P_{i,p,T_p}^{exp.out} = \Delta P_{i,p,T_p}^{DG} + \sigma_{k,T_p} \Delta P_{k,p,T_p}^{BSS} - P_{i,p,T_p}^{loss} + \sum_{i,n,T_p} P_{i,t}^{NDERs} \quad , \forall i, p \in T_p \tag{7.28}$$

$$\Delta Q_{i,p,T_p}^{exp.out} = \Delta Q_{i,p,T_p}^{DG} + \sum_{i,n,T_p} Q_{i,t}^{NDERs} \quad , \forall i, p \in T_p \tag{7.29}$$

Constraint (7.30), guarantees that the DGs generation, is still less than the load demand as the V/f control was failed at the first level, so the ESP power import is needed. Constraint (7.31), shows the permissible limit of system losses, after adjustments to the power factor correction.

$$\Delta P_{i,p,T_p}^{DG} + \Delta P_{k,T_p}^{BSS} + \sum_{i,n,T_p} \Delta P_{i,p,T_p}^{NDERs} < \sum_{i,T_p} \Delta P_{i,p,T_p}^{load}, \forall i, p \in T_p \tag{7.30}$$

$$P_{i,l,T_p}^{loss,min} mp_{i,l,T_p} \leq \sum_{i=1}^{N} P_{i,l,T_p}^{loss} \leq P_{i,l,T_p}^{loss,max}, mp_{i,l,T_p} \geq 0, \forall i \in T_p \tag{7.31}$$

7.2.2 Market Model for Internet of Energy Provider

The main idea of restructuring the electricity market, is to gain maximum benefit for the buyers, by creating a competitive environment. In the proposed strategy, it is assumed that there is more than one energy import choice is made available and that these choices come in the form of the internet of energy providers. Three entities mainly participate in the market model. These entities are, 1) the internal service providers on behalf of the multi-microgrid area. as the buyers 2) the internet of energy providers, as the sellers 3) the internet of energy, as the choice provider for most economical solutions. However, a static monopoly, exploitation model exists in the case of one buyer and many sellers, so arguably the buyer can exploit the sellers, by setting low prices so that they can gain profit. Two main types of contracts are available in such situations these are the one day-ahead market and the one hour-ahead mechanism [155]. So in both methods, the availability of the generation mix, trades and bids are determined on per day or a per hour basis, respectively. Each internet of energy provider will compete to sell electricity to the multi-microgrid area and as a result, the price will typically decrease as every service provider tries to underbid each other. It is also assumed that

one or multiple internet of energy provider(s), can be chosen as qualifier bidders, if one seller could not meet the necessary requirements of overcoming the certain emergency situation. Hence, the overall objective function for internet of energy providers, can be defined as

$$OF_{IOEP} = OF_{Trans.Access} + OF_{EEL} \tag{7.32}$$

In which the first part of (7.32), relates to the minimization of the internet of energy provider, pricing for providing transmission access, to the distribution network operator in emergency situations and defined as:

$$OF_{Trans.Access} = P^{imp/expo} \times time \times NAI \times Cost^{energy} \tag{7.33}$$

where $P^{imp/expo}$ is the required power transaction for the troubled microgrid, $time$ describes how long the transaction will take place, NAI , is the network availability index and it is defined as

$$NAI = capacity^{line} \times load\ factor \tag{7.34}$$

Now if $load\ factor > 1$, then cost will remain as base charge /kW but if $load\ factor < 1$, then the distribution network operator will charge the highest price. The last part of (7.33), relates to cost of energy transfer in $/kWh.

For the second part of (7.32), let us assume that ω is the internet of energy providers bidding price and L is the economic benefit of the internal service provider. By using the monopoly price, R is the total revenue which increases with an increase in L. The main objective is to choose L, such that the profit Pr, would be maximized and given by

$$Pr(L) = R(L) - \omega(L).L \tag{7.35}$$

Suppose at the maximum profit $P'(L) = 0$, so for the purpose of maximization

$$0 = R'(L) - \omega'(L).L - \omega(L) \tag{7.36}$$

where $\omega'(L)$ is the derivative of the function $\omega(L)$, rearranging eq (7.36) gives

$$R'(L) = \omega'(L).L + \omega(L) \tag{7.37}$$

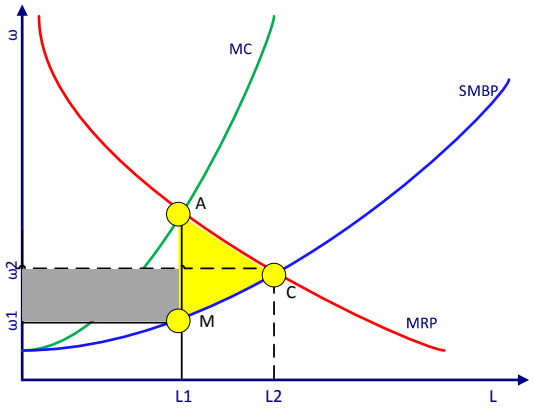

Fig 7.2 Overview of economic cost curves for market model

Table 7.1Time slots and SMBP for IOEPs [157]

IOEPs		
GST = 10% of (Supply charge & Consumption)		
Supply Charge = $\boldsymbol{\omega_{IOEP1.sup}}$ \$/day Supply charge for additional MGs = $\boldsymbol{\omega_{IOEP1.AMGs}}$ \$/day		
Time Slot	Timings	$\boldsymbol{\omega_{IOEP}}$ (\$/kWh)
Peak	[3]Weekdays : 11am to 5pm (Summer) Weekdays : 7am to 11am (Winter) Weekdays : 5pm to 9pm (Winter)	ω_{x1}
*Weekday Shoulder	Weekdays : 11am to 5pm (Summer) Weekdays : 7am to 11am (Winter) Weekdays : 5pm to 9pm (Winter)	ω_{x2}
Weekend Shoulder	7am to 9pm	ω_{x3}
*Off-Peak	Everyday 9pm to 7am	ω_{x4}

*Shoulder and off-peak mean the more consumption shifted to these times the more will be the saving for electricity cost.

Now the left hand side of this equation is the marginal revenue (MR), produced for the multi-microgrid area in the case of an extra *P* being generated due to increased *L*, and the right hand side is the marginal cost (MC) of the electricity, from internet of energy providers, due to extra cost requested from internal service provider, in a case of an emergency situation. So MC will be higher than the supplied bidding cost from ESPs. The economic cost curves for the market model is shown in Fig. 7.2. The grey triangle describes the competitive social surplus e.g. benefit for both consumer and supplier [156] and the triangle ACM highlighted in yellow is

the deadweight loss *(DWL),* or the allocative inefficiency e,g. it is the loss of economic efficiency and described as

$$DWL = DWL^{IOEP} + DWL^{ISP} \tag{7.38}$$

where

$$DWL^{IOEP} = Cost^{ISP}_{monoply} \tag{7.39}$$

$$DWL^{ISP} = Cost^{SMBP} + Cost^{GST} + Cost^{supply} \tag{7.40}$$

DWL is composed of two parts: The first part (7.39), describes that due to the monopoly the internal service provider, can take advantage of monopoly pricing and this causes economic efficiency loss, for the internet of energy providers. The second part (7.40), relates to the environment of competition, in which each provider tries to be a qualified bidder, which causes the DWL on internet of energy providers side. However, on the other hand, this situation will result in an overall increase of $R(L)$ for the multi-microgrid area. Hence, the cost of electricity bidding prices provided by internet of energy providers, are assumed to be, smart bidding prices (SMBP). However, due to monopoly, it will be bounded by the conditions of *R(L)*. The main aim of the SMBP is to encourage the multi-microgrid area customers to shift their usage of electricity to off-peak hours by offering reasonably low prices as compared to peak load hours. Second and third costs in (7.40), are general sales tax (GST) cost on the overall consumption and the electricity supply cost (both of these costs are applied irrespective of the usage of electricity and are taken to be an excess burden and should be paid by the internal service provider on the total import power from the ESPs). The idea of timing the days and the corresponding estimated costs for the SMBP is taken from the Synergy Western Australia [157] and are shown in Table 7.1. To this end, OF for the economic efficiency los,s can be formulated as

$$OF_{EEL} = P^{IOEP} DWL^{IOEP} + P^{ISP} DWL^{ISP} \tag{7.41}$$

s.t.

$$\sum_{ESPs} MC > \sum_{ESPs} SC \tag{7.42}$$

$$SMBP = \begin{cases} \omega_{min}, & if\ \omega_{min} \geq \omega(L) \\ \omega(L), & if\ \omega_{min} \leq \omega(L) \end{cases} \tag{7.43}$$

$$e = \frac{R'(\omega) - \omega}{\omega} \tag{7.44}$$

$$EBP \leq\ (\omega_{IOEP} + \omega_{sup.cost}) \times \%\ GST \tag{7.45}$$

Constraint (7.42), is for the economic cost curves of SPs and (7.43), is the relationship between SMBP and multi-microgrid area monopoly, pricing to maximise(L). Now with all the internet of energy providers, being governed by the state of competition, the rate of exploitation will be equal to zero i.e. $e = 0$ in (7.44). The total electricity bidding price will be the combination of the internet of energy providers bidding price, supply charges and tax on the total cost, as described in Constraint (7.45).

7.2.3 Operation of Distribution Network Operator

The third part of (7.1), is related to the operation of the distribution network operator that connects the selected, troubled microgrid(s) with the SPs by using the ISS.

$$OF_{DNO} =\ P^{line\ loss} \times Cost^{switchable\ lines} \tag{7.46}$$

s.t.

$$\sum_{state=1}^{n} ISS_{operation} \leq T_x\ , \tag{7.47}$$

$$\forall\ \text{ISS} = 1,2, \ldots, \text{n}\ \&\ T_x =\ T_{x_1} +\ T_{x_2} + T_{x_3}$$

The basic operation of the distribution network operator, is to determine the available SPs and their respective distance, from the troubled microgrid(s), to calculate the line losses along with cost of switching between the SPs transmission lines as shown in (7.46). In Eq (7.47), the main function of the ISS, is to automatically shift between the SPs connected and intentional

islanding operation modes. The cost of ISS can be based on the opening, closing and re-closing states. For this purpose, a multi-agent based control method, is assumed for ISS operation [158], as described in the research issue 4 in chapter 3. Thus, the operational stages of ISS, can be divided into three states such as: 1) closing the ISS after getting the signal from the DNO. 2) the energy transaction duration 3) the ISS opening after the power/ supply balance is achieved within the troubled microgrids. So the total operational time for the ISS will be the addition of three states, so that if $T_{x_1} = x$ seconds, then $T_{x_2} = x \times 60\ minutes$, and $T_{x_3} = 2x$ seconds respectively.

7.3 Numerical Results of Simulations

The formulated market optimization problem, is assessed by performing the exhaustive simulations in Matlab. As an example, a network consisting of three microgrids and two internet of energy providers, is assumed as shown in Fig. 7.3. The assumed data for the transmission lines, in the considered network and the respective distance of each microgrid and internet of energy provider, from distribution network operator, is illustrated in Fig. 7.3. It is to be noted here, that communication lines are not displayed in the shown net-work, but the protocols are the same as those previously described in Fig. 2. The microgrids are assumed to have the same topology inside themselves. Although in reality, this scenario is not possible, this assumption is made, for the sake of reducing and simplifying the complexity of the situation. The impedance data for the microgrids internal structure, is taken from [29] and all values used in case studies are taken in kW units.

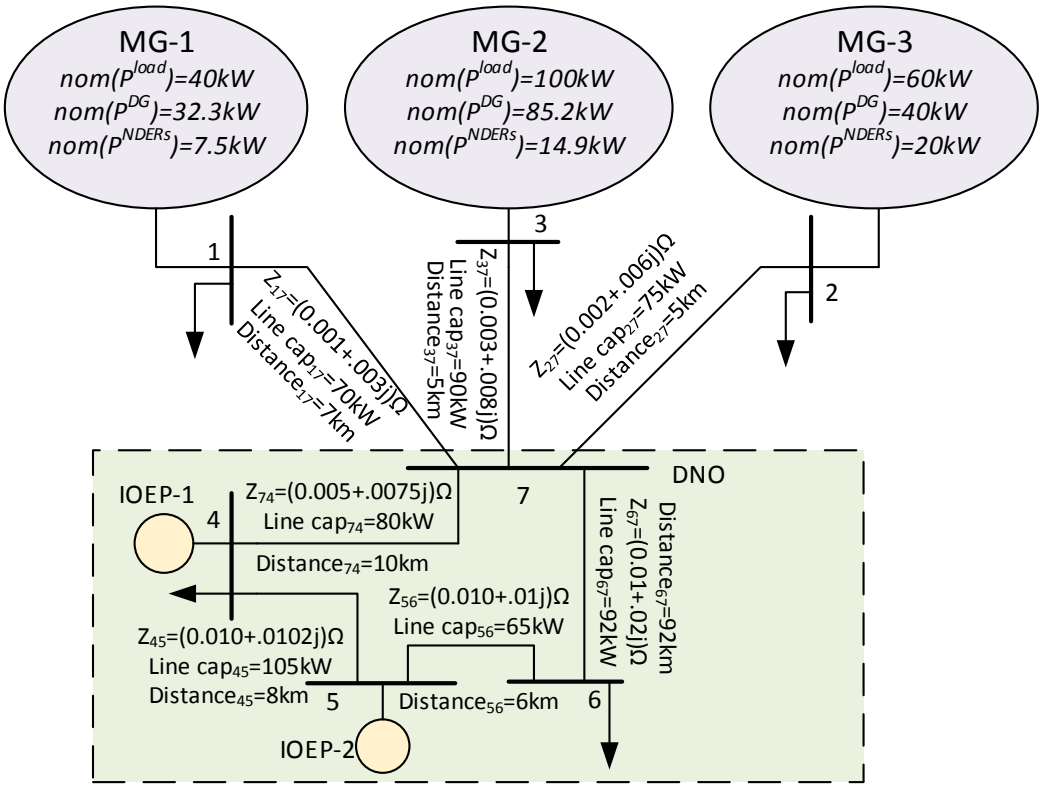

Fig 7.3 Considered network topology along with line impedances and respective distance of each line from the central position of distribution network operator.

Table 7.2 Nominal capacities of DERs of microgrids in multi-microgrid area

Photovoltaic		Diesel Generator	
P_{PV}^{cap}	10 kW	P_{DG}^{min}	13 kW
Wind		P_{DG}^{max}	80 kW
P_{wind}^{cap}	15 kW	Storage System	
Load		Capacity	70 kW
P_{load}^{cap}	100 kW	SOC_{LIMIT}	20% - 90%
$P_{BSS}^{CH,MAX}$	14 kW	$P_{BSS}^{DCH,MIN}$	65 kW

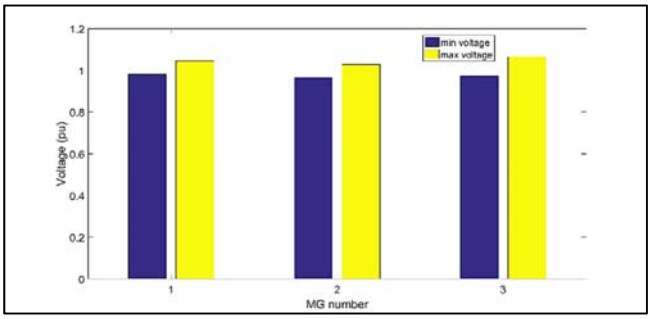

(a)

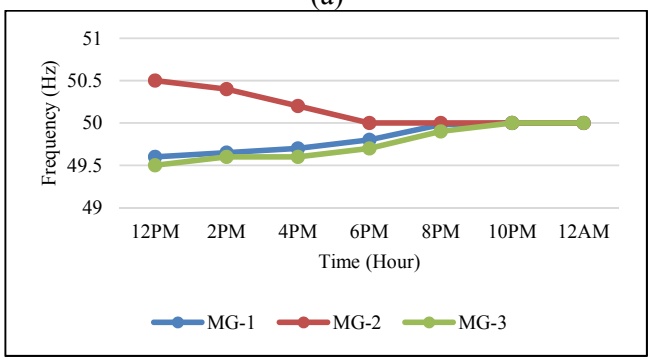

(b)

Fig 7.4 (a) Highest and lowest voltage levels, of each microgrid in multi-microgrid area (b) Sample of frequency for each microgrid

The nominal capacities of the DERs existing inside the microgrids, are presented in Table 7.2, whilst all of the costs data which has been used in the simulations is presented in Table 7.3. The maximum and minimum rangesof the technical impacts of the voltage and frequency of each microgrid in islanded mode, are depicted in Fig. 7.4a and 7.4b respectively.

The Genetic Algorithm is the solver being utilized here to identify the best feasible solution for the market optimization of the assumed network. This analysis is done for a total of 150 iterations. In each iteration, at first, a population is initialized with multiple chromosomes, which includes the droop set points of the DDERs and the NDERs in microgrids, the BSS state of operation, the power exchange with shared service providers, the power export/import to/from the IEOPs and the transmission lines power loss. Secondly OF in (7.1), is calculated for the optimal solution, along the constraints application as previously presented in Section III of this paper so as to realize the evaluation criteria. Once the parent

solution pool is formed by the selection procedure, then the off springs are created by the recombination process. The top scaling, heuristic cross-over and adaptive feasible mutation, are used as the Genetic Algorithm operators.

Finally, the developed market optimization technique will continue until the minimum desired cost is achieved for the considered MGs cluster, to overcome the emergency situation. The Pseudo code of optimization algorithm, is shown here.

Table 7.3 Assumed cost data for numerical analysis

Cost data for DERs of microgrids used in internal service provider operation				
	C^{DG}	0.1$/kWh	C_{DG}^{adj}	0.15$/kWh
	C^{emi}	0.02$/kg	C_{emi}^{adj}	0.025$/kg
	$C_{inturruption}^{NDERs,load}$	0.3$/kWh	∂	0.003kg/kWh
	$C_{lifeloss}^{BSS}$	10$/kWh	$C_{inturruption}^{adj}$	0.35$/kWh
Cost data for market model analysis				
Electricity price offered by microgrids in multi-microgrid area network MG-1 = 0.52$/kWh , MG-2 = 0.49$/kWh , MG-3 = 0.45$/KWh $Cost^{energy}$= 0.75$/kWh				
SMBP offered by IOEPs				
IOEP-1			IOEP-2	
	$\omega_{IOEP1.sup}$	0.3$/h	$\omega_{IOEP2.sup}$	0.32$/h
	$\omega_{IOEP1.AMGs}$	0.15$/h	$\omega_{IOEP2.AMGs}$	0.17$/h
	ω_{x11}	0.52$/kWh	ω_{x21}	0.37$/kWh
	ω_{x12}	0.26$/kWh	ω_{x22}	0.15$/kWh
	ω_{x13}	0.21$/kWh	ω_{x23}	0.18$/kWh
	ω_{x14}	0.13$/kWh	ω_{x24}	0.1$/kWh
Technical permissible limits $f^{nom} = 50$ Hz; $f^{min} = 49.5$ Hz; $f^{max} = 50.5$ Hz $V^{nom} = 1$pu; $V^{min} = 0.975$ pu; $V^{max} = 1.075$ pu				
Cost data for distribution network operator operation $Cost^{switchable\ lines}$= 2$				
ISS operational states with respective costs				
State	Closing	Operation	Opening	Re-closing
Time (includes DNO request)	$T_{x_1} = 2-3sec$	T_{x_2}= 40-60 min	$T_{x_3} = 4-6\ sec$	If needed then 3-7 sec after DNO request
$Cost^{SL}$	0.1$	0.8$ for 1 hr and 0.5$ for every extra hour requested	0.1 $	0.3$

Algorithm: The Genetic Algorithm Solver for market optimization technique.

1. *for* MG-1 to MG-N
2. Define the output of secondary controller based on DERs set-points ;
3. Declare the MG(s) as a TMG;
4. Define the minimum and maximum bounds for NDERs/loads curtailment, the DGs, the BSSs and power transaction for each MG in the multi-microgrid area;
5. end
6. Initialize GA parameters (initial population, individual fitness evaluation, selection and recombination)
7. Generate initial population with all selected control variables and constraints, along with the crossover and mutation probabilities;
8. Define the optimization stopping criteria;
9. *while* iterations <= Iteration ^{maximum}
10. *for* function tolerance =< 1e-6 and ΔT <= t (sec)
11. Define the number of SPs and the MG(s) which are not participating as the shared service providers;
12. Recognize the MG(s) isolated from the cluster, due to emergency conditions ;
13. Call the modified Gauss–Seidel-based power flow analysis function ;
14. Identify the DDERs, the BSS and the NDERs outputs, load demand, SoC of the BSSs, frequency and voltage deviation for the MG(s), in the multi-microgrid area and the TMG(s);
15. Calculate cost of the DG, the cost of emissions, the BSSs life loss cost, curtailment of load/NDDs cost (if any , the DWL, power loss in transmission ,lines cost;
16. Calculate the cost of the power transaction (import/export) for each TMG(s), in multi-microgrid area;
17. Evaluate the equality, inequality and boundary constraints;
18. If the feasible solution is not converged "OR" constraints are not met, then repeat lines (13 to 17) by applying small increase in the integer variables tolerance;
19. Calculate $\boldsymbol{OF_{ISP}, OF_{IOEP}}$ $\boldsymbol{and}$ $\boldsymbol{OF_{DNO}}$ along with their weightings, using (2), (30) and (44) ;
20. Calculate OF, using equation (1), for each individual population;
21. end
22. Define the most feasible population of the current iteration and identify the best chromosomes with high rank fitness;
23. Update the values of the chromosomes within the selected population and limit them with boundary constraints and tolerance;
24. end

Let us consider case study-I (numerically described in Table 7.4), in which MG-2 is declared as a troubled microgrid, with the nominal frequency of 50.6 Hz and the voltage maximum limit being on 1.095pu (both are above permissible limits as defined in Table 7.3). The main reason for this is because the DG is operating at 62kW, while its nominal capacity is

65kW, its' load is 77kW and the NDERs contribution is 12 kW, while the BSS is present with standby mode of operation. As the data has been collected on basis of 'one day ahead', so the time slot for this study, is noted as the weekend shoulder. Without a developed optimization strategy, the best solution is to do the NDERs curtailment of 9kW, so that both the frequency and the voltage will be within the permissible limits. A sample operation profile of MG-2, is shown in Fig 7.5.

This developed strategy, proposes to export power of 10 kW to the shared service providers and the internet of energy providers. Therefore, the distribution network operator will recommend the power export to the MG-3 and IOEP-2, as the best feasible solution. In this way, the MG-3 will couple with the MG-2 and form a power sharing environment, between two neighbors. MG-3 will work as shared service provider (load is 36kW, DG is operating at 25kW, NDERs contribution is 9kW, BSS has discharged for 2kW to accommodate the load). Now the MG-2 export of the 2.2kW to the MG-3 with the transmission line loss of 0.2kW, while 7.8kW is transmitted to IOEP-2 out of which 0.7 kW is wasted as power loss due to the distance of 8km from common central node of distribution network operator. The minimum cost of operation for this solution is calculated to be 13.41$ (out of which OF_{ISP} is 4.81$, OF_{IOEP} is 6.62$ and OF_{DNO} is 1.98$ respectively). The related costs to each OF are presented in Fig. 7.6.

It is clear from the pictorial representation provided, that the maximum cost is to be paid by IOEP-2 (i.e. 4.13$/kWh) and it matches the idea that the extra burden of the supply cost and the GST is also included. But an interesting fact revealed herein, is that as this emergency situation happened on a weekend shoulder time, the SMBP is as relatively low as 0.21 $/kWh. Similarly, the minimum cost has emerged for the shared service provider (i.e. MG-3 in this case), due to the fact that it is available, on minimum distance from the distribution network operator (i.e. at 5km as shown in Fig. 7.3). Therefore, the corresponding transmission line loss,

is relatively low. Similarly, due to the application of the proposed optimization technique, the technical aspects of the troubled microgrid (i.e. MG-2 in this study) has been settled down i.e. maximum voltage reaches to 1.044 pu and the frequency is exactly 50Hz, due to interconnection with IOEP-2.

Table 7.4 Numerical values observed for case study-I. In order to overcome the emergency situation, of over generation within a single troubled microgrid, presented inside a multi-microgrid area

Initially observed data							
Observed TMG	TMG status	f^{nom} (Hz)	V^{max} (pu)	P^{DG} (kW)	P^{load} (kW)	P^{NDERs} (kW)	Time slot
MG-2	Over generated	50.6	1.095	62	77	12	Weekend

Market optimization solution									
P^{expo}_{Total} (kW)	Available SSP	Selected IOEP	P^{load}_{SSP} (kW)	P^{DG}_{SSP} (kW)	P^{NDER}_{SSP} (kW)	P^{BSS}_{SSP} (kW)	P^{expo}_{SSP} (kW)	P^{expo}_{IOEP} (kW)	$P^{line\ loss}$ (kW)
10	MG-3	IOEP-2	36	25	9	2 (discharge)	2.2	7.8	0.9

OF ($) = 13.41$					
OF_{ISP}($)	4.81	OF_{IOEP}($)	6.62	OF_{DNO}($)	1.98

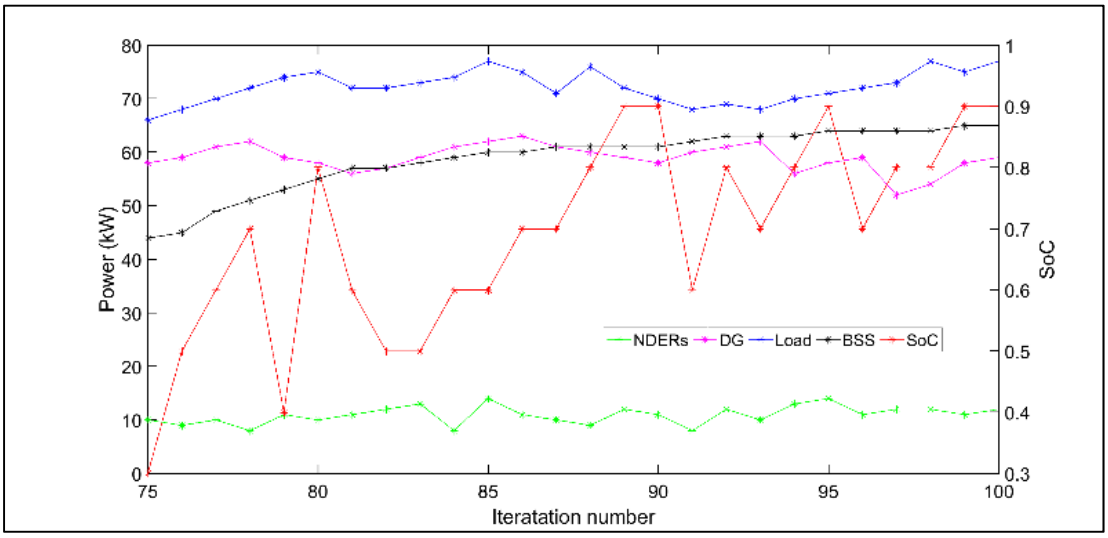

Fig 7.5 Sample operation profiles for 25 iterations out of a total of 150 iterations in case study-I, when MG-2 is under emergency situation, of over generation

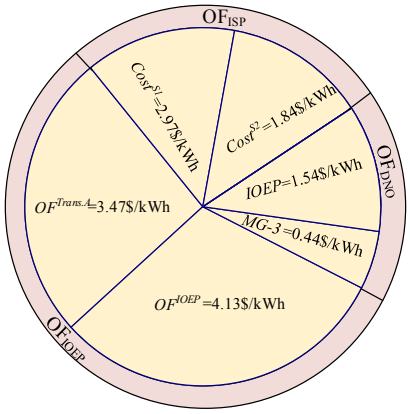

Fig 7.6. Contribution of each OF, in reaching the optimal solution to accommodate the emergency situation of the over generation of case study-I

Now let us consider another case study-II (numerically described in Table 7.5), in which MG-2(with nominal frequency of 50.6 Hz and voltage maximum limit is on 1.035 pu e.g. both are above the permissible limits) and MG-3 (with nominal frequency of 49.23 Hz and the voltage maximum limit is on 0.991 pu e.g. the. Frequency and voltage both are below the permissible limit) are declared as troubled microgrids. In the MG-2 (load is 32 kW, DG is operating at 30.8 kW with 1.3 kW coming from the NDERs) and MG-3 (load is 43kW, DG is operating at 29.8kW with 13.2kW coming from the NDERs). As the data has been collected on a day-ahead basis, the time period for this study is noted in peak hours. Sample operation profiles, for both troubled microgrid(s) are shown in Fig 7.7. Without a developed optimization strategy, the best solution is to perform a load curtailment of the total 3kW in MG-2, and NDERs curtailment of 5kW in MG-3 so that both the frequency and the voltage will be within permissible limits.

The developed strategy, proposes to export power of total 3.5 kW, from MG-3 to MG-2, whilst no internet of energy provider will be used to overcome an emergency situation. Therefore, the distribution network operator will recommend the power import from

Table 7.5 Numerical values observed for the case study-II, in order to overcome the emergency situation of over loading and over-generation in the multiple TMG(s), present inside the multi-microgrid area.

Initially observed data								
Observed TMG	TMG status	f^{nom} (Hz)	V^{max} (pu)	P^{DG} (kW)	P^{load} (kW)	P^{NDERs} (kW)	P^{BSS} (kW)	Time slot
MG-2	Overloaded	50.6	1.035	30.8	32	1.2	-	Peak
MG-3	Over-generated	49.23	0.099	29.8	43	13.2	-	
		Market optimization solution						
$\boldsymbol{P^{imp}_{Total}}$ (kW)	Available SSP	Selected IOEP	P^{expo}_{SSP} (kW)	Distance from DNO (km)			$P^{line\ loss}$ (kW)	
2.9	MG-3	-	3.5	5			0.4	
OF ($) = 9.2$								
$\boldsymbol{OF_{ISP}}$($)		8.9	OF_{IOEP}($)	-		OF_{DNO}($)	0.4	

MG-3 as the most feasible solution. In this way, 2.9 kW is transmitted from MG-3 out of which 0.4 kW, is wasted as a power loss, due to the distance of 2 km from the common central node of the distribution network operator. The minimum cost of operation for this solution, is calculated as 9.2$ (out of which OF_{ISP} is 8.9$, OF_{DNO} is only 0.4$ whileOF_{IOEP} is having no cost because they are not participating in overcoming the emergency situation). It is clear from the pictorial representation, that maximum cost is to be paid by MG-2 (i.e. 9.2$/kWh). However, an interesting fact revealed here, is that as this is an emergency situation that occurred during the peak weekday hours, the SMBP is relatively high but as no IOEP is taking part into this case study so SMBP is not applied at all.

Now let us consider another case study-III (numerically described in Table 7.6), in which MG-3(with nominal frequency of 49.38Hz and voltage maximum limit is on 0.0986pu e.g. both are below the permissible limits as defined in Table 7.3) and MG-1 (with nominal frequency of 49.41Hz and the voltage maximum limit is on 1.037 pu e.g. the. frequency is below the

permissible limit, whilst the voltage is within the normal range) are declared as troubled microgrids. In the MG-3 (load is 54kW, DG is operating at 39kW with 8kW coming from the NDERs and 7kW is the power support from the BSS) and MG-1 (load is 23kW, DG is operating at 16kW with 6kW coming from the NDERs and only 1kW of power support from the BSS). As the data has been collected on a day-ahead basis, the time period for this study is noted in peak hours. Sample operation profiles, for both troubled microgrid(s) are shown in Fig 7.7. Without a developed optimization strategy, the best solution is to perform a load curtailment of the total 12kW, so that both the frequency and the voltage will be within permissible limits.

The developed strategy, proposes to import power of 12 kW, from both the internet of energy providers, whilst no shared service provider will be usedto overcome an emergency situation. Therefore, the distribution network operator will recommend the power import from

Table 7.6 Numerical values observed for the case study-III, in order to overcome the emergency situation of over loading in the multiple TMG(s), present inside the multi-microgrid area.

Initially observed data								
Observed TMG	TMG status	f^{nom} (Hz)	V^{max} (pu)	P^{DG} (kW)	P^{load} (kW)	P^{NDERs} (kW)	P^{BSS} (kW)	Time slot
MG-1	Overloaded	49.41	1.037	16	23	6	1	Peak
MG-3		49.38	0.098	39	54	8	7	
	Market optimization solution							
P^{imp}_{Total} **(kW)**	Available SSP	Selected IOEP	P^{expo}_{IOEP} (kW)	Distance from DNO (km)			$P^{line\ loss}$ (kW)	
12	-	IOEP-1	11	10			2.3	
		IOEP-2	4	5			0.7	
OF ($) = 23.64$								
OF_{ISP}**($)**		7.2	OF_{IOEP}($)	12.3		OF_{DNO}($)	4.14	

IOEP-1 and IOEP-2 as the most feasible solution. In this way, 11kW is transmitted from IOEP-1 out of which 2.3 kW, is wasted as a power loss, due to the distance of 10km from the common central node of the distribution network operator, whilst 4kW is imported from IOEP-2, out of

which 0.7kW, is being wasted as the transmission line power loss. The minimum cost of operation for this solution, is calculated as 23.64$ (out of which OF_{ISP} is 7.2$, OF_{IOEP} is 12.3$ and OF_{DNO} is 4.14$ respectively). The related costs with each OF are shown in Fig. 7.8.

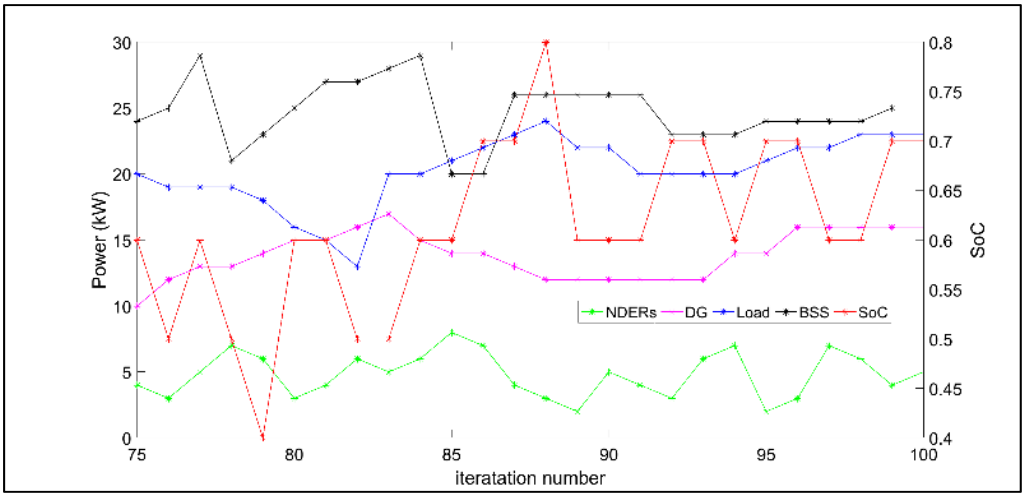

(a)

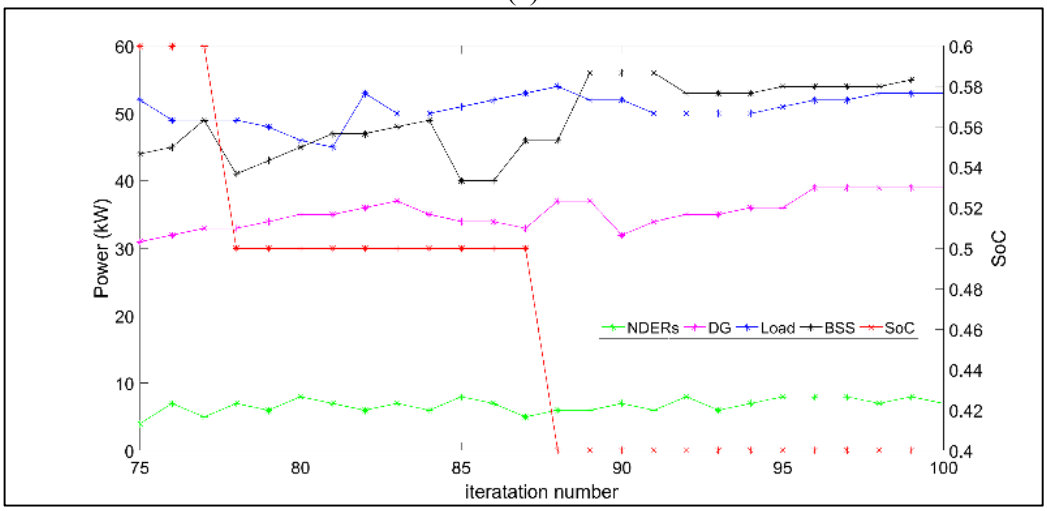

(b)

Fig 7.7. Sample operation profiles for 25 iterations out of total 150 iterations, in case study-III, when MG-1 (a) and MG-3 (B), are in an emergency situation created by over loading

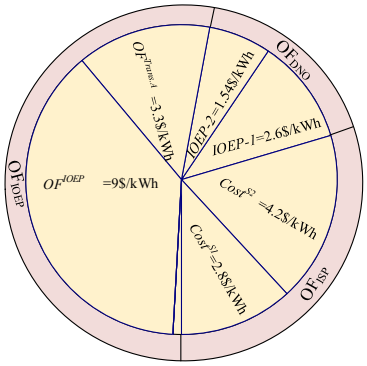

Fig 7.8 Contribution of each OF in reaching the optimal solution to accommodate the emergency situation of overloading and over generation of multi-microgrid area's TMG(s)

It is clear from the pictorial representation, that maximum cost is to be paid by IOEP-1 (i.e. 9$/kWh) and it matches the idea, that extra burden of the supply cost and the GST is also included. However, an interesting fact revealed here, is that as this is an emergency situation that occurred during the peak weekday hours, the SMBP is relatively high for IOEP-1 as 0.52 $/kWh, while IOEP-1 is importing power of 3.3kW at the relatively low cost of 0.37$/kWh. Similarly, the IOEP-1, is at a greater distance of 10km from the distribution network operator, as compared to IOEP-1, thus the transmission line losses for IOEP-1, are 2.6kW while the IOEP-1, is presenting with a lower loss of 1.54kW. Similarly, due to the application of the proposed optimization technique, the technical aspects of the troubled microgrids (e.g. MG-3 and MG-1, in this study), has been settled down. For instance, the MG-3 maximum voltage reaches to 1.035 pu and MG-1 voltage is steady at 1.038pu, while both microgrids are working within the permissible limits of frequency as well.

7.4 Summary

This chapter provides a strategy for the market optimization of remote area microgrids by utilizing the interaction between microgrids and the internet of energy providers, with the

help of the distribution network operator. The distribution network operator and each of the microgrids have their own objectives for minimizing the overall cost of the operations. The optimal control of the entire network, is achieved by using the heuristic optimization approach of Genetic Algorithm. Case studies are done on a sample network of two internet of energy providers and three microgrids. The simulation results show that stochastic decisions end with the optimal value of the operation cost, permissible limits of voltage level and minimum efficiency loss. The results also highlight the significance of utilizing SMBP costs, which gives substantial benefit to microgrid customers. Compared to the previous efforts made in the literature about microgrids, market optimization, this work gives liberty to the internet of energy providers, for providing consent to export or import power, in certain emergency situations of multi-microgrid areas. The interaction amongst distribution network operators and microgrids for the integration of the internet of energy providers have also been taken into account, to ensure the safe operation of the network.

Chapter 8. Conclusions and Recommendations

This chapter summarises the general findings of the thesis. Some recommendations for future research in the areas of the thesis, are also introduced here.

8.1 Conclusions

The general conclusions of the thesis are:

(1) The evaluation and analysis of two different events, reveal that, over a considered standalone microgrid network, realised in Matlab, it is seen that the top function of the scaling operator, helps the floating point-genetic algorithm solver, to yield a 1-5% lower value for the best fitness function, compared to the other scaling functions. The results were validated by a Monte Carlo study.

(2) Based on the economic analysis of the formulated fitness function, it is evident that if the combination of a suitable diesel generator, photovoltaic system, wind turbines and a battery energy storage system is used, then , it is to be noted that scaled fitness functions, can also be applied for solving the optimisation problems of the large interconnected systems, within a floating point-genetic algorithm solver; however, a standalone hybrid microgrid, was considered as the non-linear test case, in this research because it can observed as larger deviations in its voltage and frequency, due to the variability of its loads and the NDERs. The analysis illustrates that the suggested hybrid microgrid system, is a feasible system that can be used to meet the sudden change in

loads, with the help of scaling, crossover and the mutation operator, an effective cost of operation is generated, for an off-grid microgrid.

(3) From the sensitivity analysis, the optimal control variables, in a standalone microgrid placed in an emergency situation, such as an overloading and excessive generation of the NDERs, leads to unacceptable voltage and/or frequency deviations and can be overcome by the interplay of the various functions of the scaling operator.

(4) The proposal of a multi-stage supervisory emergency controller, for eliminating the overloading and excessive generation emergencies of remote area microgrids, has shown effective results to overcome the emergency situation. It is activated as soon as the voltage and frequency of the microgrid, drop beyond the safe mode and determine a set of actions to eliminate the emergency, and recover the microgrid to the safe mode of operation.

(5) The considered actions to take are the soft actions such as, adjustment of the droop parameters of the droop regulated systems and charging/discharging control of the BSSs, intermedial actions such as the power exchange with one or more neighbouring microgrids, as well as the hard actions such as load-shedding or renewable curtailment, which are considered in a sequential basis. The several case studies concluded that, the emergency situation can be eliminated by using a combination of all actions of the controller or by using separated actions of the controller. It is worth mentioning here, that the proposed controller has chosen the best optimal solution in every situation, along with the permissible limits of voltage and frequency.

(6) The distribution network operator and each of the microgrids, have their own objectives for minimizing the overall cost of operation. It is revealed by the simulation results, that stochastic decisions end with an optimal value of the operation costs, permissible limits of the voltage level and minimum loss of efficiency. The results also highlight the

significance of utilizing the SMBP costs which give substantial benefit to the microgrid customers. The interaction amongst the distribution network operators and using the microgrids for integration of the internet of energy providers, proves to be a sound strategy in resolving a sudden emergency situation, within microgrid clusters.

8.2 Recommendations for Future Research

Some future research topics in the area of this thesis are presented below:

(1) The BSS, is the only utilised energy storage system, in this research; however, in order to control and minimise the economics of microgrids, applications of flywheels can be considered, as a probable energy storage system, in future analyses.

(2) In this research, only remote area microgrids are analysed in standalone, coupled or grid connected modes of operation. Similar analysis, can also be performed for microgrids working in cooperation with utility or private generation companies. This idea can provide significant benefits in terms of cost, by including the concept of competitive bidding strategies, for outsider companies and creating an environment of competition amongst them.

(3) The optimisation technique, only focuses on achieving the minimum operating cost, with permissible limits of voltage and frequency, to resolve an emergency situation for remote area microgrid clusters. Setting up the priority list of customers and allowing them to participate in the operation horizon, by introducing demand response programs, could prove to be a useful and helpful way to understand the consumption of the microgrid, the demand response incentives and the contribution of each customer to the load shedding plan and so forth.

(4) The inclusion of an electric vehicle in the modelled structure of the microgrid and employing that vehicle as an active, participative, element, instead of remaining a

typically passive load. This inclusion could benefit both the system operators and the electric vehicle owners. This action would also increase the resilience and controllability of the entire, considered network.

Appendices

Appendix I

The assumed data for 38-bus microgrid topology is tabulated below.

Table A: Control Parameters of DERs in the considered 38-Bus microgrid system

DER	Bus No.	K_P	K_Q	f_o	V_o	R_x	X_x
		(p.u.)	(p.u.)	(p.u.)	(p.u.)	(p.u.)	(p.u.)
DG	1	0.0045	0.0362	0.9777	1.02	0.0030	0.0288
BSS	34	0.0015	0.0725	0.9792	1.02	0.0030	0.0288
WT	35	0.0023	0.0217	0.9770	1.02	0.0030	0.0288
WT	36	0.0023	0.1087	0.9766	1.02	0.0030	0.0288
PV	37	0.0008	0.0217	0.9769	1.02	0.0030	0.0288
PV	38	0.0006	0.0215	0.9762	1.02	0.0030	0.0288

Table B: Network parameters for the 38 bus microgrid system [150]

Line impedance in p.u.					Loads on to-node (p.u.)	
F	T	R p.u.	X p.u.	S_L	P	Q
1	2	0.000574	0.000293	0.5	0.1	0.6
2	3	0.00307	0.001564	2	0.09	0.04
3	4	0.002279	0.001161	0.5	0.12	0.08
4	5	0.002373	0.001209	1	0.06	0.03
5	6	0.0051	0.004402	1	0.06	0.02
6	7	0.001166	0.003853	3	0.2	0.1
7	8	0.00443	0.001464	3	0.2	0.1
8	9	0.006413	0.004608	2	0.06	0.02
9	10	0.006501	0.004608	1.5	0.06	0.02
10	11	0.001224	0.000405	1.5	0.045	0.03
11	12	0.002331	0.000771	1.5	0.06	0.035
12	13	0.009141	0.007192	0.5	0.06	0.035
13	14	0.003372	0.004439	0.5	0.12	0.08
14	15	0.00368	0.003275	0.5	0.06	0.01
15	16	0.004647	0.003394	1	0.06	0.02
16	17	0.008026	0.010716	1	0.06	0.02
17	18	0.004558	0.003574	1	0.09	0.04
2	19	0.001021	0.000974	0.5	0.09	0.04
19	20	0.009366	0.00844	0.5	0.09	0.04
20	21	0.00255	0.002979	0.5	0.09	0.04
21	22	0.004414	0.005836	0.5	0.09	0.04
3	23	0.002809	0.00192	1	0.09	0.05
23	24	0.005592	0.004415	1	0.42	0.2
24	25	0.005579	0.004366	1.5	0.42	0.2
6	26	0.001264	0.000644	1.5	0.06	0.025
26	27	0.00177	0.000901	1.5	0.06	0.025
27	28	0.006594	0.005814	1.5	0.06	0.02
28	29	0.005007	0.004362	1.5	0.12	0.07
29	30	0.00316	0.00161	1.5	0.2	0.6
30	31	0.006067	0.005996	0.5	0.15	0.07
31	32	0.001933	0.002253	0.5	0.21	0.1
32	33	0.002123	0.003301	1	0.06	0.04
8	34	0.012453	0.012453	1.5	0	0
9	35	0.012453	0.012453	1	0	0
12	36	0.012453	0.012453	1.5	0	0
18	37	0.003113	0.003113	1	0	0
25	38	0.003113	0.003113	2	0	0

F=From node, T=To node, S_L= Line capacity limit in p.u.,
P=Real load in p.u., Q=Reactive load in p.u.

Appendix II

To Whom It May Concern

I, Munira Batool, contributed (designed the included methodologies, developed the associated simulation files, performed interpretations and analysis on the results, and wrote the manuscript. The overall percentage of my contribution is about 60 %.) to the journal publication entitled "A multi-level supervisory emergency control for the operation of remote area microgrid clusters" (*Journal of Modern Power Systems and Clean Energy*, 2019, doi: 10.1007/s40565-018-0481-6).

Ms. Munira Batool Signature: 

I, as a Co-Author, endorse that this level of contribution by the candidate indicated above is appropriate.

Dr. Farhad Shahnia Signature: *Farhad Shahnia*

Prof. Syed Islam Signature: 

Appendix III

To Whom It May Concern

I, Munira Batool, contributed (designed the included methodologies, developed the associated simulation files, performed interpretations and analysis on the results, and wrote the manuscript. The overall percentage of my contribution is about 60 %.) to the journal publication entitled "Impact of scaled fitness functions in a floating-point genetic algorithm to optimize the operation of standalone microgrids" (*IET Renewable Power Generation*, 2019, doi: 10.1049/iet-rpg.2018.5519).

Ms. Munira Batool Signature: 

I, as a Co-Author, endorse that this level of contribution by the candidate indicated above is appropriate.

Dr. Farhad Shahnia Signature: *Farhad Shahnia*

Prof. Syed Islam Signature: 

Appendix IV

To Whom It May Concern

I, Munira Batool, contributed (designed the included methodologies, developed the associated simulation files, performed interpretations and analysis on the results, and wrote the manuscript. The overall percentage of my contribution is about 60 %.) to the journal paper entitled "A VPP Market Model for Clustered Microgrid Optimization including Distribution Network Operations" (under 2nd review in *IET Generation, Transmission and Distribution*, GTD-2018-5275).

Ms. Munira Batool Signature: 

I, as a Co-Author, endorse that this level of contribution by the candidate indicated above is appropriate.

Prof. Syed Islam Signature: 

Dr. Farhad Shahnia Signature: *Farhad Shahnia*

Appendix V

To Whom It May Concern

I, Munira Batool, contributed (designed the included methodologies, developed the associated simulation files, performed interpretations and analysis on the results, and wrote the manuscript. The overall percentage of my contribution is about 60 %.) to the conference publication entitled "Power transaction management amongst coupled microgrids in remote areas" (IEEE PES Innovative Smart Grid Technologies (ISGT), Auckland, 2017).

Ms. Munira Batool Signature: 

I, as a Co-Author, endorse that this level of contribution by the candidate indicated above is appropriate.

Prof. Syed Islam Signature: 

Dr. Farhad Shahnia Signature: *Farhad Shahnia*

Appendix VI

To Whom It May Concern

I, Munira Batool, contributed (designed the included methodologies, developed the associated simulation files, performed interpretations and analysis on the results, and wrote the manuscript. The overall percentage of my contribution is about 60 %.) to the conference publication entitled "Master control unit based power exchange strategy for interconnected microgrids" (27th Australian Universities Power Engineering Conference (AUPEC), Melbourne, 2017).

Ms. Munira Batool Signature: 

I, as a Co-Author, endorse that this level of contribution by the candidate indicated above is appropriate.

Prof. Syed Islam Signature: 

Dr. Farhad Shahnia Signature: *Farhad Shahnia*

Appendix VII

To Whom It May Concern

I, Munira Batool, contributed (designed the included methodologies, developed the associated simulation files, performed interpretations and analysis on the results, and wrote the manuscript. The overall percentage of my contribution is about 60 %.) to the conference publication entitled "Selection of sustainable standalone microgrid for optimal operation of remote area town" (One Curtin Postgraduate Conference (OCPC), Malaysia, 2017).

Ms. Munira Batool Signature: 

I, as a Co-Author, endorse that this level of contribution by the candidate indicated above is appropriate.

Prof. Syed Islam Signature: 

Dr. Farhad Shahnia Signature: *Farhad Shahnia*

Appendix VIII

To Whom It May Concern

I, Munira Batool, contributed (designed the included methodologies, developed the associated simulation files, performed interpretations and analysis on the results, and wrote the manuscript. The overall percentage of my contribution is about 60 %.) to the conference publication entitled "Stochastic modelling of the output power of photovoltaic generators in various weather conditions" (26th Australian Universities Power Engineering Conference (AUPEC), Brisbane, 2016).

Ms. Munira Batool Signature: 

I, as a Co-Author, endorse that this level of contribution by the candidate indicated above is appropriate.

Prof. Syed Islam Signature: 

Dr. Farhad Shahnia Signature: *Farhad Shahnia*

Appendix IX

To Whom It May Concern

I, Munira Batool, contributed (designed the included methodologies, developed the associated simulation files, performed interpretations and analysis on the results, and wrote the manuscript. The overall percentage of my contribution is about 60 %.) to the book chapter entitled "Operations of a clustered microgrid" in (*Variability, Scalability, and Stability of Microgrid*, IET Press, 2019).

Ms. Munira Batool Signature: 

I, as a Co-Author, endorse that this level of contribution by the candidate indicated above is appropriate.

Prof. Syed Islam Signature: 

Dr. Farhad Shahnia Signature: *Farhad Shahnia*

References

[1] T.S. Brinsmead, J. Hayward, and P. Graham (2014) Australian electricity market analysis report to 2020 and 2030, CSIRO Technical Report No. EP141067. http://arena.gov.au/files/2014/07/CSIRO-Electricity-market-analysis-for-IGEG.pdf

[2] SWIS electricity demand outlook (2014) Technical Report, Independent Market Operator. http://wa.aemo.com.au/docs/default-source/Reserve-Capacity/soo/imo_2014-swis-electricity-demand-outlook.pdf?sfvrsn=0

[3] Sina Parhizi, Hossein Lotfi, *et al.* (2015) State of the Art in Research on Microgrids: A Review, *IEEE Access* 3:890-925.

[4] A. Zomers (2014) Remote access: context, challenges, and obstacles in rural electrification, *IEEE Power Energy Magazine* 12(4):26-34.

[5] B. Zhao, X. Zhang, J. Chen, C. Wang, and L. Guo (2013) Operation optimisation of standalone microgrids considering lifetime characteristics of battery energy storage system, *IEEE Trans. Sustainable Energy* 4(4):934-943.

[6] I. Y. Chung, W. Liu, D. A. Cartes, *et al.* (2010) Control methods of inverter-interfaced distributed generators in a microgrid system, *IEEE Trans. Industrial Applications* 46(3):1078-1088.

[7] I. P. Nikolakakos, I. A. Al-Zyoud, H. H. Zeineldin, *et al.* (2014) Enhancement of islanded droop-controlled microgrid performance via power filter design, IEEE PES General Meeting, National Harbor, USA.

[8] M. Kumar, S. C. Srivastava, and S. N. Singh (2015) Control strategies of a dc microgrid for grid connected and islanded operations, *IEEE Trans. Smart Grid* 6(4):1588-1601.

[9] S.A. Pourmousavi, M.H. Nehrir, and R.K. Sharma (2015) Multi-timescale power management for islanded microgrids including storage and demand response, *IEEE Trans. Smart Grid*, 6(3):1185-1195.

[10] P. C. Loh, D. Li, Y. K. Chai, and F. Blaabjerg (2013) Autonomous control of interlinking converter with energy storage in hybrid AC–DC microgrid, *IEEE Trans. Industrial Application*, 49(3):1374–1382.

[11] A. Banerji, S. K. Biswas, and B. Singh (2016) Enhancing quality of power to sensitive loads with microgrid, *IEEE Trans. Industrial Application*, 52 (1):360–368:doi: 10.1109/TIA.2015.2478884.

[12] A. Trentin, P. Zanchetta, J. Clare, and P. Wheeler (2012) Automated optimal design of input filters for direct AC/AC matrix converters, IEEE Trans. Industrial Electronics, 59, (7):2811-2823.

[13] D.E. Olivares, et al. (2014) Trends in microgrid control, *IEEE Trans. Smart Grid*, 5(4):1905-1919.

[14] J.P. Lopes, C. Moreira, A. Madureira (2006), Defining control strategies for microgrids islanded operation,' *IEEE Trans. Power Systems*, 21(2):916-924.

[15] J. Qin, Q. Ma, Y. Shi, L. Wang (2017), Recent advances in consensus of multi-agent systems: A brief survey, *IEEE Trans. Industrial Electronics*, 64 (6): 4972-4983.

[16] https://building-microgrid.lbl.gov/types-microgrids

[17] Families in regional, rural and remote Australia, Website, Retrieved 14-08-17. https://aifs.gov.au/sites/default/files/publication-documents/fs201103.pdf

[18] L. Byrnes, et al. (2016), Reviewing the viability of renewable energy in community electrification" *Renewable & Sustainable Energy Reviews,* 59:470-481.

[19] L. Che, and M. Shahidehpour (2014), DC microgrids: Economic operation and enhancement of resilience by hierarchical control, *IEEE Trans SmartGrid*, 5(5):2517-

2526.

[20] L. Che, M. Khodayar, and M. Shahidehpour (2014), Only connect: Microgrids for distribution system restoration, *IEEE Power Energy Magazine*, 12(1):70-81.

[21] L. Ali, and F. Shahnia (2017), Determination of an economically-suitable and sustainable standalone power system for an off-grid town in Western Australia, *Renewable Energy*, 106:243-254.

[22] F. Shahnia, M. Moghbel, A. Arefi, *et al.*(2017), Levelized cost of energy and cash flow for a hybrid solar-wind-diesel microgrid on Rottnest Island, 27th Australiasian Universities Power Engineering Conference.

[23] S.A. Arefifar, Y.A.I. Mohamed, T.H.M. El-Fouly (2012), Supply adequacy based optimal construction of microgrids in smart distribution systems,' *IEEE Trans Smart Grid*, 3(3):1491-1502.

[24] F. Katiraei, et al. (2008) 'Microgrids management,' *IEEE Power and Energy Magazine*, 6(3): pp. 54-65.

[25] Q.C. Zhong, G.Weiss (2009),Static synchronous genertaors for distributed generation and renewable energy, Power System Conference & Exposition.

[26] Y.S. Kim, E.S. Kim and S.I. Moon (2016), Frequency and voltage control strategy of standalone microgrids with high penetration of intermittent renewable generation systems,' *IEEE Trans Power Systems*, 31, (1), pp, 718-728,.

[27] S. Augustine, M.K. Mishra, N. Lakshminarasamma (2015), Adaptive droop control strategy for load sharing and circulating current minimization in low-voltage standalone dc microgrid, *IEEE Trans Sustainable Energy*, 6(1):132-141.

[28] A. Elrayyah, F. Cingoz, Y. Soze (2017), Smart loads management using droop-based control in integrated microgrid systems, *IEEE Journal of Emerging and Selected Topics in Power Electronics*, 5(3):1142-1153.

[29] I.U. Nutkani, et al. (2016), Linear decenterlized power sharing schemes for economic operation of ac microgrids, *IEEE Trans Industrial Electronics*, 63(1):225-234.

[30] A. Karapetyan, et al. (2016), 'Efficient algorithm for scalable event-based demand response management in microgrids,' *IEEE Trans Smart Grid*, doi:10.1109/TSG.2016.2616945.

[31] B.V. Solanki, A. Raghurajan (2017), Including smart loads for optimal demand response in integrated energy management systems for isolated microgrids, *IEEE Trans Smart Grid*, 8 (4):1739-1748.

[32] M.M.A Abdelaziz, E.F.El-Saadany (2015), Economic droop parameter selection for autonomous microgrids including wind turbines, *Renewable Energy*, 82:108-113.

[33] J.M. Guerrero, et al. (2011), Hierarical control of droop controlled ac and dc microgrids, *IEEE Trans Industrial Electronics*, 58(1):158-172.

[34] K. Visscher, S.D. Haan (2008), Virtual synchronous machines for frequency stabilization in future grids with a significant share of decenterlized generation, IET CIRED Seminar.

[35] M.C. Chandorkar, D.M Divan, R. Adapa (1993), Control of parallel connected inverters in standalone ac system, *IEEE Trans Industry Application*, 29(1):136-143.

[36] J.P Lopes, A. Madureira, C. Moreira (2006), Defining control strategies for microgrids islanded operation, *IEEE Trans Power Systems*, 21(2):916-924.

[37] M.H. Moradi, M. Abedini, S.M. Hosseinian (2016), Optimal operation of autonomous microgrids using HS-Genetic Algorithm, *International Journal of Electric Power & Energy Systems*, 77:210-220.

[38] A. Anvari, et al. (2016), Optimal adaptive control for effective load sharing in microgrids, 42nd Annual Conf. of IEEE Industrial Electronics Society.

[39] Y.Y. Hong, et al. (2013), Multiscenerio underfrequency load shedding in a microgrid

consisting of intermittent renewables, *IEEE Trans Power Delivery*, 28(3):1610-1617.

[40] Q. Zhou, J.W. Bialek (2007) , Generation curtailment to manage voltage constraints in distribution networks, *IET Generation, Transmission and Distribution*, 1 (3):492-498.

[41] T.H. Mehar, A. Gosh, F. Shahnia (2017), Cooperative control of battery energy storage system, *International Journal of Electric Power & Energy Systems*, 87:109-120.

[42] R.H. Lasseter (2011), Smart distribution: Coupled microgrids, *Proceedings of the IEEE*, 99:1074-1082.

[43] J. Li, Y. Liu, and L. Wu (2016), Optimal operation for community based multi-party microgrid in grid connected and islanded modes, *IEEE Trans Smart Grid,* doi: 10.1109/TSG.2016.2564645.

[44] Saeed Hasanvand, Majid Nayeripour , *et al*, (2017), Spectral clustering for designing robust and reliable multi-MG smart distribution systems, *IET Generation, Transmission & Distribution*, DOI: 10.1049/iet-gtd.2017.0671.

[45] Z. Wang, B. Chen, et al. (2016), Networked microgrids for self-healing power systems,*IEEE Trans Smart Grid*, 7(1):310-319.

[46] G Antonis, T. Sikalakis, *et al.* (2008), Centralized Control for Optimizing Microgrids Operation, *IEEE Trans Energy Conversion*, 23(1):241-248.

[47] A. Khodaei (2015), Provisional microgrids, *IEEE Trans Smart Grid,* 6 (3):1107-1115.

[48] P.C. Loh, L. Ding, *et al.* (2013), Autonomous operation of hybrid microgrid with ac and dc subgrids, *IEEE Trans Power Electronics*, 28(5):2214-2223.

[49] Z. Wang, J. Wang (2015), Self-healing resilient distribution systems based on sectionalization into microgrids, *IEEE Trans Power Systems*, 30 (6) :3139-3149.

[50] K.P. Schneider, F.K. Tuffner, *et al.* (2017), "Evaluating the feasibility to use microgrids as a resiliency resource," *IEEE Trans on Smart Grid*, 8(2): 687–696.

[51] Z. Wang, and J. Wang (2015), Coordinated Energy Management of Networked

Microgrids in Distribution Systems, *IEEE Trans Power Systems*, 30 (6): 3139-3149.

[52] Q. Li, David Wenzhong Gao, et. al, "Consensus-Based Distributed Eco-nomic Dispatch Control Method in Power Systems", IEEE Trans. Smart Grid, DOI: 10.1109/TSG.2017.2756041

[53] I. Krad, David Wenzhong Gao, et. al, "Analysis of operating reserve demand curves in power system operations in the presence of variable generation", IET Renewable power generation, vol. 11, no. 7, pp. 959–965, 2017.

[54] G Antonis, T. Sikalakis, et al., "Centralized Control for Optimizing Microgrids Operation," IEEE Trans Energy Conversion, vol.23, no.1, pp.241-248, 2008.

[55] A. Khodaei, "Provisional microgrids", IEEE Trans Smart Grid, vol 6, issue 3, pp 1107-1115, 2015.

[56] L. Che, and M. Shahidehpour, "DC microgrids: Economic operation and enhancement of resilience by hierarchical control," IEEE Trans SmartGrid, vol.5, no.5, pp.2517-2526, 2014.

[57] L. Che, M. Khodayar, and M. Shahidehpour, "Only connect: Microgrids for distribution system restoration," IEEE Power Energy Magazine, vol.12, no.1, pp.70-81, 2014.

[58] Ahmed Eltom, Wafa Elballa, *et al*.,Smart Distribution Course for 21st Century Power Sector Workforce, IEEE Trans. On Power Systems, DOI: 10.1109/TPWRS.2018.2811737

[59] A. Chaouachi, R. M. Kamel, R. Andoulsi, and K. Nagasa-ka,"Multiobjective intelligent energy management for a microgrid," IEEE Trans. Ind. Electron., vol. 60, no. 4, pp. 1688–1699, Apr. 2013.

[60] S. Tan, J. X. Xu, and S. K. Panda, "Optimization of distribution net-work incorporating distributed generators: An integrated approach," IEEE Trans. Power Syst., vol. 28, no. 3, pp. 2421–2432, Aug. 2013.

[61] Intel Hardware. Software and Technologies for Industrial Automation, Intel®, 2017.

[62] https://www.intel.com.au/content/www/au/en/industrial-automation/products-and-solutions/hardware-software-technologies.html

[63] Industrial controllers, National InstrumentsTM website, 2017. http://www.ni.com/ industrial-controller

[64] H. S. V. S. Kumar Nunna and S. Doolla, "Multiagent-based distribut-ed energy resource management for intelligent microgrids," IEEE Trans.Ind. Electron., vol. 60, no. 4, pp. 1678–1687, Apr. 2013.

[65] A. K. Marvasti, F. Yong, S. DorMohammadi, and M. Rais-Rohani,"Optimal operation of active distribution grids: A system of systems framework," IEEE Trans. Smart Grid, vol. 5, no. 3, pp. 1228–1237,May 2014.

[66] J. Wu and X. Guan, "Coordinated multi-microgrids optimal control algorithm for smart distribution management system," IEEE Trans.Smart Grid, vol. 4, no. 4, pp. 2174–2181, Dec. 2013.

[67] H. S. V. S. K. Nunna and S. Doolla, "Demand response in smart distribution system with multiple microgrids," IEEE Trans. Smart Grid,vol. 3, no. 4, pp. 1641–1649, Dec. 2012.

[68] M. Fathi and H. Bevrani, "Statistical cooperative power dispatching in interconnected microgrids," IEEE Trans. Sustain. Energy, vol. 4, no. 3,pp. 586–593, Jul. 2013.

[69] C. Yuan, M.S. Illindala, and A.S. Khalsa (2017), Modified Viterbi algorithm based distribution system restoration strategy for grid resiliency, *IEEE Trans Power Delivery*, 32 (1):310–319.

[70] F. Shahnia, S. Bourbour, and A. Ghosh (2017), Coupling neighbouring microgrids for overload management based on dynamic multicriteria decision-making, *IEEE Trans Smart Grid*, 8(2):969-983.

[71] E. Pashajavid, F. Shahnia, and A. Ghosh (2017), Development of a self-healing strategy to enhance the overloading resilience of islanded microgrids, *IEEE Trans Smart Grid*, 8 (2):868-880.

[72] Y. Zhang, L. Xie, and Q. Ding (2016), Interactive control of coupled microgrids for guaranteed system-wide small signal stability, *IEEE Trans Smart Grid*, 7 (2):1088-1096.

[73] F. Shahnia, R.P.S. Chandrasena, S. Rajakaruna, and A. Ghosh (2014), Primary control level of parallel distributed energy resources converters in system of multiple interconnected autonomous microgrids within self-healing networks, *IET Gen. Transmission & Distribution*, 8 :203-222.

[74] Y. Zhang, and L. Xie (2015), Online dynamic security assessment of microgrid interconnections in smart distribution systems, *IEEE Trans Power Systems*, 30(6):3246-3254.

[75] I.P. Nikolakakos, H.H. Zeineldin, *et al.* (2016), Stability evaluation of interconnected multi-inverter microgrids through critical clusters, *IEEE Trans Power Systems*, 31(4):3060-3072.

[76] N. Nikmehr, S.N. Ravadanegh (2016), Reliability evaluation of multi-microgrids considering optimal operation of small scale energy zones under load-generation uncertainties, *International Journal of Electrical Power & Energy Systems*, 78:80-87.

[77] S.A. Arefifar, M. Ordonez, and Y. Mohamed (2016), Voltage and current controllability in multi-microgrid smart distribution systems, *IEEE Trans Smart Grid*, doi: 10.1109/TSG.2016.2568999.

[78] F. Shahnia, and A. Arefi (2017), Eigen analysis-based small signal stability of the system of coupled sustainable microgrids, *International Journal of Electrical Power & Energy Systems*, 91:42-60.

[79] F. Shahnia (2016), Stability and eigenanalysis of a sustainable remote area microgrid

with a transforming structure, *Sustainable Energy, Grids & Networks*, 8:37-50.

[80] F. Shahnia (2016), Semi-decentralized charging and discharging control of floating batteries in microgrids, 2nd IEEE Annual Southern Power Electronics Conference (SPEC),Auckland.

[81] T.H. Mehr, A Ghosh, and F. Shahnia (2017), Cooperative control of battery energy storage systems in microgrids, *International Journal of Electrical Power & Energy Systems*, 87:109-120.

[82] R. Majumder, and G. Bag, Parallel operation of converter interfaced multiple microgrids (2014), *International Journal of Electrical Power & Energy Systems*, 55:486-496.

[83] A. Arefi, and F. Shahnia (2017), Tertiary controller-based optimal voltage and frequency management technique for multi-microgrid systems of large remote towns, *IEEE Trans Smart Grid*, doi:10.1109/TSG.2017.2700054.

[84] F. Shahnia, and A. Arefi (2016), Defining the suitable adjacent microgrids to form a temporary system of coupled microgrids, IEEE Region 10 Conference (Tencon), Singapore.

[85] J. Wang, M. Shahidehpour, and Z. Li (2009), Strategic generation capacity expansion planning with incomplete information, *IEEE Trans Power Systems*, 24(2):1002-1010.

[86] Y. Tohidi, F. Aminifar, and M. Fotuhi-Firuzabad (2013), Generation expansion and retirement planning based on the stochastic programming, *Elect. Power System Research*, 104:138-145.

[87] H. Wang, and J. Huang (2016), Cooperative planning of renewable generations for interconnected microgrids, *IEEE Trans Smart Grid*, 7(5):2486-2496.

[88] M.J. Hossain, M.A. Mahmud, F. Milano, *et al.* (2016), Design of robust distributed control for interconnected microgrids, *IEEE Trans Smart Grid*, 7(6):2724-2735.

[89] N. Nikmehr, S.N. Ravadanegh (2015), Optimal operation of distributed generations in

micro-grids under uncertainties in load and renewable power generation using heuristic algorithm, *IET Renewable Power Generation*, 9 (8):982-990.

[90] P. Suhane, *et al.* (2016), Sizing and performance analysis of standalone wind-photovoltaic based hybrid energy system using ant colony optimisation, *IET Renewable Power Generation*, 10(7):964-972.

[91] G. Ma, *et al.*(2017), Multi-objective optimal configuration method for a standalone wind-solar-battery hybrid power system, *IET Renewable Power Generation*, 11(1):194-202.

[92] P. Satapathy, S. Dhar, P.K. Dash (2017), Stability improvement of PV-BSS diesel generator-based microgrid with a new modified harmony search-based hybrid firefly algorithm*, IET Renewable Power Generation*, 11(5):566-577.

[93] M.A. Hassan, M.A. Abido (2011), Optimal design of microgrids in autonomous and grid-connected modes using particle swarm optimisation, *IEEE Trans Power Electronics*, 26(3):755-769.

[94] I.Y. Chung, *et al.* (2010), Control methods of inverter-interfaced distributed generators in a microgrid system, *IEEE Trans Industrial Applications*, 46(3):1078-1088.

[95] Z. Bo, *et al.* (2013), Operation optimisation of standalone microgrids considering lifetime characteristics of battery energy storage system, *IEEE Trans Sustainable Energy*, 4(4):934-943.

[96] H. Ayman, M. Fathi, E. Beshr, M.B. Eteiba (2015), Multi-objective optimisation of islanded microgrids, IEEE International Conference on Electrical, Computer and Communication Technologies.

[97] A. Mohsenzadeh, C. Pang. M.R. Haghifam (2017), Determining optimal forming of flexible microgrids in the presence of demand response in smart distribution systems, *IEEE System Journal*, doi:10.1109/JSYST.2017.2739640.

[98] H. Bilil, G. Aniba, H. Gharavi (2017), Dynamic appliances scheduling in collaborative microgrids system, *IEEE Trans Power Systems*, 32(3):2276-2287.

[99] M. Nemati, et al (2015). Optimisation of microgrids short term operation based on an enhanced genetic algorithm, IEEE PowerTech Conference, Eindhoven.

[100] Z. Zhao, P. Yang, et al. (2017), Dynamic characteristics analysis and stabilization of PV-based multiple microgrid clusters, *IEEE Trans Smart Grid*, doi:10.1109/TSG.2017.2752640

[101] G.K. Mahanti, A. Chakraborty, S. Das (2005), Floating-point genetic algorithm for design of a reconfigurable antenna arrays by phase-only control, 37th IEEE conference on software engineering.

[102] S.A.H. Soliman, A.A.H. Mantawy (2012), Modern optimisation techniques with applications in electric power system, Springer.

[103] J. Zhu (2015), *Optimisation of Power System Operation*, Wiley-IEEE Press.

[104] H. Song, Y. Hu, C. Jiang (2016), An automatic scaling method for obtaining the trace and parameters from oblique ionogram based on hybrid genetic algorithm, *Radio Science*, 51(12):1838-1854.

[105] X.Y. Zhang, et al. (2016), 'Kuhn-Munkres parallel genetic algorithm for the set cover problem and its application to large-scale wireless sensor networks, *IEEE Trans Evolutionary Computation*, 20(5):695-710.

[106] B. Khan, and P. Singh (2017), Selecting a meta-heuristic technique for smart micro-grid optimisation problem: A comprehensive analysis, *IEEE Access*, 5:13951-13977.

[107] V. Mohan, R. Suresh, J. Govind Singh, *et al.*(2017), Microgrid energy management combining sensitivities, interval and probabilistic uncertainties of renewable generation and loads, *IEEE Journal on Emerging & Selected Topics in Circuits & Systems*, 7(2):262-270.

[108] T.L. Vandoorn, J. De Kooning, B. Meersman, *et al.* (2013), Voltage-based droop control of renewables to avoid on–off oscillations caused by over voltages, *IEEE Trans Power Delivery*, 28(2):845-854.

[109] B. Zhao, X. Zhang, J. Chen, *et al. (2013)*, Operation optimisation of standalone microgrids considering lifetime characteristics of battery energy storage system, *IEEE Trans Sustainable Energy*, 4(4):934-943.

[110] H. Wang, and J. Huang (2016), Incentivizing energy trading for interconnected microgrids, *IEEE Trans Smart Grid*, doi: 10.1109/TSG.2016.2614988.

[111] M. Fathi, and H. Bevrani (2013), Statistical cooperative power dispatching in interconnected microgrids, *IEEE Trans Sustainable Energy*, 4(3):586-593.

[112] C. Li, F. Bosio, F. Chen, *et al.* (2017), Economic dispatch for operating cost minimization under real-time pricing in droop-controlled dc microgrid, *IEEE Journal of Emerging & Selected Topics in Power Electronics*, 5(1):587-595.

[113] Amin Khodaei (2017), Provisional microgrids planning, *IEEE Trans Smart Grid,* 8(3): 1096-1104.

[114] Intel Hardware. Software and Technologies for Industrial Automation, Intel®, 2017. https://www.intel.com.au/content/www/au/en/industrial-automation/products-and-solutions/hardware-software-technologies.html

[115] Industrial controllers, National Instruments™ website, 2017. http://www.ni.com/industrial-controller

[116] Process control and industrail automation, Analogue devices, 2017. http://www.analog.com/en/applications/markets/process-control-and-industrial-automation.html

[117] Wireless Networks, ABB, 2017. http://new.abb.com/network-management/communication-networks/wireless-networks

[118] Industrial Wireless communication, Siemens, 2017. http://w3.siemens.com/mcms/automation/en/industrial-communications/industrial-wireless-communication/pages/industrial-wireless-communication.aspx

[119] M.A. Setiawan, F. Shahnia, *et al.*(2015), Zigbee-based communication system for data transfer within future microgrids, *IEEE Trans smart grid*, 6(5):2343-2355.

[120] F. Shahnia, and S. Bourbour (2017), A practical and intelligent technique for coupling multiple neighbouring microgrids at the synchronization stage, *Sustainable Energy, Grids & Networks*, 11:13-25.

[121] Kane, and V. Verma (2013), Characterization of PV cell-environmental factors consideration, Int. Conf. on Power, Energy and Control (ICPEC).

[122] A. Fezzani, I. Hadj Mahammed, and S. Said (2014), Matlab-based modelling of shading effects in photovoltaic arrays, 15th Int. Conf. on Sciences and Techniques of Automatic Control and Computer Engineering (STA).

[123] http://au.mathworks.com/help/physmod/sps/powersys/ref/pvarray.html

[124] S. Rahman, M.A. Khallat, and Z.M. Salameh (1988), Characterization of insolation data for use in photovoltaic system analysis models, *Energy*, 13:63-72.

[125] C. Walck, *Hand-book on Statistical Distributions For experimentalists*, Internal Report SUF–PFY/96-01, 2007.

[126] http://au.mathworks.com/help/stats/betapdf.html

[127] P. Bulanyi, and R. Zhang (2014), Shading analysis and improvement for distributed residential grid connected photovoltaics systems, 52nd Annual Conference of The Australian Solar Council.

[128] M. Drif, P.J Perez, J. Aguilera et al. (2008), A new estimation method of irradiance on a partially shaded pv generator in grid connected photovoltaic systems, *Renewable Energy*, 33:2048-2056.

[129] V. Quaschning, and R. Hanitsch (1996), Influence of shading on electrical parameters of solar cells, 25th IEEE Photovoltaic Specialists Conference.

[130] I.H. Elsebaie (2012), Developing rainfall intensity-duration-frequency relationship for two regions in Saudi Arabia, *Journal of King Saud University Engineering Sciences*, 24, :131-140.

[131] B. Chitti Babu, T. Cermak, S. Gurjar et al. (2015), Analysis of mathematical modelling of PV module with MPPT algorithm, 15th IEEE Int. Conf. on Environment and Electrical Engineering (EEEIC).

[132] S. A. Arefifar, Y. A. I. Mohamed, and T. H. M. El-Fouly (2012), Supply Adequacy Based Optimal Construction of Microgrids in Smart Distribution Systems, *IEEE Trans. on Smart Grid* , 3:1491-1502.

[133] http://www.engineersedge.com/motors/diesel-generator-review.html

[134] Farid Katiraei and Chad Abbey (2007), Diesel Plant Sizing and Performance Analysis of a Remote Wind-Diesel Microgrid, Proceeding Of the IEEE-PES General Meeting.

[135] Juan P. Fossati, Ainhoa Galarza, Ander Martin-Villate, et al. (2015), A method for optimal sizing energy storage systems for microgrids, *Renewable Energy*, 77:539-549.

[136] Dirk Uwe Sauer, Heinz Wenzl (2008), Comparison of different approaches for lifetime prediction of electrochemical systems, *Journal of Power Sources*, 176:534-546.

[137] Z. Bo, Z. Xuesong, C. Jian, et al. (2013), Operation Optimisation of Standalone Microgrids Considering Lifetime Characteristics of Battery Energy Storage System, *IEEE Trans. on Sustainable Energy*, 4:934-943.

[138] D.P. Jenkins, J. Fletcher and D. Kane (2008), Lifetime prediction and sizing of lead acid batteries for microgeneration storage applications, *IET Renewable Power Generations*, 2(3):191-200.

[139] Faisal Mumtaz, M. H. Syed, Mohamed Al Hosani et al. (2016), A Novel Approach to Solve Power Flow for Islanded Microgrids Using Modified Newton Raphson With Droop Control of DG*, IEEE Trans. on Sustainable Energy*, ,7(2) :493-503.

[140] K.Y. Lee, M.A. El-Sharkawi (2008), Modern heuristic optimisation techniques, Theory and applications to power systems.

[141] R.D. Zimmerman, C.E.M. Sanchez, R.J. Thomas (2011), MATPOWER: Steady-state operations, planning, and analysis tools for power systems research and education, *IEEE Trans Power System*, 26(1):12-19.

[142] S.N. Sivanandam, S.N. Deepa (2007), Introduction to genetic algorithms, Springer Science & Business Media.

[143] Matlab Genetic Algorithm Toolbox, 2016. https://au.mathworks.com/help/gads/genetic-algorithm-options.html

[144] K.W. Kim, M. Gen, M.H. Kim (2006), Adaptive genetic algorithms for multi-resource constrained project scheduling problem with multiple modes, *International Journal of Innovative Computing, Information and Control*, 2 (1):1349-4198.

[145] F.A. Sadjadi (2004), Comparison of fitness scaling in genetic algorithms with applications to optical processing, *Proceedings of SPIE*, 5557:356-364.

[146] M. Gen, R. Cheng (2000), Genetic algorithm and engineering optimisation, John Wily and Sons, New York.

[147] R. Heilmann (2003), A branch-and-bound procedure for the multi-mode resource-constrained project scheduling problem with minimum and maximum time lags, *European Journal of Operational Research*, 144:348-365.

[148] K.L. Mak, Y.S. Wong, X.X. Wang (2000), An adaptive genetic algorithm for manufacturing cell formation, *International Journal of Manufacturing Technology*, 16, :491-497.

[149] W.G. Zhang, W. Chen, Y.L. Wang (2006), The adaptive genetic algorithms for portfolio selection problem, International Journal of Computer Science and Network Security, 6 (1):196-200.

[150] C. Li, *et al* (2016), Power flow analysis for low-voltage ac and dc microgrids considering droop control and virtual impedance, *IEEE Trans Smart Grid*, 8(6):2754-2764.

[151] Z. Wang and J. Wang, "Self-Healing Resilient Distribution Systems Based on Sectionalisation into Microgrids," IEEE Transactions on Power Systems, vol.30, pp. 3139-3149, 2015.

[152] R. Palma-Behnke et al., "A microgrid energy management system based on the rolling horizon strategy," IEEE Trans. Smart Grid, vol. 4, no. 2,pp. 996–1006, Jun. 2013.

[153] F. Shahnia, S. Bourbour, and A. Ghosh, "Coupling neighboring mi-crogrids for overload management based on dynamic multicriteria deci-sion-making," IEEE Trans Smart Grid, vol.8, no.2, pp.969-983, 2017.

[154] M. Batool, S. M. Islam, and F. Shahnia, "Master control unit base power transaction strategy for interconnected microgrids," Australasian Universities Power Engineering Conference (AUPEC), 2017.

[155] Q. Yang, D. An, W. Yu, Y. Xinyu, and F. Xinwen, "On stochastic optimal bidding strategy for microgrids," in 2015 IEEE 34th International Performance Computing and Communications Conference (IPCCC), 2015, pp. 1-8.

[156] M. H. Cintuglu, H. Martin, and O. A. Mohammed, "Real-Time Implementation of Multiagent-Based Game Theory Reverse Auction Model for Microgrid Market Operation," IEEE Transactions on Smart Grid, vol. 6, pp.1064-1072, 2015.

[157] https://www.synergy.net.au/Standard_Electriity_Prices_Charges_brochure-1.PDF

[158] Meiqin Mao, Yinzheng Tao, Liu chen Chang, et. al. "An Intelligent Static Switch Based on Embedded System and Its Control Method for A Mi-crogrid",Innovative Smart Grid

Technologies - Asia (ISGT Asia), 2012.

Every reasonable effort has been made to acknowledge the owners of copyright materials. I would be pleased to hear from any copyright owner who has been omitted or incorrectly acknowledged.